

**Molecular mechanisms
of astrocyte vesicle fusion
at synaptic interfaces**

Dissertation

for the award of the degree
“Doctor rerum naturalium” (Dr. rer. nat.)
Division of Mathematics and Natural Sciences
of the Georg-August-Universität Göttingen

submitted by
Anne C. Wolfes

born in
Boston (MA), USA

Göttingen, 4th September 2015

Thesis committee members:

Camin Dean, PhD (reviewer)

Trans-synaptic signaling, European Neuroscience Institute, Göttingen

Prof. Dr. Reinhard Jahn (reviewer)

Department of Neurobiology, Max Planck Institute for Biophysical Chemistry, Göttingen

Prof. Dr. Swen Hülsmann

Department of Neurophysiology, University Medical Center, Göttingen

Extended thesis committee members:

Dr. Hauke Werner

Department of Neurogenetics, Max Planck Institute for Experimental Medicine, Göttingen

Prof. Dr. Michael Hörner

Department of Cellular Neurobiology, Schwann-Schleiden Research Center, Göttingen

Prof. Dr. Thomas Dresbach

Department of Anatomy, University Medical Center, Göttingen

Date of the oral examination: 28th September 2015

Affidavit

I hereby declare that the PhD thesis entitled “Molecular mechanisms of astrocyte vesicle fusion at synaptic interfaces” was written independently and with no other sources and aids than quoted.

Göttingen, 4th September 2015

Anne C. Wolfes

“You're scared?

We're all scared.

But that doesn't mean we're cowards.

We can take these dead-eyed, we can take 'em!

With science!”

(Bruce Campbell as Ash in Sam Raimi's "Army of Darkness")

Acknowledgements

I am deeply grateful to Dr. Camin Dean for giving me the opportunity of joining her lab and heading out to work on a fun project that left me so much room for being creative and testing ideas. With her encouragement and guidance, I learned to count on my strengths, and that being a scientist is not just a job description. Thank you for your support, believing in me, and for letting us all work in line with our biorhythms.

I would also like to thank Prof. Reinhard Jahn and Prof. Swen Hülsmann for taking such an active part in the thesis committee meetings. I am sincerely thankful for their input and guidance.

Humans are social animals, and I was lucky enough to feel this every day at the lab thanks to my wonderful colleagues. Everyone was always happy to help or feed me; in particular, I thank Ankit Awasthi for giving me data and whatever I needed from his incredibly well-stocked snack drawer, Vinita Bharat for giving me GFP constructs, cookies, and hugs, Christiane Bolleyer for giving me coffee after swimming in ice-cold water and fantastic birthday cake, Charlie Gilbride for giving me regular doses of sweet, sweet Britishness and fun scientific discussions, Joaquín Hurtado for showing me how to slice brains and making me laugh (even if he constantly stole my pens), Markus Stahlberg for giving me viruses and hazelnut coffee (that were both essential to my work), Saheeb Ahmed for showing me his Western blot magic, and Binu Ramachandran for giving me mouse perfusion skills.

I am also grateful for Dr. Wiebke Möbius and Torben Ruhwedel for having me over at their electron microscopy unit although they were swamped with work, and for sharing their cake and tea with me.

I also want to thank Prof. Michael Hörner, Mirja Blötz, Christiane Becker, and Dr. Synnöve Beckh for helping me through the jungle of documents and regulations (and their grey zones). You made my life a lot easier! I also thank Matthias Weyl and Tim Amelung for stopping me from throwing my computer out the window. I thank Frank Kötting and Stephan Bachmann for giving me great equipment and batteries.

As always, I am grateful for the scarily many years of Christoph. Aside from just being yourself, thank you too for helping me find an acronym for my cell culture protocol. We should run a lab together and be inventors, like when we met.

I am indebted to Claudius Eiffert a.k.a. the poster thief, the fast food freak, the encyclopedia of movies, the rock star, the physiotherapist, and the comic artist. You made even the last week seem easy (albeit exhausting), fun, and fed me when I probably would have lived solely on peanut butter and pizza.

Last but not least, I want to thank my family. You are very strange. I have no words for all the love (and acceptance), and I thank you for really sticking to my request of as little contact as possible during intense work phases. Mama, Papa, thank you for giving me optimism and telling me that nothing is impossible. It's true. Penny, Robert – although I am jealous of your skin pigmentation, you mean the world to me. Thanks for showing me why.

Table of Contents

List of Figures and Tables	9
Abbreviations.....	10
1. Abstract.....	12
2. Introduction	13
2.1 Astrocytes in the healthy brain	13
2.2 Astrocytes in neurodevelopmental diseases.....	17
2.3 Astro-neuronal communication and the tripartite synapse.....	19
2.3.1 Signalling through ions and Ca ²⁺ activity.....	20
2.3.2 Signalling through molecules	23
2.4 Gliotransmitters	24
2.5 Release mechanisms of astrocytes.....	26
2.5.1 Non-vesicular and vesicular release	26
2.5.2 Studying gliotransmitter release: Astrocyte culture systems.....	30
2.6 Vesicle-associated proteins in astrocytes.....	33
2.6.1 SNARE proteins in astrocytes.....	33
2.6.2 Synaptotagmins in astrocytes.....	36
2.7 Aim of the project.....	38
3. Materials and Methods	39
3.1 Materials	39
3.1.1 Antibodies.....	39
3.1.2 Animals	43
3.2 Methods.....	45
3.2.1 Cell culture	45
3.2.2 Immunocytochemistry	52
3.2.3 Histological analysis	53
3.2.4 Immunoblotting	55
3.2.5 Electron microscopy	57
3.2.6 Transfection and antibody internalisation assays.....	58
3.2.7 Adeno-associated viruses for Ca ²⁺ imaging.....	60
3.2.8 Microscopy	61
3.2.9 Data analysis	62

4. Results	64
4.1 Characterisation of different astrocyte cultures.....	64
4.1.1 Specific media alter astrocyte morphology, protein expression, and proliferation	64
4.1.2 Ca ²⁺ signalling profiles in different astrocyte cultures.....	75
4.2 Evidence for vesicles in astrocytes	81
4.2.1 Astrocytes contain vesicular organelles	81
4.2.2 Astrocytes express vesicle-associated proteins.....	83
4.2.3 Vamp2-harboured vesicles: Localisation and recycling	85
4.2.4 Syt-harboured vesicles: Localisation and recycling	95
4.3 Syt7 in development and synaptogenesis.....	107
4.3.1 Syt7 is developmentally regulated in astrocytes	107
4.3.2 Synapse number decreases when astrocytes lack Syt7	109
5. Discussion.....	113
5.1 Astrocyte morphology and protein expression depend on the medium	114
5.2 Ca²⁺ signalling differs amongst astrocyte culture methods.....	116
5.2.1 Astrocytic Ca ²⁺ signalling occurs in somata, branchlets, and microdomains	117
5.2.2 Co-culture and NB+H astrocytes exhibit similar Ca ²⁺ signalling profiles	119
5.3 Astrocytes express some vesicle-associated proteins, including synaptotagmins	122
5.4 Vamp2 and Syt7 mark distinct vesicle populations in astrocytes	125
5.4.1 Vamp2 is rarely localised to endosomes in astrocytes.....	127
5.4.2 Syt7 is not localised to lysosomes	128
5.5 Astrocytic Syt7 is involved in synaptogenesis.....	129
5.6 Astrocytes developmentally regulate Syt7 and Hevin.....	131
5.7 Conclusion and future directives	134
Bibliography	135
Curriculum Vitae	158

List of Figures and Tables

- Fig. 1:** Classical view of brain cell positions.
- Fig. 2:** The tripartite synapse.
- Fig. 3:** Structure and function imply heterogeneity of astrocytic Ca^{2+} signalling.
- Fig. 4:** Vesicle subtypes of membrane trafficking.
- Fig. 5:** Immunopanning steps for isolating astrocytes.
- Fig. 6:** SNARE proteins involved in vesicle fusion with the plasma membrane.
- Fig. 7:** Simplified Syt structure.
- Fig. 8:** Conditioned medium from co-cultures makes astrocytes more similar to co-culture and IP astrocytes by morphology.
- Fig. 9:** Secondary antibody controls for immunocytochemistry.
- Fig. 10:** Different media yield morphologically different astrocytes.
- Fig. 11:** HBEGF promotes astrocyte proliferation.
- Fig. 12:** Older tissue yields fewer but viable astrocytes.
- Fig. 13:** Co-culture and NB+H astrocytes show Ca^{2+} events distinct from MD and IP cultures.
- Fig. 14:** Cultured astrocytes contain different vesicular organelles.
- Fig. 15:** Astrocytes express vesicle-associated proteins.
- Fig. 16:** Endogenous Vamp2 is distributed sparsely in astrocyte monocultures.
- Fig. 17:** Vamp2 partly co-localises with endosomal proteins in MD astrocytes.
- Fig. 18:** Astrocytes recycle Vamp2-harboured vesicles in cell cultures.
- Fig. 19:** TeNT blocks GFP-Vamp2 vesicle recycling in astrocytes *in vivo*.
- Fig. 20:** Astrocytes express several synaptotagmin isoforms.
- Fig. 21:** Testing Syt7 antibodies on Wt and *Syt7^{-/-}* samples.
- Fig. 22:** Syt1 expression near astrocytes *in vivo*.
- Fig. 23:** Syt staining appears punctate in co-culture and NB+H astrocytes.
- Fig. 24:** Syts do not co-localise with Vamp2 in NB+H astrocytes.
- Fig. 25:** Syt7 and Lamp1 do not co-localise in astrocytes.
- Fig. 26:** Astrocytes recycle some Syt7-harboured vesicles.
- Fig. 27:** Astrocytes do not take up anti-GFP antibodies via GFP-Syt17-harboured vesicles.
- Fig. 28:** Syt7 is developmentally regulated in astrocytes.
- Fig. 29:** Neurons have fewer synapses when grown on *Syt7^{-/-}* astrocytes.
- Fig. 30:** Hevin is developmentally regulated in astrocytes, and partly co-localises with Syt7.
- Fig. 31:** Model of Hevin released from astrocytes during synaptogenesis

Table 1: Common and recently developed astrocyte monoculture protocols.

Table 2: Comparing our results on astrocytic Ca^{2+} signalling to slices and *in vivo* data.

Abbreviations

Aldh1L1	aldehyde dehydrogenase 1 family member L1
β III tub	beta III tubulin
bp	base pairs
BSA	bovine serum albumin
$^{\circ}$ C	degrees Celsius (centigrades)
DAPI	4'-6-Diamidino-2-phenylindole
ddH ₂ O	double distilled (or miliQ) water
EDTA	ethylened acid
E	embryonic day
e.g.	exempli gratia
EEA1	early endosome antigen 1
<i>g</i>	standard gravity
Gfap	glial fibrillary acidic protein
GFP	green fluorescent protein
HRP	horse radish peroxidase
IP	immunopanning, refers to the IP culture method (Foo et al., 2011)(McCarthy and de Vellis, 1980)(McCarthy and de Vellis, 1980)(McCarthy and de Vellis, 1980)(McCarthy and de Vellis, 1980)
iPSC	induced pluripotent stem cell
Itgb5	integrin beta 5
kDa	kilodalton
M	Molar
Map2	microtubule-associated protein 2
Mbp	myelin basic protein
MD	refers to the MD culture method (McCarthy and de Vellis, 1980)
μ M	micromolar
mM	millimolar
min	minutes
ml	milliliter
μ g	microgram
μ l	microliter
NB+H	refers to the NB+H culture method developed here
ng	nanogram
n.s.	non-significant
μ m	micrometer
nm	nanometer
<i>p</i>	<i>p</i> value
P	postnatal day
PAGE	polyacrylamide gel electrophoresis
PBS	phosphate buffered saline
PCR	polymerase chain reaction
s	seconds
SDS	sodium dodecyl sulfate
SEM	standard error of the mean
Snap	synaptosomal-associated protein
Stx	syntaxin

Syp	synaptophysin
Syt	synaptotagmin
TSP1	thrombospondin1
Wt	wild-type
w/v	weight per volume
U	unit (for enzyme activities)
UV	ultraviolet
V	Volt
Vamp	vesicle-associated membrane protein
vGluT	vesicular glutamate transporter

1. Abstract

Astrocytes are key to neuronal trophic support, development, and synaptic signalling and plasticity. Astrocytes can detect synaptic events at tripartite synapses –a major site of bidirectional communication between neurones and astrocytes– and alter synaptic function by gliotransmitter release. This is reflected in basic research studies as well as neurodevelopmental disease models, where astrocyte-derived factors shape synapse structure and function. Despite the many roles of astrocytes in brain (patho-) physiology, the mechanisms that underlie release of gliotransmitters to affect astro-neuronal communication are poorly understood.

To investigate astrocytic signalling at synaptic interfaces and which molecules mediate astrocytic vesicle fusion, I developed a simple and economical protocol for growing more “*in vivo*-like” astrocyte monocultures. In comparison to other astrocyte monocultures, spontaneous Ca^{2+} signalling in astrocytes of my protocol was more similar to that of astrocytes co-cultured with neurones. Moreover, I observed distinct subcellular domains in which different Ca^{2+} event types occurred that were similar to those of astrocytes in slices and *in vivo*.

Using this culture protocol, I confirmed that astrocytes express several vesicle-associated proteins, two of which localised to two distinct vesicle populations that underwent recycling: Vamp2 and Syt7. Vamp2 was previously found in astrocytes, and cleaving Vamp2 by clostridial toxins blocks Ca^{2+} -dependent glutamate release from astrocytes. Syt7, which is implicated in lysosomal secretion in different cell types (but also regulates synaptic vesicle replenishment), is a Ca^{2+} sensor with high Ca^{2+} affinity that has not yet been reported in astrocytes. The Ca^{2+} signalling patterns I observed in cultured astrocytes provide a context for Syt7-mediated vesicle fusion, which I further investigated using *Syt7*^{-/-} mouse cultures: When co-cultured with *Syt7*^{-/-} astrocytes, wild-type neurones had fewer synapses. Further, I showed that Syt7 and the synaptogenic factor Hevin are developmentally regulated and partially co-localise in cultured astrocytes. These data suggest that Syt7 may regulate vesicular Hevin release from astrocytes, which in turn shapes how neuronal circuits develop. Astrocytic exocytosis contributes to neurodevelopmental diseases, where aberrant astrocytic Hevin release has been implicated in epileptogenesis. Together, these data support that astrocytic Syt7 (and perhaps other Syts) may mediate the release of astrocytic factors that are important for brain development.

2. Introduction

2.1 Astrocytes in the healthy brain

Already over a century ago, Santiago Ramón y Cajal suggested a greater role for glia than just acting as ‘glue’ that keeps neurones together (García-Marín et al., 2007). Indeed, the main classes of glia play diverse and indispensable roles in nervous system physiology, from the myelinating oligodendrocytes in the brain or Schwann cells in the periphery to microglia (dubbed the brain’s immune system), and astrocytes, which maintain the blood-brain barrier and provide metabolic and homeostatic support for neurones. Glia likely contribute to the high cognitive abilities in humans, as from the bottom of the evolutionary tree to the top, the ratio of glia to neurones increases (Nedergaard et al., 2003; Sherwood et al., 2006). Astrocytes especially may contribute to intelligence, as a recent study suggests, in which mice with human astrocytes performed better in learning and memory tests than littermates (Han et al., 2013).

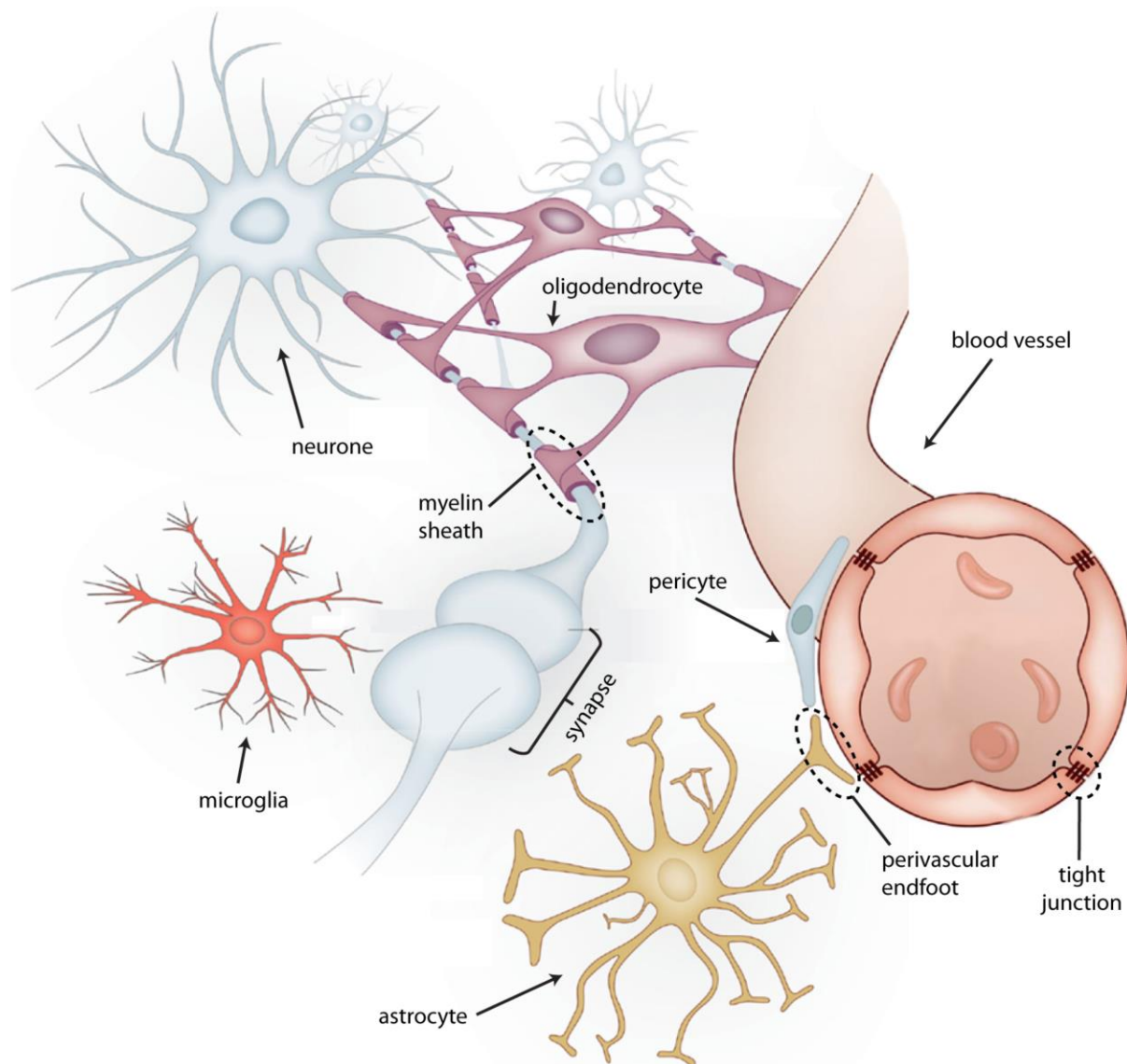


Fig. 1: Classical view of brain cell positions

Schematic image of neurones with zoomed-in view of a synapse, glia, microglia, oligodendrocytes enwrapping axons with myelin sheaths, and an astrocyte contacting blood vessels via a perivascular endfoot. Together with pericytes (which also surround blood vessels), astrocytes form the blood-brain barrier, with tight junctions that restrict molecule and even small ion fluxes. Thus, compounds cannot easily cross the blood-brain barrier, which is a significant caveat for developing drugs that target neurones or glia in the brain. Modified image from Sankowski et al. (2015).

In the past few decades, glia have gained more attention, and their importance for neuronal network function is no longer thought to be restricted to structural, immune, and trophic support: Microglia and astrocytes in particular were shown to directly affect synaptic signalling and plasticity (Araque et al., 1999; Perea et al., 2009; Santello et al., 2012; Schafer et al., 2013), and oligodendrocytes and Schwann cells also provide nutrients to the axons they

ensheath and communicate with neurones (Fields et al., 2014). Among these three major types of glia, the most subtypes and versatile functions were described for astrocytes.

The different domains taken up by morphologically distinct astrocytes already hint at their high degree of specialisation. By brain area, astrocytes are categorised into cortical white matter fibrous astrocytes and grey matter protoplasmic astrocytes, cerebellar Bergmann glia, retinal Müller cells, and radial glia which first appear in the developing brain (and give rise to other astrocytes) but also exist in specialised adult brain areas where neurogenesis occurs (i.e. the subventricular zone along the walls of the lateral ventricles and the subgranular zone within the dentate gyrus of the hippocampus).

On a subcellular scale, astrocytes feature structurally different and specialised domains, e.g. astrocytic endfeet, which contact blood vessels (Fig. 1). The term “astrocytic process” has been used ambiguously, but a specific nomenclature for astrocyte morphology was recently suggested (Tong et al., 2013): The large, primary processes of astrocytes (branches) split into smaller branchlets, which in turn separate into even thinner, specialised processes including endfeet (which contact the vasculature) and leaflets (which contact synapses).

Although all of the astroglial subtypes mentioned above are considered astrocytes, a common marker protein that labels all astrocytes has yet to be identified. However, glial fibrillary acidic protein (Gfap) and aldehyde dehydrogenase 1 family member L1 (Aldh1L1) have been used to label the majority of astrocytes (Cahoy et al., 2008; Yang et al., 2011), although Aldh1L1 was also found in postnatal neural stem cells (Foo and Dougherty, 2013). Other markers expressed by astrocytes also label neurones, like Nestin (Messam et al., 2000), which is expressed by immature astrocytes and neural precursor cells, or S100 β , which predominantly marks mature astrocytes but also other brain cells like oligodendrocytes (Donato et al., 2013; Steiner et al., 2008). The lack of a common astrocyte marker again illustrates how specialised different subtypes of astrocytes are. Indeed, astrocytes are multi-taskers and fundamental to the blood-brain barrier, trophic support of neurones, ion homeostasis, development, and synaptic signalling and plasticity (Volterra and Meldolesi, 2005).

As shown in Fig. 1, the blood-brain barrier is formed by specialised astrocytic processes called endfeet, which wrap around blood vessels (Parri and Crunelli, 2003). Such contacts allow astrocytes to retrieve nutrients from the bloodstream and pass these on to neurones, e.g. astrocytes take up glucose via glucose transporters in their endfeet (Fernandez-Fernandez et al., 2012; Prebil et al., 2011). At the same time, astrocytic endfeet are also

involved in spatial $[K^+]$ buffering, thus contributing to ion homeostasis. Local extracellular $[K^+]$ increases (as caused by action potentials) can trigger undesired action potentials in neighbouring neuronal processes, and in situations with increased neural activity, favour epileptic discharge – but when astrocytes take up excess K^+ from the extracellular space, high $[K^+]$ is quickly dispersed through gap junctions to other astrocytes, and finally released into the bloodstream (Walz, 2000). Astrocytes also take up excess glutamate. Like faulty K^+ buffering, excess extracellular glutamate can also contribute to epilepsy by causing hyperexcitation and seizures, and is cytotoxic at high concentrations (Seifert and Steinhäuser, 2013). Interestingly, clinical hallmarks of epileptic patients also include dysfunctional astrocytic glutamate transporters and glutamine synthetase (GS), which converts glutamate into glutamine, a key source for neuronal glutamate and thus neurotransmitter release.

However, glutamate is not only taken up by astrocytes, but alongside other molecules, can also be released from astrocytes to alter synaptic signalling and plasticity (Barker and Ullian, 2010; Perea et al., 2009). The role of glial factors in synaptic function and communication between astrocytes and neurones will be discussed in more detail in chapter 2.3.2.

Astrocytes not only provide support of neural network activity, but in development they also guide neurones (Del Puerto et al., 2013) and directly affect myelination (Ishibashi et al., 2006) and synaptogenesis (Allen, 2013; Pfrieger, 2002). Key to steering such developmental processes, the release of astroglial factors has become a major focus within the field, not least because of the implications for neurodevelopmental diseases (Sloan and Barres, 2014a). For example, astrocyte-secreted factors contribute to the abnormal morphology of dendritic spines in fragile X syndrome and Down's syndrome, and also amplify epilepsy and neuropathic pain (Eroglu, 2009).

2.2 Astrocytes in neurodevelopmental diseases

In terms of diseases associated with astrocytes, epilepsy first comes to mind. This disorder is characterised by epileptic seizures due to hyperexcitability and abnormal brain development (Caleo, 2009). As described in the previous chapter, astrocytes are key to spatial K^+ and glutamate buffering, to prevent neurones from firing uncontrollably. Of note, dysfunctional astrocytes increase neuronal excitability and thereby exacerbate epileptic seizures (Gómez-Gonzalo et al., 2010). Apart from adult astrocyte dysfunction in epilepsy, early postnatal development has recently received more attention as a contributing factor to epilepsy, since defective synapse elimination and/or refinement can also add to neuronal hyperexcitability (Bozzi et al., 2012). Epilepsy is also considered a neurodevelopmental disorder, since neuronal connections are established and refined soon after birth. Interestingly, astrocytes greatly influence synaptogenesis (e.g. by secreting synaptogenic factors), including synaptic elimination and remodelling (Clarke and Barres, 2013).

Apart from neuronal circuit development, the importance of astrocytes for normal brain function becomes painfully clear in Alexander disease, which is a rare disorder caused by Gfap mutations in most cases. The majority of patients experience developmental delays, regression and seizures, and rarely survive until adulthood (Brenner et al., 2009). Although astrocytic dysfunction sits at its core, Alexander disease was initially described as a white matter disease (leukodystrophy) because of hypertrophic astrocytes scattered all throughout the white matter. Other astroglipathies may therefore underlie disorders categorised as neuronal or myelin-related.

In fact, Rett syndrome is one such astroglipathy that was first attributed to neuronal dysfunction. Rett syndrome is characterised by a lack of the transcriptional repressor methyl-CpG-binding protein 2 (MeCP2), without which patients first lose acquired developmental progress and then develop autistic traits, cognitive impairment, and respiratory abnormalities that often lead to premature death (Chahrouh and Zoghbi, 2007). Recently, astrocytes were found to express MeCP2 (Ballas et al., 2009). Further, wild-type (Wt) neurones developed abnormal dendrite morphology when exposed to either astrocytes or conditioned medium from mutant mouse cell cultures that lack MeCP2. These dendritic abnormalities were partially restored (along with normal movement and breathing) after conditional re-installing of MeCP2 function only in astrocytes of mutant mice. In a screen for differential gene expression in Wt and mutant mice lacking MeCP2, the genes for two secreted proteins (chromogranin B and lipocalin-2) were significantly downregulated (Delépine et al., 2015) in

MeCP2 knockout mice. The authors of this study suggested that astrocytes secrete less chromogranin B and lipocalin-2 in MeCP2 knockout mice, which in turn may lead to neuronal abnormalities in MeCP2-lacking mutant mice. These findings suggest that astrocytes play a more central role in Rett syndrome than neurones (Lioy et al., 2011).

Another astrocyte-secreted factor, thrombospondin1 (TSP1) was identified as a key mediator of dendritic spine development and is implicated in Down's syndrome (Garcia et al., 2010). Similarly to the Rett syndrome studies described above, Wt neurones developed abnormal dendritic spine number and density, as well as synaptic defects when cultured with astrocytes from Down's syndrome patients. However, reinstating normal TSP1 levels rescued these effects.

Another example of a neurodevelopmental disorder with astrocyte dysfunction at its centre is fragile X syndrome, which entails autistic traits, epilepsy, and motor and cognitive impairments (Hagerman and Stafstrom, 2009). In a mouse model of fragile X syndrome, Wt astrocytes prevented mutant neurones from developing abnormal dendrites with fewer synapses as compared with cultures of only mutant cells (Jacobs and Doering, 2010).

Astrocyte-related neurodevelopmental diseases also include psychiatric diseases like autism and schizophrenia. Autism is partially attributed to abnormal synapse development and an imbalance of excitatory / inhibitory connections, and several genes implicated in autistic disorders affect synaptogenesis (Walsh et al., 2008). In schizophrenia, dysregulated glutamate homeostasis is thought to underlie psychosis, and is accompanied by fewer astrocytes that express less glutamate transporter EAAT2 (also known as Glt-1) (Bauer et al., 2010; Moghaddam and Javitt, 2012). In addition, schizophrenic patients have fewer synaptic connections than non-schizophrenic patients (Bennett, 2009; Glantz and Lewis, 2000), illustrating that this disorder too has neurodevelopmental features.

In summary, astrocytic dysfunction is central to many neurodevelopmental diseases: For the disorders described above, common symptoms like epileptic seizures and abnormal synapse formation and function are all linked to astrocytic dysfunction (Molofsky et al., 2012). In these cases, the term “neurodevelopmental disease” is misleading, since several such conditions have equally central “gliodevelopmental” aspects. Taken together, these studies demonstrate that studying astrocytes is not just a matter of understanding brain physiology, but also pathology.

2.3 Astro-neuronal communication and the tripartite synapse

The previous chapters outlined how astrocytes support both neuronal circuit function and development. This support is far from passive: Astrocytes actively signal to and receive input from neurones (and other glia) via ions (primarily Ca^{2+} but also Na^+ and K^+) and molecules (e.g. glutamate, ATP). Using these diverse signalling agents, astrocytes influence both synaptic signalling and plasticity (Araque and Navarrete, 2010; Fellin et al., 2006a).

The importance of astrocytes at synapses is mirrored by the number of their perisynaptic processes: Each protoplasmic astrocyte contacts $\approx 100,000$ synapses in rodents, and up to 2 million synapses in humans (Oberheim et al., 2006). Thus, the idea of “tripartite synapses” was introduced (Araque et al., 1999) to stress that synapses include not just pre- and postsynaptic neurones, but astrocytic processes, too (Fig. 2). Notably, microglia also shape synaptic connections, so that referring to “quad-partite synapses” may be even more appropriate (Schafer et al., 2012, 2013). However, the term “tripartite synapse” will be used here to highlight communication between astrocytes and neurones.

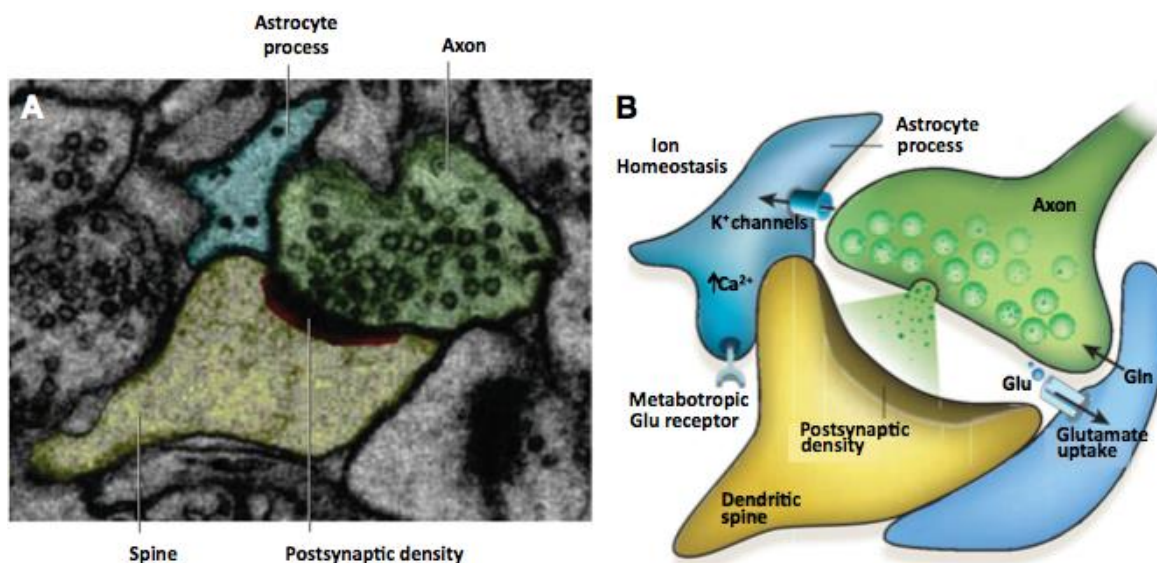


Fig. 2: The tripartite synapse

A Electron micrograph showing a pre- (green) and a post-synaptic (yellow) neuronal process, contacted by an astrocyte (blue). **B** Scheme (using the same colour code) illustrating that astrocytes mediate K^+ ion homeostasis and are capable of sensing extracellular glutamate (Glu) via Glu receptors (both processes can trigger astrocytic Ca^{2+} signalling), and that astrocytes also take up glutamate to convert it to glutamine (Gln) as a source for glutamate in neurones. Modified images from Eroglu and Barres (Eroglu and Barres, 2010).

2.3.1 Signalling through ions and Ca²⁺ activity

Unlike neurones, astrocytes are electrically non-excitabile and can't generate action potentials, but rather show a linear relationship between injected current and membrane potential changes; yet, they also express voltage-dependent ion channels in their processes (Barres, 1991; Steinhäuser, 1993). Instead of using action potentials to communicate with each other, astrocytes employ Ca²⁺, Na⁺, and K⁺ signalling through gap junctions, ion transporters, and channels in their membranes (Rose and Karus, 2013; Sontheimer, 1994; Verkhratsky and Steinhäuser, 2000). Here, we focus on Ca²⁺ signalling, which (although intertwined with Na⁺ and K⁺ ion fluxes) is the major ion-based signalling mechanism in astro-neuronal communication.

Ca²⁺ signalling can be observed in cell cultures but also *in vivo*, where it can occur in response to sensory stimulation (Kuga et al., 2011; Wang et al., 2006). Synaptic activity locally decreases the extracellular Ca²⁺ concentration, which in turn triggers glutamate and ATP release from astrocytes and subsequent Ca²⁺ signalling in astrocytes (Torres et al., 2012). In addition, astrocytic Ca²⁺ signalling can also prompt neuronal responses (Nedergaard, 1994; Parpura et al., 1994) and thus astrocytes modulate synaptic transmission, e.g. by inhibiting (Newman and Zahs, 1998) or increasing electrical activity (Hassinger et al., 1995). At synaptic interfaces, their fine, specialised protrusions allow astrocytes to mediate neuronal signalling in spatially restricted domains as shown by confocal and electron microscopy (Melone et al., 2011; Verkhratsky and Parpura, 2010): Aside from Ca²⁺ waves, astrocytes also exhibit isolated Ca²⁺ fluctuations in thin processes or even smaller microdomains of around 4 μm² (Di Castro et al., 2011; Shigetomi et al., 2013a) (Fig. 3).

To resolve Ca²⁺ event dynamics, genetically encoded Ca²⁺ indicators (GECIs) are a new tool that allow for fluorescent visualisation of Ca²⁺ fluctuations (Kotlikoff, 2007), e.g. GCaMP is a circularly permuted GFP variant containing a calmodulin and M13 domain of a myosin light chain kinase that fluoresces upon Ca²⁺ binding (Nakai et al., 2001). Recent GCaMP generations like the membrane-tethered Lck-GCaMP3 (Tian et al., 2012) now permit imaging Ca²⁺ events in confined subcellular regions like tripartite synapses and astrocytic microdomains (Shigetomi et al., 2010a; Tong et al., 2013).

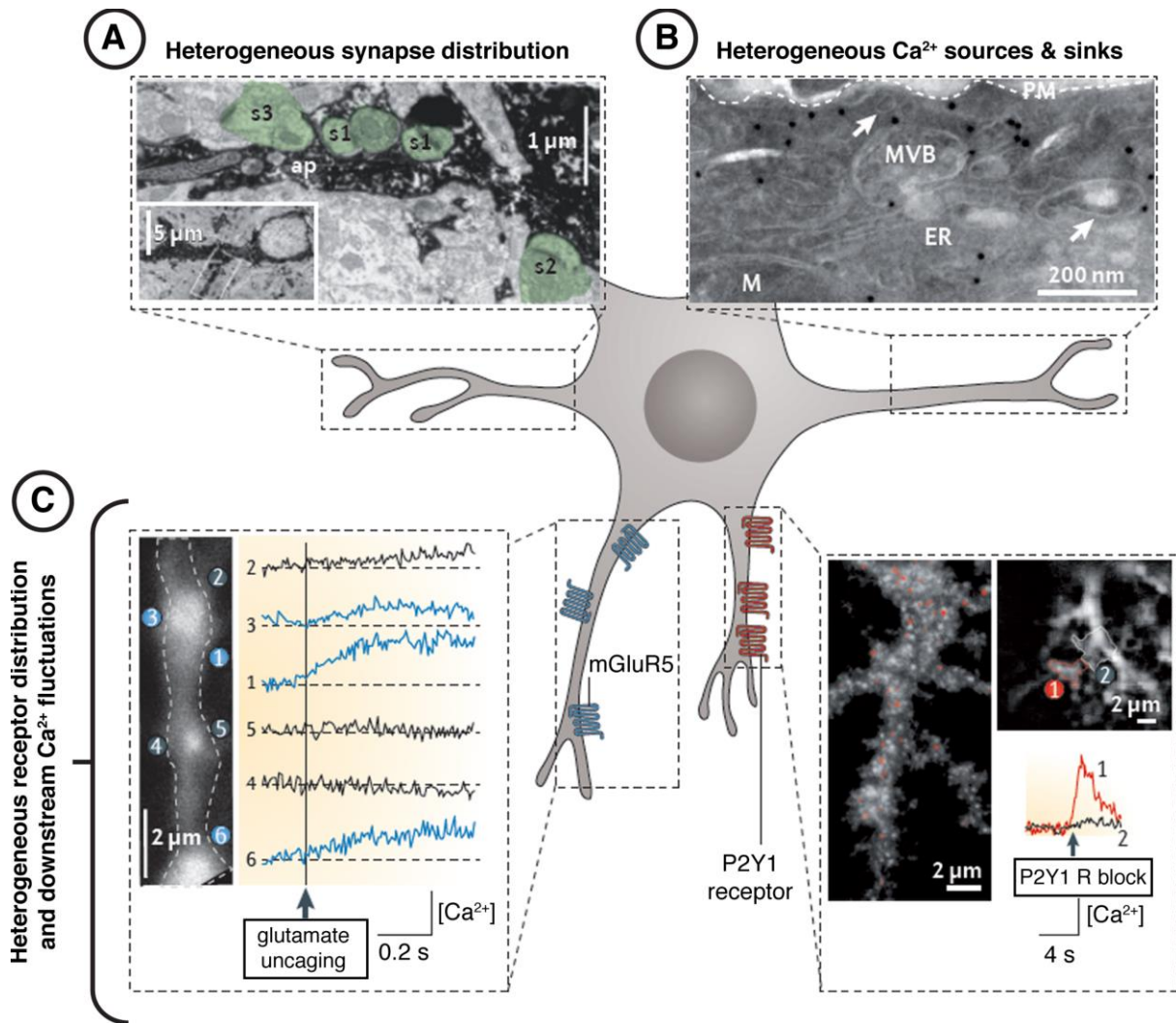


Fig. 3: Structure and function imply heterogeneity of astrocytic Ca^{2+} signalling

Astrocytes show heterogeneous synapse distribution, Ca^{2+} sources and sinks, receptor distribution, and Ca^{2+} fluctuations. **A** Electron micrograph showing heterogeneous synapse (s) distribution where each synapse is enwrapped by astrocytic processes (ap). Synapses are enwrapped completely by the astrocytic process (s1), only contacted at one side of the synaptic cleft (s2), or not contacted at all (s3). **B** Electron micrograph showing how an astrocytic process contains heterogeneous Ca^{2+} sources and sinks, e.g. mitochondria (M) and the endoplasmic reticulum (ER). Other structures include multivesicular bodies (MVB), vesicular compartments (arrow), and the plasma membrane (PM, white dashed line). **C** Data from Ca^{2+} imaging studies in astrocytic processes showing heterogeneous G protein-coupled receptor distribution and downstream Ca^{2+} fluctuations. Left: Two-photon glutamate uncaging causes local Ca^{2+} fluctuations (via metabotropic glutamate receptor 5 (mGluR5)) in some subdomains (blue traces) of astrocytic processes (white dashed line), but not in other subdomains (black traces). Right: STED image showing uneven distribution of purinergic P2Y1 receptors (red) along astrocytic processes (grey scale). Within the same process, two distinct domains respond differently to local application of the P2Y1 receptor agonist 2MeSADP (square image and graph below). Modified image from (2014).

Aside from astro-neuronal signalling, astrocytic Ca^{2+} signals can also arise independently of neuronal stimuli; these Ca^{2+} signals are capable of inducing intracellular Ca^{2+} waves that can spread to neighbouring astrocytes or affect neuronal signalling (Nett et al., 2002; Parri et al., 2001). This suggests that astrocytic Ca^{2+} signalling can occur on a large scale but also within specialised domains, either spontaneously, in response to, or leading to neuronal stimulation. In terms of bidirectional communication between astrocytes and neurones, Ca^{2+} signalling events are both diverse and specific at once.

2.3.2 Signalling through molecules

Apart from Ca^{2+} -mediated signalling, astrocytes and neurones also communicate through molecules to a large extent. A major site of molecular signal exchange is the tripartite synapse, at which neurones release neurotransmitters (e.g. glutamate). From a metabolic perspective, neurotransmitters like glutamate are taken up by astrocytes, where glutamate is converted into glutamine and passed to neurones for replenishing synaptic vesicles with glutamate. However, astrocytes also express neurotransmitter receptors (e.g. ionotropic and metabotropic glutamate, GABA, and purinergic receptors), by which they can sense neurotransmitter release from neurones (Verkhratsky, 2009). When neurotransmitters bind to their astrocytic receptors, they can elicit intracellular Ca^{2+} signalling in astrocytes, and via gap junctions cause Ca^{2+} waves in neighbouring glia (Dani et al., 1992; Scemes and Giaume, 2006).

In the case of glutamate, it was suggested that astrocytes sense glutamate at synaptic interfaces via the metabotropic glutamate receptor (mGluR) 5 (Panatier et al., 2011). However, this receptor was recently shown to be expressed only until postnatal week 3, and mGluR3 was instead proposed as an astrocytic glutamate sensor due to its developmentally unrestricted expression (Sun et al., 2013). This example demonstrates that signalling mechanisms between astrocytes and neurones may differ between early postnatal, adolescent, and adult cells.

Another example of how astrocytes respond to neurotransmitter release is that they in turn release transmitters (e.g. ATP) themselves and thus modulate synaptic plasticity (Pouget et al., 2014; Zhang et al., 2003). In fact, astrocytes were shown to release several molecules that act as transmitters at neuronal synapses; when such chemical signals are released from astrocytes (often in a Ca^{2+} -dependent manner), they are referred to as gliotransmitters. Gliotransmitter release has received much attention, particularly because of the multitude of release mechanisms that are implied, i.e. non-vesicular and vesicular release. This aspect of astro-neuronal signalling –gliotransmitters and their release mechanisms– are discussed in more detail in chapters 2.4 and 2.5.

2.4 Gliotransmitters

A true gliotransmitter is defined as any compound that (1) is synthesised or stored in glia, (2) is released in a regulated fashion following physiological or pathological stimuli, (3) induces fast (millisecond / second) responses in adjacent cells, and (4) has functions in (patho-) physiology (Parpura and Zorec, 2010). In astrocytes, the best-studied gliotransmitters include glutamate, adenosine triphosphate (ATP), and D-serine, all of which have been proposed to be released in a Ca^{2+} -dependent manner (Henneberger et al., 2010; Jacob et al., 2014; Kim et al., 2015a; Navarrete et al., 2012). Since research on astrocytic gliotransmitters is quite extensive, the most prominent examples of gliotransmitter function will be given below to provide an overview of how astrocytic compounds affect neuronal network function.

One of the first gliotransmitters to be identified was glutamate. Synaptic stimulation can elicit astrocytic glutamate release, which in turn modulates synaptic signalling and plasticity (Perea et al., 2009; Sasaki et al., 2011). For instance, neuronal activity triggers astrocytes to release glutamate, which binds to nearby neuronal *N*-methyl-D-aspartate (NMDA) receptors (Jourdain et al., 2007). As a result, neurotransmitter release probability is enhanced, i.e. astrocyte-derived glutamate directly affects synaptic transmission.

Astrocytes also release ATP into the extracellular space, where ATP is hydrolysed to adenosine. Adenosine then inhibits presynaptic neurotransmitter release and thereby coordinates neuronal network function (Carlsen and Perrier, 2014; Pascual et al., 2005). Further, astrocyte-derived ATP can evoke Ca^{2+} signals in neighbouring astrocytes, since inhibiting ATP receptors or enzymatically degrading ATP led to diminished Ca^{2+} waves in astrocytes (Bowser and Khakh, 2007).

Astrocytes express high levels of serine racemase, which converts L- to D-serine (Schell et al., 1995; Wolosker et al., 1999), which is then released by astrocytes. Similar to astrocyte-derived glutamate, D-serine binds to NMDA receptors (Mothet et al., 2000). At tripartite synapses, neuronal NMDA currents are amplified when astrocytes continuously release D-serine, favouring synaptic potentiation. Astrocytic leaflets tightly ensheath or retract from tripartite synapses of the supraoptic nucleus in virgin versus lactating rodents, respectively. At these highly dynamic synapses, synaptic depression takes place when astrocytic processes are more distant from the synapse – showing a role for astrocyte-derived D-serine in metaplasticity (Panatier et al., 2006).

In summary, gliotransmitters directly affect synaptic signalling and plasticity (e.g. glutamate, D-serine), coordinate synaptic networks (e.g. ATP), and evoke Ca^{2+} signalling in

neighbouring astrocytes (e.g. ATP), which may in turn release other gliotransmitters. Astrocytes employ a great diversity of release mechanisms, which can be classified as non-vesicular or vesicular, as discussed in chapter 2.5. Using several different release mechanisms may allow astrocytes to compartmentalise their seemingly contradictory properties (e.g. sinks for extracellular neurotransmitters vs. astrocytic glutamate release) via spatial (distinct subcellular domain) and temporal specificity (Fields and Stevens-Graham, 2002).

2.5 Release mechanisms of astrocytes

2.5.1 Non-vesicular and vesicular release

Astrocytes employ several distinct release mechanisms (e.g. for gliotransmission), which can be divided into non-vesicular and vesicular release.

Non-vesicular release in astrocytes entails numerous mechanisms that can broadly be categorised into channel-mediated (via cell swelling-induced anion channel opening, connexin hemichannels, pannexin channels, and ionotropic receptors) and transporter-mediated release (via reversal of uptake by plasma membrane transporters, antiporters, and organic anion transporters).

Channel-mediated release occurs in response to cell volume changes or ligand binding to channel receptors that change the conformation of the channel. Of the three gliotransmitters mentioned earlier –glutamate, D-serine, and ATP– cell swelling-regulated anion channels were only reported as permeable to glutamate (Kimelberg et al., 1990; Takano et al., 2005). Connexin hemichannels (also known as connexons) constitute half of a cell-cell channel, while pannexin channels (also known as pannexons) reside within the membrane of a single cell (Sosinsky et al., 2011). In contrast to cell swelling-regulated anion channels, connexin hemichannels and pannexin channels allow both glutamate (Barbe et al., 2006; Ye et al., 2003) and ATP (Cotrina et al., 1998, 2000; Dahl, 2015) to pass. Similarly, ionotropic purinergic receptors also mediate glutamate (Duan et al., 2003; Fellin et al., 2006b) and ATP release from astrocytes (Bowser and Khakh, 2007).

Transporter-mediated release is a mechanism with bidirectional effects, e.g. as glutamate exits the astrocyte through reversal of uptake by plasma membrane transporters, K^+ enters the cells (Malarkey and Parpura, 2008). Reversal of uptake by plasma membrane transporters passage glutamate (Szatkowski et al., 1990; Volterra et al., 1996) and D-serine (Ribeiro et al., 2002), but ATP release by this mechanism was not reported. Antiporters in astrocytes were only shown to release glutamate (and take up cystine in exchange) (Baker et al., 2002; Warr et al., 1999), while organic anion transporters mediate both glutamate (Rosenberg et al., 1994) and ATP (Anderson et al., 2004; Queiroz et al., 1999) release.

Astrocytes likely recruit different release mechanisms according to the type of stimuli they receive and the subcellular domain from which substances are released. In support of this, a recent study in cultured astrocytes revealed two non-vesicular, channel-mediated types of glutamate release, where G-protein coupled receptor activation led to opening of the

glutamate-permeable K^+ channel Trek-1 (with fast kinetics) or the Ca^{2+} -activated anion channel Best1 (with slow kinetics) (Woo et al., 2012). Interestingly, channels mediating fast glutamate release (Trek-1) were mostly localised to the cell body and processes, whereas channels mediating slower glutamate release (Best1) were mostly localised to astrocytic microdomains.

Numerous studies suggest that in addition to non-vesicular release mechanisms, glutamate, ATP, and D-serine can also be exocytosed via vesicles in a Ca^{2+} -dependent manner. Three classes of vesicles were found in astrocytes: lysosomes (Jaiswal et al., 2007; Li et al., 2008; Zhang et al., 2007), large dense-core vesicles / secretory granules (Coco et al., 2003; Prada et al., 2011; Ramamoorthy and Whim, 2008), and small synaptic-like microvesicles (Bergersen and Gundersen, 2009; Bergersen et al., 2012; Bezzi et al., 2004; Jourdain et al., 2007; Martineau et al., 2013). These and other astrocytic organelles (including recycling endosomes) are summarised in Fig. 4.

In contrast to non-vesicular mechanisms, vesicular release from astrocytes requires vesicular organelles to transport cargo (e.g. gliotransmitters) to the cell membrane and undergo Ca^{2+} -dependent exocytosis. On a molecular level, vesicle fusion is mediated by vesicle-associated proteins, which are examined in more detail in chapter 2.6. Thus, three hallmarks of vesicle exocytosis are vesicular organelles, Ca^{2+} dependency, and vesicle-associated proteins capable of affecting vesicle fusion.

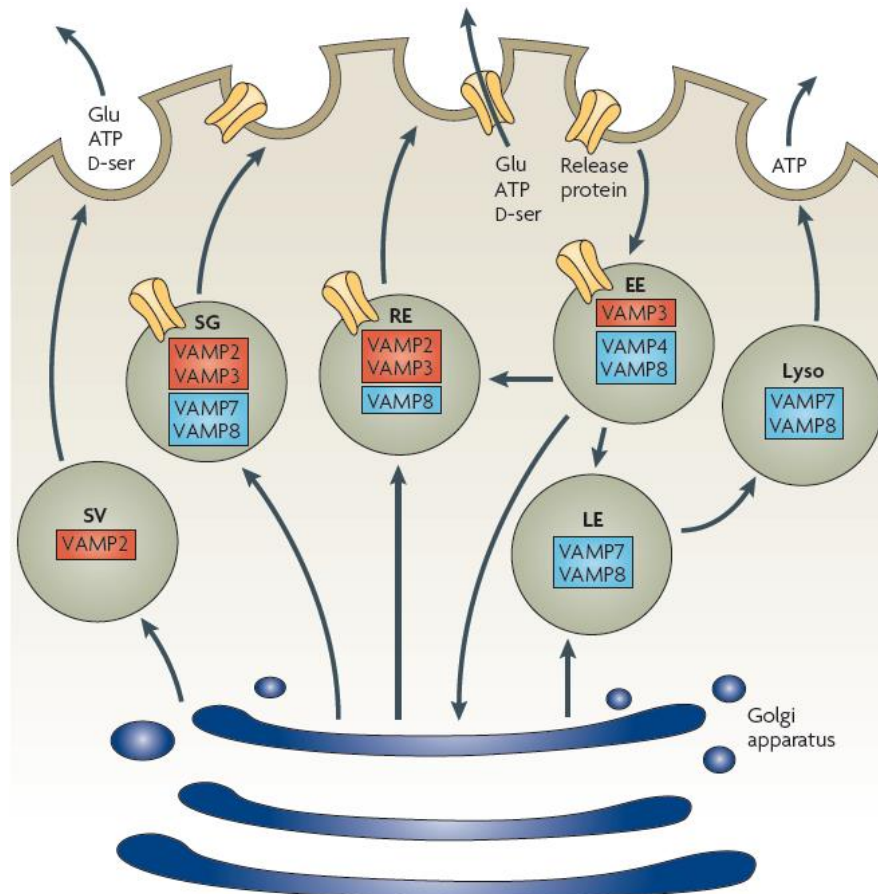


Fig. 4: Vesicle subtypes of membrane trafficking

Schematic diagram showing different vesicle subtypes and their respective vesicle-associated membrane proteins (VAMPs), i.e. synaptic vesicles (SV, comparable to small synaptic-like microvesicles in astrocytes), secretory granules (SG), recycling endosomes (RE), early (EE) and late (LE) endosomes, and lysosomes (Lyso). Vesicle diameter can range from 30-50 nm (SVs), ≈ 300 nm (SG), 60-2000 nm (RE), and 60-3000 nm (LE and Lyso). Example transmitters include glutamate (Glu), ATP, and D-serine (D-ser). Image taken from Hamilton and Attwell (2010).

Much of the initial support for vesicular exocytosis has come from astrocyte monocultures, which meet these three criteria: They express several vesicle-associated proteins (Montana et al., 2006; Parpura and Zorec, 2010), contain vesicular organelles with diameters similar to synaptic and dense-core vesicles / secretory granules (Martineau et al., 2013; Singh et al., 2014), and release gliotransmitters like glutamate in a Ca^{2+} -dependent manner (Bezzi et al., 1998; Innocenti et al., 2000; Pasti et al., 2001; Zhang et al., 2004a). Similar observations were made in brain slices and *in vivo*, where astrocytes too express vesicle-associated proteins or their mRNA (Mittelstaedt et al., 2009; Schubert et al., 2011), feature vesicular organelles (Hur et al., 2010; Williams et al., 2006), and show Ca^{2+} -dependent gliotransmitter release (Kang et al., 2013; Rossi et al., 2000). Thus, whether or not

astrocytes employ release through vesicles in general is no longer a question – but if these vesicles undergo regulated release, and if so, what the underlying molecular mechanisms, vesicle subtypes, and cargo are, is a matter of debate.

2.5.2 Studying gliotransmitter release: Astrocyte culture systems

A lot of what we know about gliotransmitter release from astrocytes has come from cell culture systems. Although *in vivo* experiments are superior to cell cultures by physiological parameters, cell culture experiments give access to experimental manipulations that can help dissect molecular mechanisms within living cells. Since astrocytes share a lot of the same transmitter molecules and receptors with neurones, molecules present in astrocytic versus neuronal processes (that are closely connected) are difficult to distinguish in co-cultures of astrocytes and neurones. Although fluorescence-activated cell sorting (FACS) can be used to reliably isolate astrocytes (Dutly and Schwab, 1991; Foo, 2013a; Sergent-Tanguy et al., 2003), this method identifies cells by GFP expression (e.g. under the control of an astrocyte-specific promoter, which may not be expressed in all astrocytes) and restrains cell health so that cell cultures are difficult to maintain (Foo, 2013a).

To study gliotransmitter release in astrocytes isolated from neurones, a protocol for growing so-called “MD” astrocyte monocultures was developed 35 years ago that has led to numerous advances in the astrocyte field (McCarthy and de Vellis, 1980). Since then, several other monoculture protocols have been designed aimed at culturing more physiologically relevant astrocytes. The four major approaches to date are listed below and include MD astrocytes, immunopanned (IP) astrocytes, astrocytes derived from induced pluripotent stem cells (iPSCs), and astrocytes grown in 3D matrices (Table 1).

Table 1: Common and recently developed astrocyte monoculture protocols

Comparison of the commonly used MD culture method with three recently published protocols, listing advantages and disadvantages of each protocol, as well as the cell source and the original reference.

Culture method	Cell source	Advantages	Potential disadvantages
MD (McCarthy & de Vellis, 1980)	perinatal (often P0-2)	simple, quick, cheap	polygonal morphology, protein expression profile unlike freshly isolated astrocytes (Foo et al., 2011), uses serum
IP (Foo et al., 2011)	P0-14	stellate morphology, gene expression like freshly isolated astrocytes, serum-free	lengthy protocol, requires many reagents
iPSC-derived (Krencik & Zhang, 2011)	iPSCs	human astrocytes, can use cells from “disease-specific tissue”, maintain for months, serum-free	takes more than 3 months to prepare (and longer to mature)
3D matrix (Puschmann et al., 2013; Placone et al., 2015*)	P1-3	stellate, 3D morphology, serum-free*, murine/human	requires 3D matrices

The central steps of the MD method are culturing cells in serum-containing Dulbecco's Modified Eagle Medium (DMEM), and shaking them after 7-10 days in culture. At this point, neurones and all non-astrocytic glia detach from the culture dish, so that only astrocytes remain after shaking. MD astrocytes develop a polygonal (not stellate as *in vivo*) morphology, and express high Gfap levels (a sign of pathology in brain regions like the cortex (Zamanian et al., 2012)). Simply growing cells in the same medium (without shaking) also yields polygonal, non-neuronal cells that express predominantly astrocyte markers like Gfap, Aldh1L1, and Vimentin (Du et al., 2010; Souza et al., 2013). This suggests that much of the differentiation into polygonal astrocytes may be due to medium composition, and not due to preparation methods (i.e. shaking to remove other cell types).

In contrast to MD astrocytes, IP astrocytes morphologically resemble astrocytes *in vivo*, although the protocol to generate IP astrocytes is long, requires many reagents, and yields only few cells (Foo et al., 2011). Other drawbacks include that astrocytes are selected by a single astrocyte-specific cell surface antibody, possibly selecting for just a subset of astrocytes (since no common astrocyte marker exists) and are kept at room temperature for hours during immunopanning (Fig. 5), which may compromise cell viability. Compared with MD astrocytes, most cortical IP astrocytes express similar Gfap levels, suggesting that although IP astrocytes are more *in vivo*-like in terms of morphology, they may still represent reactive astrocytes.

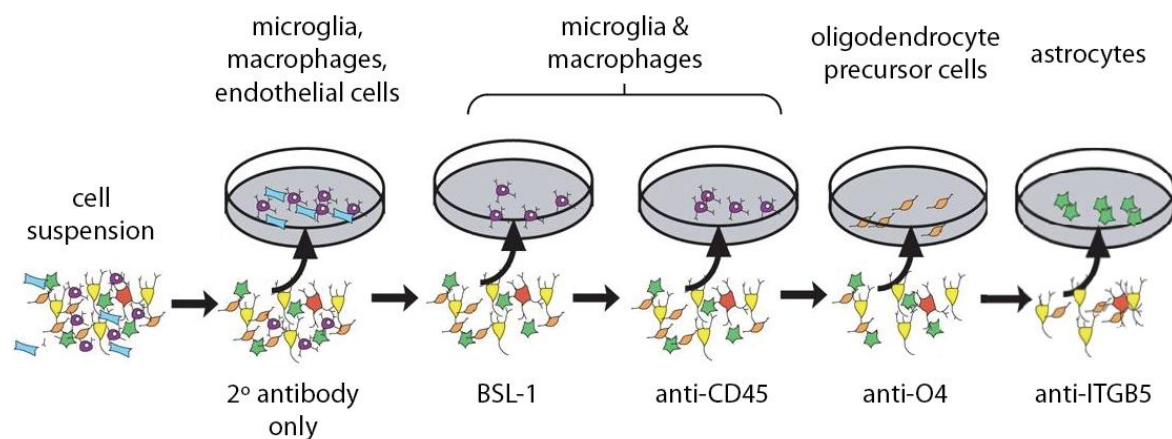


Fig. 5: Immunopanning steps for isolating astrocytes

For generating immunopanned (IP) astrocytes, a cell suspension is prepared from early postnatal rats or mice, which is subjected to a series of negative and one final positive immunopanning step to isolate astrocytes. Above each dish, the targeted cell type is noted, while the respective probes attached to the dish surfaces are indicated below each dish. In each step, different cell types are selected for by first a secondary (2°) antibody only to target non-specific binding of mostly immune-responsive cells, then by BSL-1 (a bacterial lectin to target microglia and macrophages) and antibodies against CD45, O4, and finally ITGB5. Modified from Foo et al. (2011).

Another difference between MD and IP astrocytes is the medium, i.e. serum-containing DMEM versus a serum-free mix of DMEM and Neurobasal medium that includes the heparin-binding EGF-like growth factor (HBEGF). While HBEGF is expressed in the brain from embryonic day 14 onwards (and is upregulated during astrogliogenesis), HBEGF promotes astrocyte migration (Faber-Elman et al., 1996) and proliferation in culture (Kornblum et al., 1999). Hence, HBEGF may support astrocyte survival, proliferation, and/or differentiation (Puschmann et al., 2013) – which would be reflected in astrocyte morphology and behaviour.

These attributes of HBEGF were recently incorporated in a protocol for growing 3D astrocyte monocultures (Puschmann et al., 2013). Apart from promoting an *in vivo*-like morphology of astrocytes, HBEGF quality is consistent (unlike serum, which is prone to varying batch quality), resulting in more consistent cultures, while still enhancing astrocyte proliferation as much as serum (Puschmann et al., 2014). However, some cell culture techniques benefit from 2D cell cultures, e.g. imaging Ca^{2+} signalling within processes of one or several astrocytes or total internal reflection fluorescence microscopy, which is only possible within a single optical plane.

Using a protocol beginning with iPSCs, human astrocytes can be generated, matured, and maintained in serum-free medium with a combination of growth factors (Krencik and Zhang, 2011). Like IP astrocytes, these iPSC-derived astrocytes are also Gfap-positive and may thus represent reactive astrocytes.

Protocols for 3D astrocyte monocultures demonstrate that non-reactive astrocytes (which only express little Gfap and Vimentin) can be cultured. And protocols using different medium for cultured astrocytes suggest that chemically defined media including HBEGF are superior to serum-containing media not just by ensuring quality standards, but also by promoting *in vivo*-like astrocyte morphology and protein expression.

2.6 Vesicle-associated proteins in astrocytes

Astrocytes express several vesicle-associated proteins that are implicated in vesicular fusion in other cells, e.g. synaptic vesicle fusion in neurones. Vesicle-associated proteins can refer to proteins integral to or associated with membranes of exocytotic vesicles (e.g. lysosomes, dense-core vesicles / secretory granules, small synaptic-like microvesicles, or recycling endosomes), or endocytotic vesicles (e.g. early or late endosomes).

2.6.1 SNARE proteins in astrocytes

Every cell expresses soluble NSF attachment protein receptor (SNARE) proteins, which are involved in intracellular membrane trafficking (Jahn and Scheller, 2006), and mediate docking and fusion of vesicles with their respective target membranes. SNARE proteins are required for endocytotic (Deák et al., 2004) and exocytotic vesicle fusion, and have been studied extensively in the context of neuronal synaptic vesicle exocytosis. During synaptic transmission, an incoming action potential causes voltage-gated Ca^{2+} channels in the axon terminal to open, so that intracellular $[\text{Ca}^{2+}]$ increases. As a result, synaptic vesicles fuse with the pre-synaptic plasma membrane; the SNARE complex orchestrates this fusion. Four proteins (one vesicular SNARE, Vamp2 (also known as synaptobrevin), the plasma membrane protein syntaxin1, and two copies of the plasma membrane associated protein Snap25 (a target SNARE) make up the SNARE complex (Fig. 6) which promotes fusion. The Ca^{2+} sensor synaptotagmin (Syt) 1 triggers fast synchronous fusion in response to Ca^{2+} -binding to its two C2 domains, which causes it to bind tightly to SNARE proteins and to insert into lipid bilayers (Chapman, 2002).

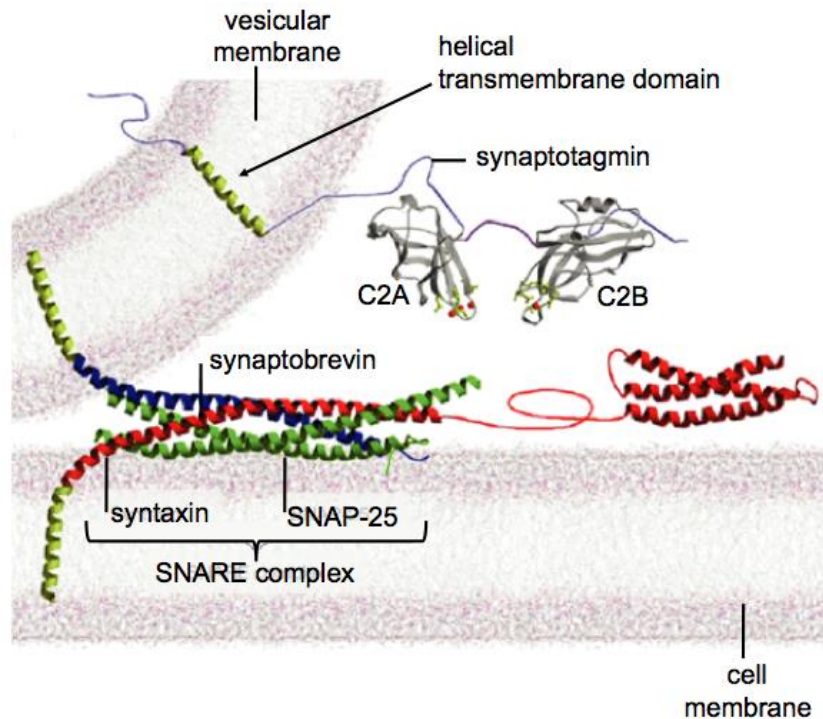


Fig. 6: SNARE proteins involved in vesicle fusion with the plasma membrane

Synaptic vesicles fuse with the cell membrane via the SNARE proteins synaptobrevin / Vamp2, syntaxin, and Snap25 (SNAP-25). Synaptotagmin is associated with the vesicular membrane via its helical transmembrane domain. When the intracellular Ca^{2+} concentration rises due to an incoming action potential, Ca^{2+} binds to the C2 domains of synaptotagmin, causing conformational changes that lead to partial insertion of synaptotagmin into the plasma membrane, and the SNARE complex promotes fusion of the vesicle and plasma membranes, causing vesicle cargo to be released into the extracellular space. Modified image from Chapman (2002).

Some of these fusion-related proteins also exist in astrocytes. Astrocytes express not only Vamp2 (and Vamp3 or cellubrevin), but also syntaxin isoforms 1, 2, 3, and 4 (Bal-Price et al., 2002; Jefinija et al., 1997; Paco et al., 2009; Tao-Cheng et al., 2015), Snap23, and Syt isoforms 4, 7, and 11 – thus, astrocytes may release gliotransmitters via exocytotic vesicles in a similar manner to neurones (Hamilton and Attwell, 2010; Volkhardt, 2002).

The majority of studies reporting the presence of SNARE proteins in astrocytes have used cultured astrocytes (Montana et al., 2006), and reports have been conflicting (e.g. Syt1 and the pre-synaptic vesicle protein synaptophysin (Syp) were both detected in astrocytes by immunostainings (Maienschein et al., 1999), but were not found in subsequent studies (Fiacco et al., 2009)). The presence of only few SNAREs, e.g. Vamp2 (Zhang et al., 2004b) and Vamp3 (Bezzi et al., 2004; Wilhelm et al., 2004), were confirmed by experiments in slices or *in vivo*.

Functional studies illustrate that vesicle-dependent exocytotic release from astrocytes likely involves several SNARE proteins (Jeftinija et al., 1997; Parpura et al., 1995; Verderio et al., 1999). For instance, cleaving syntaxin1 with botulinum toxin C leads to reduced glutamate baseline and evoked glutamate release (Bal-Price et al., 2002; Jeftinija et al., 1997). The release of another gliotransmitter, D-serine, is strongly reduced when blocking Vamp2 and 3 function by tetanus toxin (Mothet et al., 2005).

Moreover, overexpressing a dominant-negative domain of vesicular SNARE (dnSNARE) showed that inhibiting SNARE complex formation also decreases astrocytic glutamate release in astrocytes of the transgenic dnSNARE mouse model (Pascual et al., 2005; Zhang et al., 2004b). In dnSNARE mice, astrocyte-derived adenosine (hydrolysed from ATP) was identified as a key gliotransmitter for regulating neuronal circuits (Fellin et al., 2009).

The majority of evidence to date suggests that astrocytes most likely do express SNARE proteins, but how these proteins co-operate to potentially regulate fusion, and which vesicles they localise to is less well understood, possibly because of variable results from cell culture and *in situ* studies (Montana et al., 2006; Schubert et al., 2011). Interestingly, astrocytes express several Syt isoforms (in cultures, slices, and *in vivo*), suggesting that they may regulate exocytosis of gliotransmitters or other substances.

2.6.2 Synaptotagmins in astrocytes

The Syt isoforms are central mediators of vesicular exocytosis, of which Syt1, 4, and 7 are evolutionarily conserved (Andrews and Chakrabarti, 2005). All Syt isoforms contain C2 domains, and with the exception of Syt17, all Syts have a helical transmembrane domain by which they are incorporated into membranes (Fig. 7).

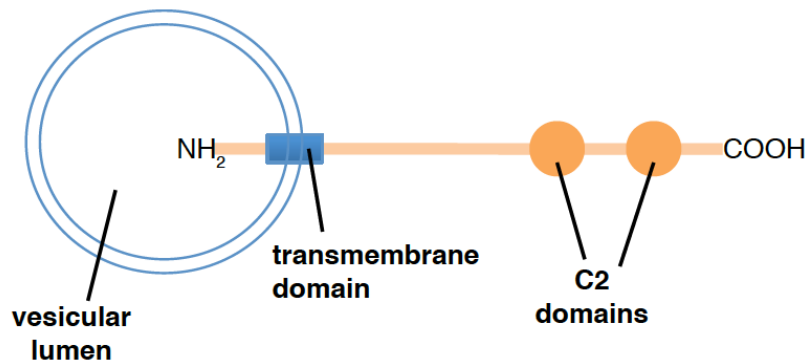


Fig. 7: Simplified Syt structure

Syts contain Ca²⁺-binding C2 domains, which in some Syts (e.g. 1, 2, 3, 4, 6, 7, 9, and 10) allow Ca²⁺-sensing. Syts are incorporated into membranes via a helical transmembrane domain (except for Syt17, which lacks this domain), thus exposing their N terminus to the lumen of vesicles.

Regulated synaptic vesicle exocytosis in neurones occurs in response to local Ca²⁺ rises, which are detected by the Ca²⁺ sensor Syt1. *In vitro* fusion assays revealed that only some Syts trigger Ca²⁺-dependent vesicle fusion (e.g. Syt1 and 7) while others (e.g. Syt4, 8, 11, and 12) act as inhibitors of vesicle fusion (Bhalla et al., 2008; Dean et al., 2009; Potokar et al., 2008).

In astrocytes, which feature large intracellular Ca²⁺ fluctuations, vesicle fusion may also be regulated by Ca²⁺-sensing via Syts. Although astrocytes do not express Syt1, there are other candidates: Astrocytes express the mRNA of Syt4, 7, and 11 (and low levels of Syt5 mRNA) *in vivo* (Cahoy et al., 2008; Mittelsteadt et al., 2009). Syt isoform proteins were further detected in astrocytes, including Syt4 (Malarkey and Parpura, 2011) and Syt17 (Camin Dean, unpublished data). The 17 known mammalian Syt isoforms are structurally and functionally distinct (Bhalla et al., 2008; Hui et al., 2005), which favours the idea that Syts may affect several different intracellular membrane trafficking pathways and thus localise to different vesicle subtypes (Schiavo et al., 1998; Südhof, 2002).

Syt4 was reported to mediate astrocytic glutamate release, since Syt4 knockdown experiments in astrocytes led to less Ca²⁺-dependent glutamate release from astrocytes (Zhang

et al., 2004a). *Syt4*^{-/-} mice exhibit altered hippocampal function and memory deficits (Ferguson et al., 2004a, 2004b), implying that Ca²⁺-dependent glutamate release by astrocytes may contribute to learning and memory.

Syt7 shows the highest Ca²⁺-binding affinity of the Syt isoforms (Hui et al., 2005). Syt7 is mostly associated with lysosomes in cultured neurones, fibroblasts, and macrophages (Arantes and Andrews, 2006; Flannery et al., 2010; Martinez et al., 2000). In neuroendocrine cells, Syt7 was found on large dense-core vesicles / secretory granules, where it mediates Ca²⁺-dependent exocytosis of these vesicles (Fukuda et al., 2004; Wang et al., 2005), although a later study reported that Syt7 is on endosomal but not large dense-core vesicles of endocrine and neuroendocrine cells (Monterrat et al., 2007). Revealing yet another potential site of action, Syt7 was recently reported to mediate synaptic vesicle replenishment in neurones (Liu et al., 2014).

Compared with Syt4 and 7, much less is known about Syt11 and 17. In macrophages, Syt11 acts as a negative regulator of tumor necrosis factor and interleukin-6 secretion, and associates with recycling endosomes, lysosomes, and even phagosomes (Arango Duque et al., 2013). Since Syt17 lacks a transmembrane domain, it is not always considered a “true” Syt, although Syt17 contains C2 domains and is vesicle-associated (Takamori et al., 2006). Syt17 is also referred to as B/K protein, and was detected within membranes of the trans-Golgi network, which is the cell’s centre for lysosomal and secretory vesicle assembly (Fukuda and Mikoshiba, 2001a).

Only little is known about astrocytic Syt isoforms, and the vesicles they are associated with, and how and if they are relevant for vesicle recycling is unknown. Unlike other vesicle-associated proteins, whose presence in astrocytes *in vivo* is under debate, Syt mRNA was clearly linked to astrocytes, suggesting that some Syts are involved in astrocytic vesicle trafficking and / or fusion.

2.7 Aim of the project

Astrocytes represent the glial cell type with the most diverse functions, many of which require that astrocytes release molecules like gliotransmitters (to mediate synaptic signalling and plasticity) or synaptogenic factors (to shape developmental processes). Astrocyte dysfunction underlies many common neurodevelopmental disorders, e.g. epilepsy and Down's syndrome. In both health and disease, astrocytes are closely connected to neurones by structure and function, and astrocytes and neurones communicate reciprocally, e.g. at tripartite synapses.

To ensure normal brain function, astrocytes employ many different release mechanisms, with evidence for non-vesicular (through channels and transporters) and vesicular release (through lysosomes, dense-core vesicles, or small synaptic-like microvesicles). Astrocytes contain vesicular organelles that correspond to all exocytotic vesicle types by size, express several vesicle-associated proteins implicated in vesicle fusion, and release gliotransmitters in a Ca^{2+} - and SNARE protein-dependent manner (Montana et al., 2006). Nonetheless, regulated vesicular exocytosis in astrocytes is under debate (Fiacco et al., 2009; Martineau, 2013; Sloan and Barres, 2014b; Vardjan and Zorec, 2015), in part because much of the evidence for this mechanism comes from cell culture studies of polygonal, reactive astrocytes.

The purpose of this project was to analyse candidate molecules involved in astrocytic vesicle fusion (i.e. Vamp2 and different Syt isoforms), their role in vesicle recycling, and effects of specific glial compounds released at synaptic interfaces. Thus, we aimed to contribute to a better understanding of molecular mechanisms of astrocytic release, and their role in synaptic function. To analyse the presence of candidate vesicle-associated proteins involved in astrocytic vesicle fusion, we developed a simple protocol for growing stellate, more “*in vivo*-like” astrocyte monocultures. Further, distinct types of astrocytic Ca^{2+} events (as required for regulated vesicular release) were observed in different subcellular domains in these stellate cultured astrocytes, as observed in brain slices and *in vivo* (Shigetomi et al., 2013a; Srinivasan et al., 2015).

3. Materials and Methods

3.1 Materials

All chemicals were from Carl Roth (Germany) unless otherwise indicated.

3.1.1 Antibodies

3.1.1.1 Antibodies for immunopanning astrocytes

The following primary antibodies were used for the immunopanning protocol:

anti-mouse CD45 (BD Biosciences Pharmingen, 550539)

anti-O4 (Millipore, MAB345)

anti-human integrin beta 5 (eBioscience, 14-0497-82)

The following secondary antibodies were used for the immunopanning protocol:

goat anti-mouse IgG+IgM (H+L) (Jackson ImmunoResearch, 115-005-044)

goat anti-mouse IgM μ -chain specific (Jackson ImmunoResearch, 115-005-020)

goat anti-rat IgG H+L (Jackson ImmunoResearch, 112-005-167)

3.1.1.2 Antibodies for immunostainings

The following primary antibodies were used for immunocytochemistry and immunohistochemistry:

mouse anti-ALDH1L1 (NeuroMab, cat. no.: 75164)

rabbit anti-EEA1, diluted 1:500 (Synaptic Systems, cat. no.: 237002)

guinea pig anti-GFAP, diluted 1:1000 (Synaptic Systems, cat. no.: 173005)

mouse anti-GFP, diluted 1:2000 (Abcam, cat. no.: ab1218)

rabbit anti-GFP, diluted 1:2000 (Abcam, cat. no.: ab290)

chick anti-GFP, diluted 1:2000 (Abcam, cat. no.: ab13970)

goat anti-Hevin, diluted 1:1000 (R&D Systems, cat. no.: AF2836)

chick anti-Map2, diluted 1:5000 (Biosensis, cat. no.: C-1382-50)

rabbit anti-Rab7, diluted 1:500 (Abcam, cat. no.: ab74906)

guinea pig anti-synaptophysin, diluted 1:1000 (Synaptic Systems, cat. no.: 101004)
mouse anti-Syt1, diluted 1:2000 (Synaptic Systems, cat. no.: 105101)
guinea pig anti-Syt1, diluted 1:2000 (Synaptic Systems, cat. no.: 105105)
rabbit anti-Syt4, diluted 1:500 (Synaptic Systems, cat. no.: 105043)
mouse anti-Syt7, diluted 1:500 (NeuroMab, cat. no.: 75-265)
rabbit anti-Syt7, diluted 1:200 (Synaptic Systems, cat. no.: 105173)
mouse Syt11, diluted 1:500 (Abnova, cat. no.: h00023208-m03)
rabbit anti-Syt17, diluted 1:2000 (Abcam, cat. no.: ab76274)
mouse anti- β III-tubulin, diluted 1:100 (Abcam, cat. no.: ab78078)
rabbit anti-Vamp2, diluted 1:1000 (Synaptic Systems, cat. no.: 104202)
guinea pig anti-Vamp2, diluted 1:500 (Synaptic Systems, cat. no.: 104204)

The following secondary antibodies were used for immunocytochemistry and immunohistochemistry:

donkey anti-goat Alexa488, diluted 1:1000 (Invitrogen, cat. no.: A-11055)
donkey anti-mouse Alexa488, diluted 1:1000 (Invitrogen, cat. no.: A-21202)
goat anti-rabbit Alexa488, diluted 1:1000 (Invitrogen, cat. no.: A-11008)

goat anti-guinea pig Alexa546, diluted 1:2000 (Invitrogen, cat. no.: A-11074)
goat anti-rabbit Alexa546, diluted 1:2000 (Invitrogen, cat. no.: A-11010)

goat anti-guinea pig Alexa647, diluted 1:1000 (Invitrogen, cat. no.: A-21450)
donkey anti-mouse Alexa647, diluted 1:1000 (Invitrogen, cat. no.: A-31571)

3.1.1.3 Antibodies for immunoblotting

The following primary antibodies were used:

mouse anti-Aldh1L1, diluted 1:500 (NeuroMab, cat. no.: 75140)
mouse anti-Cd11b, diluted 1:200 (Abcam, cat. no.: ab8879)
mouse anti-GAPDH, diluted 1:1000 (Enzo Life Sciences, cat. no.: 11101127)
guinea pig anti-GFAP, diluted 1:1000 (Synaptic Systems, cat. no.: 173005)
goat anti-glypican6, diluted 1:2000 (R&D Systems, cat. no.: AF1053)
goat anti-Hevin, diluted 1:2000 (R&D Systems, cat. no.: AF2836)
chick anti-Mbp, diluted 1:2000 (Abcam, cat. no.: ab106583)
mouse anti-Nestin, diluted 1:1000 (Synaptic Systems, cat. no.: 312011)
mouse anti-Rab3a, diluted 1:2000 (Synaptic Systems, cat. no.: 107111)
mouse anti-S100 β , diluted 1:200 (Abcam, cat. no.: ab4066)
mouse anti-Snap25, diluted 1:1000 (Synaptic Systems, cat. no.: 111011)
mouse anti-synaptophysin, diluted 1:2000 (Millipore, cat. no.: mab368)
mouse anti-Syt1, diluted 1:2000 (Synaptic Systems, cat. no.: 105101)
mouse anti-Syt3, diluted 1:1000 (NeuroMab, cat. no.: 75-269)
rabbit anti-Syt4, diluted 1:1000 (Synaptic Systems, cat. no.: 105043)
rabbit anti-Syt5, diluted 1:500 (Synaptic Systems, cat. no.: 105053)
rabbit anti-Syt7, diluted 1:1000 (Synaptic Systems, cat. no.: 105173)
mouse anti-Syt11, diluted 1:500 (Abnova, cat. no.: h00023208-m03)
rabbit anti-Syt17, diluted 1:1000 (Abcam, cat. no.: ab76274)
mouse anti-syntaxin1, diluted 1:2000 (Synaptic Systems, cat. no.: 110011)
goat anti-thrombospondin1, diluted 1:400 (R&D Systems, cat. no.: AF3074)
guinea pig anti-Vamp2, diluted 1:2000 (Synaptic Systems, cat. no.: 104204)
rabbit anti-Vamp4, diluted 1:100 (Synaptic Systems, cat. no.: 136002)
rabbit anti-vGluT1, diluted 1:1000 (Synaptic Systems, cat. no.: 135303)
guinea pig anti-vGluT2, diluted 1:1000 (Synaptic Systems, cat. no.: 135404)
rabbit anti-vGluT3, diluted 1:2000 (Synaptic Systems, cat. no.: 135203)
rabbit anti-Vimentin, diluted 1:1000 (Synaptic Systems, cat. no.: 172002)

The following secondary antibodies were used:

HRP-coupled monoclonal mouse antibody, diluted 1:2000 (Bio-Rad, cat. no.: 1706516)

HRP-coupled rabbit polyclonal antibody, diluted 1:2000 (Bio-Rad, cat. no.: 1706515)

HRP-coupled guinea pig polyclonal antibody, diluted 1:5000 (Abcam, cat. no.: ab97155)

HRP-coupled goat polyclonal antibody, diluted 1:5000 (Abcam, cat. no.: ab6741)

3.1.2 Animals

All animals used for experiments in this dissertation were bred and kept in the mouse facility of the European Neuroscience Institute or the animal facility of the University Medical Center in Göttingen, Germany. All experiments were performed in accordance with the guidelines for German animal welfare. All animals were euthanised by CO₂.

3.1.2.1 Mouse lines

Wild-type C57B6/J mice were used for histological analysis and brain lysate preparation for immunoblots, while *Syt7*^{+/+} or *Syt7*^{-/-} mice were used for tissue culture preparations.

3.1.2.2 Mouse tail biopsy and PCR

Mouse tail biopsies were prepared by digesting tails with 7 µl 10 mg/ml proteinase K in 500 µl lysis buffer (100 mM Tris-HCl (pH 8.5), 5 mM EDTA (pH 8.0), 0.2% SDS, 200 mM NaCl) while shaking for 6 hrs or overnight at 55 °C. Subsequently, samples were centrifuged in tabletop centrifuges at maximum speed for 10 min. For each sample, the resulting supernatant was transferred to a fresh eppendorf tube and precipitated with 500 µl isopropanol and mixed well. Samples were then centrifuged again at maximum speed for 10 min, after which the supernatants were removed and 200 µl 70% ethanol were used to wash each pellet by centrifuging for another 10 min at maximum speed. Next, the ethanol was removed and the pellets dried for subsequent resuspension in 100 µl ddH₂O.

For each sample, 2 µl DNA were transferred to fresh PCR tubes, and mixed with 48 µl of the following PCR mix:

for one PCR sample:

5	µl	10 X buffer
0.4	µl	25 mM dNTPs
1	µl	10 µM forward primer
1	µl	10 µM reverse primer
0.25	µl	Taq DNA polymerase
40.25	µl	<u>ddH₂O</u>
48	µl	total / reaction (+ 2 µl DNA)

Samples were then placed in thermocyclers for the PCR to amplify specific DNA segments (Mullis et al., 1986; Saiki et al., 1988).

To separate the PCR products, 2% (w/v) agarose gels in 1X TAE buffer (including SYBR® Safe DNA Gel Stain, ThermoFisher Scientific) were loaded with PCR samples and 100 bp DNA ladder (ThermoFisher Scientific, Germany) in a separate lane. DNA bands were separated by horizontal gel electrophoresis at 75 V for 1 h. To document genotyping results, pictures were obtained using a UV illuminator with the INTAS imaging system.

3.2 Methods

3.2.1 Cell culture

The following types of cortical cultures were prepared: Co-cultures of neurones and glia, astroglial-enriched cultures using the MD method (McCarthy and de Vellis, 1980), the NB+H protocol explained below, or immunopanning (IP) astrocytes (Foo, 2013b; Foo et al., 2011).

3.2.1.1 Preparing cultures from E19 rat cortices

Co-cultures, MD, and NB+H (but not IP) astrocytes were prepared from E19 Wistar rat pups by standard cell culture preparations (Dichter, 1978; McCarthy and de Vellis, 1980) with minor modifications. Pregnant rats were euthanised by CO₂ so that rat pups could be removed from the uterus. The embryonic sacs were opened, the pup heads cut off with scissors, and the heads were placed in 4 °C cold dissection medium (10 mM HEPES (Gibco, cat. no.: 15630080) in Hank's Balanced Salt Solution (Gibco, cat. no.: 14170112)). Next, brains were isolated, their meninges removed, and the cortices isolated, cut into small pieces and collected in a tube filled with 4 °C cold dissection medium. Cortex pieces were incubated in 0.25 % trypsin-EDTA (Gibco, cat. no.: 25200056) in a 37 °C waterbath. After 20 min, trypsin-EDTA was removed and the tissue was washed in 4 °C dissection medium three times. After the last washing step the tissue was triturated by pipetting up and down in 1 ml NB+ (2% B27 supplement (Gibco, cat. no.: 17504044), 2 mM Glutamax (Gibco, cat. no.: 35050061), 5000 U/ml penicillin and 5000 µg/ml streptomycin (Gibco, cat. no.: 15070063) in Neurobasal medium (Gibco, cat. no.: 21103049)). The cell suspension was then filtered through a 100 µm nylon cell strainer (BD Biosciences, cat. no.: 352360), pre-wet with 4.5 ml NB+. Next, another 4.5 ml NB+ were added to wash out cells stuck to the cell strainer. Using the Trypan Blue (Sigma, cat. no.: T8154) exclusion technique, cells were counted and plated on cell culture dishes pre-equilibrated with medium in a Hera Cell 240i cell culture incubator (Thermo Scientific) at 37 °C and 5% CO₂.

3.2.1.2 Co-cultures of neurones and glia

Co-cultures were plated at a density of 50,000 cells / well on 12 mm glass coverslips pre-equilibrated with NB+ in the incubator (or 2×10^6 cells/dish for generating samples for Western blots). All glass coverslips and 10 cm dishes were coated with 0.04% PEI in ddH₂O for 24 hrs, then washed twice with ddH₂O prior to adding medium / cells. Cell cultures were then maintained in the incubator.

In addition to E19-derived rat co-cultures, P0-derived mouse co-cultures were also prepared from C57B6/J wild-type (Wt) or *Syt7*^{-/-} mice: For Fig. 22, Wt rat neurones were plated onto day *in vitro* (DIV) 7 mouse *Syt7*^{-/-} astrocytes (generated using the MD method described below). To control for this difference in species (which may otherwise contribute to the effect we saw), we also prepared rat neurones plated onto DIV7 Wt mouse astrocytes. However, co-cultures of mouse neurones plated onto DIV7 mouse astrocytes would serve validate our findings.

3.2.1.3 MD and NB+H astrocyte monocultures

For MD and NB+H astrocyte monocultures, cells were plated in DMEM+ (10% FCS (Invitrogen, cat. no.: 10500064), 5000 U/ml penicillin, 5000 µg/ml streptomycin in DMEM (Gibco, cat. no.: 41966029)). These cultures were exclusively plated at a density of 500,000 cells / 10 cm dish, and passaged on day *in vitro* (DIV) 7.

On DIV7, 10 cm dishes were placed on a shaker (Heidolph Rotamax 120) within the incubator and shaken at 110 rpm for 6 hrs. After shaking, the medium (including loosened neurones and non-astrocytic glia) was exchanged with pre-heated 1X PBS, which was then replaced by 37 °C warm 0.25% trypsin-EDTA. Astrocytes were then incubated in the incubator in trypsin for 5 min. Next, 5 ml DMEM+ were added to inactivate the trypsin. Cells were loosened by forcefully pipetting them off the dish and transferred to a 50 ml Falcon tube. Cell suspensions were then centrifuged in an eppendorf centrifuge 5810 R at 4,000 rpm (3,220 x g) for 4 min at 20 °C. The supernatant was then removed and the pellet was re-suspended in 10 ml DMEM+ for MD astrocytes, or NB+ containing 5 ng/ml heparin-binding epidermal growth factor (HBEGF; Sigma, cat. no.: 4643) for NB+H astrocytes. Cells were plated at a density of 5,000 cells / well on 12 mm glass coverslips (PEI-coated as described above for plating co-cultures). Astroglial-enriched cultures were then maintained in the incubator, and half the medium was exchanged once a week.

3.2.1.4 Immunopanning astrocytes

Astrocyte monocultures were also generated by immunopanning (IP) (Foo et al., 2011). We prepared cultures according to the recently published protocol with minor modifications (Foo, 2013b).

Required compounds:

Griffonia simplicifolia lectin BSL-1 (Vector Labs, cat. no.: L-1100); 20 mg/ml in 1X PBS

0.4% DNase, 12,500 units/ml (Worthington, cat. no.: LS002007)

1X Earle's Balanced Salt Solution (Sigma, cat. no.: E6267)

50 mM Tris-HCl pH 9.5, sterilised

Dulbecco's Modified Eagle Medium (DMEM, Gibco, cat. no.: 41966029)

fetal calf serum (FCS, Gibco, cat. no.: 10437-028)

heparin-binding epidermal growth factor (HBEGF, Sigma, cat. no.: 4643)

L-cysteine hydrochloride monohydrate (Sigma, cat. no.: C7880)

Neurobasal medium (Gibco, cat. no.: 21103-049)

papain (Worthington, cat. no.: LS 03126)

penicillin/streptomycin (Gibco, cat. no.: 15070063)

trypsin 30,000 units/ml stock (Sigma, cat. no.: T9935)

D(+)-glucose,

1X dPBS

EDTA

NaHCO₃

BSA (Sigma, cat. no.: A8806)

trypsin inhibitor (Worthington, cat. no.: LS003086)

transferrin (Sigma, cat. no.: T-1147)

putrescine (Sigma, cat. no.: P5780)

progesterone (Sigma, cat. no.: P8783)

sodium selenite (Sigma, cat. no.: S5261)

sodium pyruvate

L-glutamine

N-acetyl cysteine (Sigma, cat. no.: A8199)

The following solutions were prepared before immunopanning:

Enzyme stock solution (200 ml)

10X EBSS (E7510)	20 ml	(final conc. 1X)
30% D(+)-glucose	2.4 ml	(final conc. 0.46%)
1 M NaHCO ₃	5.2 ml	(final conc. 26 mM)
50 mM EDTA	2 ml	(final conc. 0.5 mM)
<u>ddH₂O</u>	<u>170.4 ml</u>	

brought to 200 ml with ddH₂O and filtered through 0.22 µm filter; stored at 4 °C in cell culture room

Inhibitor stock solution (500 ml)

10X EBSS (E7510)	50 ml	(final conc. 1X)
30% D(+)-glucose	6 ml	(final conc. 0.46%)
1 M NaHCO ₃	13 ml	(final conc. 26 mM)
<u>ddH₂O</u>	<u>431 ml</u>	

brought to 500 ml with ddH₂O and filtered through 0.22 µm filter; kept at 4 °C in cell culture room

10X low Ovomuroid (200 ml)

dPBS	150ml
BSA	3g
<u>trypsin inhibitor</u>	<u>3g</u>

pH 7.4; brought to 200 ml with dPBS and filtered; stored aliquots at -20 °C

10X high Ovomuroid (200 ml)

dPBS	150ml
BSA	6g
<u>trypsin inhibitor</u>	<u>6g</u>

pH 7.4; brought to 200 ml with dPBS and filtered; stored aliquots at -20 °C

100X Sato (50 ml)

Neurobasal	50 ml	
transferrin	500 mg	(final conc. 100 µg/ml)
BSA	500 mg	(final conc. 100 µg/ml)
putrescine	80 mg	(final conc. 16 µg/ml)
progesterone	12.5 µl of 2.5 mg/100 µl EtOH stock	(final conc. 60 ng/ml; 0.2 µM)
<u>sodium selenite</u>	<u>500 µl of 4 mg+10 µl 1 N NaOH in 10 ml Neurobasal</u>	<u>(final conc. 40ng/ml)</u>

filtered through pre-rinsed 0.22 µm filters; stored aliquots at -20 °C

IP astrocyte base medium (300 ml)

50% Neurobasal	145.5 ml
50% DMEM	145.5 ml
100 U penicillin; 100 µg/ml streptomycin	6 ml P/S stock
1 mM sodium pyruvate	- (already included in medium)
292 µg/ml L-glutamine	- (already included in medium)
1X SATO	3 ml 100X stock
5 µg/ml N-acetylcysteine	1.5 mg

30% FCS in 50/50 mixture of DMEM and Neurobasal

30% fetal calf serum in 50% DMEM/ 50% Neurobasal; filtered through 0.22 µm filter

Protocol

IP dishes were prepared by coating six 15 cm Petri dishes with 25 ml 50 mM Tris-HCl (pH 9.5) per dish and the following secondary antibodies (listed in 3.1.1.3) overnight at 4 °C:

1x secondary only plate:	60 µl anti-mouse IgG+IgM (H+L)
1x BSL1 plate:	20 µl BSL-1
1x CD45:	60 µl anti-rat IgG
2x O4 plate:	60 µl anti-mouse IgM µ-chain specific
1x ITGB5 plate:	60 µl anti-mouse IgG+IgM (H+L)

The following day, 22 ml enzyme stock solution were added to a 50 ml Falcon tube and bubbled with CO₂ until the solution turned from red to orange. The enzyme stock solution was then kept in the waterbath set to 34 °C. Similarly, 2 x 21 ml and 1 x 10ml inhibitor stock solutions were bubbled but then kept at room temperature. 1.5 ml 10X low Ovo and 100 µl 0.4% DNase were added to each of the two 21 ml aliquots of bubbled inhibitor stock (low Ovo), while 2 ml 10X high Ovo and 20 µl 0.4% DNase were added to the 10 ml aliquot of bubbled inhibitor stock solution (high Ovo). Further, 70 ml 0.2% and 40 ml 0.02% BSA were prepared in 1X dPBS and kept at 4 °C.

Except for the BSL-1 plate, each panning dish was washed with 1X PBS three times, after which 12 ml 0.2% BSA were added together with the following primary antibodies (listed in 3.1.1.3) or compounds:

1x secondary only plate:	(only 0.2% BSA)
1x BSL1 plate:	(leave unwashed and uncoated)
1x CD45:	20 μ l anti-CD45 antibodies
2x O4 plate:	20 μ l anti-O4 antibodies
1x ITGB5 plate:	20 μ l anti-Itgb5 antibodies

Plates were incubated in primary antibody for ≥ 2 hours at room temperature before use.

Dissection

P7 rat pups were sacrificed by decapitation with scissors, and brains were isolated and further dissected in 4 °C cold 1X dPBS under a light microscope in a semi-sterile dissection hood. Meninges and all tissue apart from the cerebral cortex were swiftly removed. 20 minutes before the end of dissection, 100 units papain (81.32 μ l) and 3.6-4.2 mg L-cysteine were mixed in 34 °C warm enzyme stock solution. Cortices were transferred into small drops of 4 °C 1X dPBS and cut into ≈ 1 mm³ pieces with a No. 10 scalpel blade.

Dissociation

20 ml enzyme solution (including papain and L-cysteine) were filtered through a 0.22 μ m filter (Millipore, cat. no.: SLGV013SL) and added to the brain pieces alongside 100 μ l 0.4% DNase. Brain pieces in enzyme solution were bubbled with CO₂ for 40 min on a 34 °C heat block (and shaken every 10 minutes). Next, digested brain pieces were collected in a Falcon tube and washed five times with 4.5 ml low Ovo solution. After the last wash, 4 ml low Ovo solution were added, and the brain pieces were triturated by pipetting. At the top of the suspension, single cells accumulated (vs. small and larger brain pieces sinking to the bottom) and were removed using a 1 ml pipette, and added to a separate Falcon tube with 4 ml low Ovo solution. In between, trituration steps were repeated (including the addition of 4.5 ml low Ovo solution) until the majority of brain pieces were gone.

Next, 12 ml high Ovo solution were carefully layered beneath the single cell suspension. The Falcon tube with the cell suspension / high Ovo solution biphasic mix was then centrifuged at 110 x g for 5 min at 4 °C to ensure complete inhibition of papain. The supernatant was then discarded and the cell pellet was resuspended in 9 ml 4 °C cold 0.02%

BSA. The solution was then filtered into a 50 ml Falcon tube through an autoclaved 30 μm^2 Nitex mesh to remove remaining chunks of tissue, after which the filter was washed with 3 ml 4 °C cold 0.02% BSA. The Falcon tube with the cells was then left in the waterbath at 37 °C for 30-45 min to allow antigens to return to the cell surface.

Immunopanning

All following steps were performed at room temperature. Panning dishes were washed with 1X dPBS three times, after which the cell suspension was passed through a series of immunopanning steps:

1. “secondary only” plate (which had not been incubated with any primary antibodies) for 10 min, shaking once at the 5 min time point
2. BSL-1 plate for 10 min, shaking once at the 5 min time point
3. CD45 plate for 20 min, shaking once at the 10 min time point
4. O4 dish #1 for 15 min, shaking once at the 7.5 min time point
5. O4 dish #2 for 15 min, shaking once at the 7.5 min time point
6. Itgb5 dish for 40 min, shaking once at the 20 min time point

Subsequently, the Itgb5 dish was washed with dPBS five times. Next, 200 U trypsin were added to 8 ml pre-equilibrated 1X EBSS and pipetted onto the Itgb5 dish which was then incubated at 37 °C for 3 min. After this, the side of the dish was tapped to dislodge and resuspend cells with 20 ml pre-equilibrated 30% FCS (in 1:1 Neurobasal / DMEM). The cells were then added to a fresh Falcon tube, to which 200 μl DNase were added; the Falcon tube was then centrifuged at 170 x g at 4 °C for 11 min. Next, the supernatant was discarded and the cell pellet was resuspended in 0.02% BSA. Cells were counted by the Trypan Blue exclusion method, and plated at a density of 30,000 cells / well on 12 mm PEI-coated coverslips in pre-equilibrated IP astrocyte medium (IPm; 5 ng / ml HBEGF in 1:1 Neurobasal / DMEM). Cultures were maintained in the incubator, and half the medium was exchanged once a week.

3.2.2 Immunocytochemistry

Immunocytochemistry was performed according to standard protocols (Whitelam, 1995) with minor modifications.

3.2.2.1 Sample preparation

On DIV14, 16, or 21, cell cultures were fixed for 30 min in 4% paraformaldehyde in 0.1 M phosphate buffer, after which samples were washed in 1X PBS for 5 x 3 min. Samples were then stored in 1X PBS at 4 °C or immediately used for immunostaining.

3.2.2.2 Immunostaining of cell cultures

Samples were incubated in buffer D (2% donkey serum, 0.1% Triton-X-100, and 0.05% NaN₃ in 2X PBS) for 30 min, and subsequently incubated with primary antibodies (diluted in buffer D) at 4 °C overnight.

The following day, samples were washed in 1X PBS for 5 x 3 min, after which secondary antibodies (diluted in buffer D) were added and incubated at room temperature in the dark for 2 hrs. In some cases, fluorescent staining reagents targeting F-actin (phalloidin Atto390 (Sigma, cat. no.: 50556) or phalloidin AlexaFluor647 (Invitrogen, cat. no.: A-12379)) were added to label the cytoskeleton during the last 30 minutes of incubation with secondary antibodies. After secondary antibody incubation, samples were washed in 1X PBS for 5 x 3 min. Next, the coverslips were mounted in Fluoromount mounting reagent (Diagnostic BioSystems, cat. no.: K048) on glass slides. In some cases, 10 μM DAPI (Invitrogen, cat. no.: D1306) was added to the mounting reagent. After mounting, the edges of coverslips were sealed with transparent nail polish. Samples were stored at 4 °C in the dark.

3.2.2.3 Fluorescein In Situ Apoptosis Detection

For the apoptosis test comparing IP and NB+H astrocytes grown in HBEGF-containing with HBEGF-free media, the ApopTag® Fluorescein In Situ Apoptosis Detection Kit (Millipore, cat. no.: S7110) was used according to the manufacturer's recommendations.

3.2.3 Histological analysis

3.2.3.1 Transcardial mouse perfusion

Several preparations were made in advance: 4% paraformaldehyde and 1X PBS were kept on ice and hypodermic needles (Sterican / B. Braun) were set aside for pinning down mice. The pumping speed of the Masterflex C/L PWR pump (Cole Palmer) was tested and adjusted using water. The butterfly venipuncture set (B. Braun, cat. no.: 4056388) was set up with its tubing in a dH₂O-filled beaker, while the tubing of the butterfly needle was placed into a Falcon tube containing 1X PBS on ice.

Adult C57B/6J mice were anaesthetised by CO₂. After testing if mice were fully unconscious (e.g. by pinching the paw), they were swiftly pinned down on a styropor block. The chest and abdomen were sprayed with ethanol and opened with scissors just beneath the skin. Next, the ribcage was opened and the butterfly needle was inserted into the left ventricle of the heart, while a small incision was made on the right atrium, causing PBS to rinse the bloodstream. After all blood was rinsed out, the tubing connected to the butterfly needle was moved from the Falcon tube containing PBS and placed in the paraformaldehyde-containing Falcon tube on ice, so that the mouse tissue was fixed as paraformaldehyde was pumped through the blood vessels.

Once mice were fully perfused with paraformaldehyde, the pump was stopped to allow for tissue dissection.

3.2.3.2 Sample preparation

Immediately after transcardial perfusion, mouse heads were cut off using scissors, sprayed with ethanol, and the brains were removed and transferred to 4% paraformaldehyde in fresh Falcon tubes for overnight storage.

The following day, brains were washed in 1X PBS 2 x 2 hrs, after which brains were moved to Falcon tubes containing 30% sucrose solution and kept at room temperature overnight. By the next day, brains had sunk down to the bottom of the tube, at which point they were frozen in cryomolds containing Tissue Tek O.C.T. compound on dry ice. Frozen brains were then loaded onto the Leica CM1850UV cryostat to cut cryosections, which were collected in ethylene glycol and stored at 4 °C overnight.

3.2.3.3 Immunostaining of cryosections

Cryosections were washed with 1X PBS for 3 x 20 min; all washing steps were performed on a horizontal shaker. Cryosections were then incubated in buffer D for 2 hrs at room temperature. Next, the samples were incubated in primary antibodies for 24 hrs at 4 °C on a horizontal shaker, after which samples were washed for 3 x 20 min with 1X PBS. Following this, secondary antibodies were applied at 4 °C overnight, and afterwards, samples were washed with 1X PBS for 3 x 20 min. After the last washing step, 1 ml 1X PBS was pipetted onto a glass slide, into which a single cryosection was placed using a brush. Excess PBS was removed using a 100 µl pipette and kimwipes, after which 10 µl Fluoromount mounting reagent was added onto the cryosection. A 25 mm coverslip was carefully placed on top of the sample, and after the mounting reagent had dried, the coverslips were sealed with nail polish.

3.2.4 Immunoblotting

Immunoblotting was performed according to standard protocols (LaRoche, 2009), with minor modifications.

3.2.4.1 Sample preparation of cell cultures

DIV9, 14, and 21 cultures were washed with 1X PBS, which was then replaced by 500 µl fresh 1X PBS. Using a cell scraper (CytoOne, cat. no.: CC76000220), cells were detached from the culture dish, and this cell suspension was transferred into an eppendorf tube. The cell suspension was then triturated five times using a 27 gauge needle (HSW Fine-ject, cat. no.: 4710004020), after which samples were centrifuged at 400 x g in an eppendorf centrifuge 5424 for 10 min at 4 °C. Next, the supernatant was moved to a fresh tube, which was centrifuged as before. After transferring the supernatant to a fresh tube, protein concentration was determined using the BCA protein assay kit (Novagen, cat. no.: 712853) according to the manufacturer's recommendations.

3.2.4.2 Sample preparation of brain lysate

Brain lysate was prepared as a positive control for proteins expressed *in vivo*. Adult C57B/6J mice were euthanised by cervical dislocation. Brains were isolated and transferred to a Petri dish with 4 °C homogenisation buffer (320 mM sucrose, 4 mM HEPES-KOH, pH 7.4) on ice. Next, brains were dissected further and then placed in 1.5 ml eppendorf tubes containing 500 µl homogenisation buffer on ice. Brains were then homogenised using a homogenator rod set to 900 rpm in a laboratory stirrer (VWR VOS 14 S40) in a 4 °C cold room. After this, tubes with homogenised brain lysate were centrifuged at 1,000 x g for 10 min at 4 °C. Supernatant was aliquoted and snap-frozen in liquid nitrogen for storage at -80 °C.

3.2.4.3 Gel electrophoresis

The outer gel running chamber was filled with anode buffer (1 M Tris in dH₂O, adjusted to pH 8.9), and cathode buffer (1 M Tris, 1 M Tricin, 1% SDS in dH₂O) was added to the inner cassette, into which 1.5 mm thick 10% acrylamide running gels (including 5% stacking gels) were placed. After this, 5 µg of each sample were loaded alongside a molecular weight

marker (PageRuler™ prestained protein ladder by Fermentas, cat. no.: SM0671). Gel electrophoresis was started at 60 V, and after 15 min, switched to 100 V for another hour.

3.2.4.4 Immunoblot transfer

After gel electrophoresis, the running gel with the samples was equilibrated in blotting buffer (200 mM glycine, 25 mM Tris, 0.04% SDS, 20% methanol) for 10 min. Fibre pads, nitrocellulose membranes, and filter papers were also equilibrated in blotting buffer. The blotting sandwich in the blot transfer apparatus, was stacked as follows (cathode to anode end): one fibre pad, one filter paper, the gel, one nitrocellulose membrane, one filter paper, one fibre pad. The transfer was started at 100 mA, and run for 1 h.

3.2.4.5 Protein detection

Following the transfer, membranes were blocked in 5% milk in PBS-T (0.05% Tween 20 in 1X PBS) for 1 h, and then incubated in primary antibodies in 5% milk in PBS-T at 4 °C overnight. The next day, membranes were washed in 1X PBS for 5 x 5 min, and then incubated in secondary antibodies in 5% milk in PBS-T at 4 °C overnight. Subsequently, each membrane was washed in 1X PBS for 5 x 5 min, followed by applying ECL solution (1.28% (w/v) Tris-HCl and 0.23% (w/v) luminol Na⁺ salt (Sigma, cat. no.: A4685-1g) in dH₂O (pH 8.6), 0.01% P-coumaric acid (Sigma, cat. no.: 9008-5g) in DMSO, 0.008% H₂O₂) to the membrane for 1 min. Protein detection was achieved using the Fujifilm LAS-3000 imaging system (R&D Systems). Membranes intended for re-probing were washed in 1X PBS for 10 min, followed by a 1 h block in 5% milk in PBS-T.

3.2.5 Electron microscopy

Sample preparation was done with assistance from Torben Ruhwedel (MPI for Experimental Medicine, Göttingen, Germany), and images were acquired by Dr. Wiebke Möbius (MPI for Experimental Medicine, Göttingen, Germany).

3.2.5.1 Sample preparation

Epon embedding

Briefly, 2-week-old cell cultures (co-cultures, MD, IP, and NB+H astrocyte monocultures) were fixed in 1% paraformaldehyde solution for 1 h. Samples were subsequently washed in 1X PBS and then embedded in Epon (Epon embedding steps included osmification, dehydration, and Epon impregnation).

Cutting sections of Epon embedded cultures

Epon embedded cultures were cut on a microtome (Ultracut S, Leica, Germany). Using a diamond knife (Diatome Ultra 45 °), ultra-thin (50 nm) sections were cut and collected on double-sized slot grids (2mm-1mm, AGAR Scientific, UK). Samples were then coated with formvar polyvinyl, and contrasted.

Contrasting ultra-thin sections

Grids with samples were placed upside-down on drops of the following series of solutions:

1. uranyl acetate (covered from light sources) for 30 min
2. ddH₂O for 1 min
3. Reynolds lead citrate for 6 min
4. ddH₂O for 4x 1 min

The grids were then dried with filter paper and stored at room temperature until imaging.

Imaging

Samples were imaged by Dr. Wiebke Möbius, using the Zeiss EM900 (Zeiss, Germany) and a wide-angle dual speed 2K CCD camera (TRS, Germany).

3.2.6 Transfection and antibody internalisation assays

The following plasmid DNA was used for the antibody internalisation assays: pHluorin-Vamp2, pHluorin-Syt7, and pHluorin-Syt17; all constructs contained an ampicillin-resistance gene. The plasmid DNA listed here had previously been tested by overexpression of pHluorin-coupled Syts in HEK cells and subsequent immunostaining, where antibodies recognised overexpressed Syts (Camin Dean, unpublished).

For tetanus toxin (TeNT) experiments, purified TeNT light chain peptides were a gift from Dr. Yongsoo Park and Prof. Reinhard Jahn (Max Planck Institute for Biophysical Chemistry, Göttingen, Germany) TeNT peptides were introduced to cells by transfection, which had previously been successful (Kuo et al., 2010).

3.2.6.1 Plasmid DNA amplification

E. coli strain XL-1 Blue cells (Stratagene, cat. no.: 200249) were thawed on ice. 100 µl of the cells were mixed with 100-500 ng plasmid DNA in a fresh tube and incubated on ice for 15 min. Bacteria were heat-shocked at 42 °C for 1 min, and immediately placed back on ice for 2 min. Next, 900 µl LB medium (Roth, cat. no.: X968.1; prepared according to the manufacturer's recommendations) were added, and then shaken at 800 rpm using an eppendorf thermomixer (for 1.5 ml tubes) at 37 °C for 1 h. Using an ethanol-sprayed, bent glass pipette, 200 µl of the bacterial mix was spread over a 10 cm LB-agar plate (that contained 0.5% yeast extract, 1% tryptone (pH 7), 1% NaCl, and 1.5% agar in LB medium), together with 100 µg/ml ampicillin (Roth, cat. no.: K029.2) or 50 µg/ml kanamycin (Roth, cat. no.: T832.3). Plates were then incubated at 37 °C overnight.

The next day, single isolated bacterial colonies were selected and each was added to an Erlenmeyer flask containing 100 ml pre-warmed LB medium with 50 µg/ml of the respective antibiotic. Flasks were incubated at 300 rpm and 37 °C for 16-24 hrs. After that, bacterial suspensions were centrifuged at 3,220 x g and 20 °C for 15 min. Supernatants were discarded and pellets were resuspended in 1X PBS. This suspension was centrifuged once more, and the supernatant was discarded. The resulting plasmid DNA was purified using the Qiagen Plasmid Maxi kit (Qiagen, cat. no.: 12162) according to the manufacturer's recommendations. DNA concentration was measured using a NanoPhotometer *Implen* (Montreal Biotech Inc.).

3.2.6.2 *Transfecting cultures*

Cell cultures were transfected in 24-well plates, in serum-free media pre-heated to 37 °C. For each coverslip, 1 µl LipofectamineTM 2000 transfection reagent (Invitrogen, cat. no.: 11668027) was added to 50 µl medium in an eppendorf tube and in a separate tube, 0.7 µg plasmid DNA was added to 50 µl medium. Both mixes were incubated at room temperature for 5 min before mixing them. The mix of lipofectamine reagent and DNA was then incubated for 30 min.

For co-cultures, medium was removed and saved, and 400 µl of fresh pre-heated Neurobasal medium was added to each well of the co-cultures. For astrocyte monocultures, medium was discarded, and 400 µl of fresh pre-heated DMEM (without serum) was added per well to the astrocytes. Next, 100 µl of the lipofectamine / DNA mix was added to each well and incubated at 37 °C and 5% CO₂ for 2.5 hrs. Afterwards, medium was removed, and cells were washed once in fresh pre-heated medium. Finally, the saved medium was added back to co-cultures, while astrocyte monocultures received fresh pre-heated medium.

Transfected cells were used for the antibody internalisation assay 2 days after transfection.

3.2.6.3 *Antibody internalisation assays*

Coverslips with cell cultures that had been transfected two days earlier were moved into new 24-well plate wells, in which anti-GFP antibodies (diluted 1:500) were mixed into pre-heated stimulating solution (50 µM glutamate, 10 mM KCl, 135 mM NaCl, 2 mM CaCl₂, 5.5 mM glucose, 2 mM MgCl₂, and 20 mM HEPES) or non-stimulating solution (2 mM KCl, 143 mM NaCl, 2 mM CaCl₂, 5.5 mM glucose, 2 mM MgCl₂, and 20 mM HEPES). Cells were kept in the incubator for 10 min, after which they were moved to new wells containing 4% paraformaldehyde for fixation for 30 min. After this step, samples were treated as described in 3.2.2.2.

3.2.7 Adeno-associated viruses for Ca²⁺ imaging

The vector plasmid pZac2.1 gfaABC1D-Lck-GCaMP3 was a gift from Baljit Khakh (Addgene plasmid # 44330). Adeno-associated viral (AAV) particles of the 1/2 serotype carrying the vector plasmid were provided by Markus Stahlberg (European Neuroscience Institute, Göttingen, Germany).

3.2.7.1 Viral infection

Prior to infection, half the medium of cultures was exchanged with fresh pre-heated medium. Cultures were subsequently infected with 0.3 µl AAV particles / well of a 24-well plate, after which the next half medium exchange was performed 7 days later. Infected cultures were used for live cell Ca²⁺ imaging 10 days after infection.

In contrast to co-cultures and MD and NB+H monocultures, the AAV infection caused IP astrocyte cell health to deteriorate in 50% of the cases, so that several repetitions were necessary.

3.2.7.2 Live cell Ca²⁺ imaging

Coverslips with infected cell cultures were placed in a low profile open bath chamber (Warner Instruments, cat. no.: RC-40LP), and immediately placed on the Zeiss LSM710 confocal microscope for imaging, prior to which the imaging chamber had been filled with pre-heated non-stimulating solution (2 mM KCl, 143 mM NaCl, 2 mM CaCl₂, 5.5 mM glucose, 2 mM MgCl₂, and 20 mM HEPES). Spontaneous Ca²⁺ signalling (as indicated by GCaMP3 signal) was monitored for 200 seconds, and cells were only used during a 30-minute period (some cells become unhealthy after periods of over 45 minutes). Acquisition rate was one image per second.

3.2.8 Microscopy

Fixed samples (of immunocyto- and immunohistochemistry) but also GCaMP3-infected, live cell cultures were imaged using the Zeiss LSM 710 confocal microscope (Zeiss, Germany), equipped with 405, 488, 561, and 633 nm lasers. Images were obtained using Zen Black software. Within the same experiment, image acquisition, settings for light intensity, electron multiplication (EM gain), and exposure time were kept the same.

The following objectives were used for fixed samples:

20X / 0.8 objective (Zeiss, Plan-Apochromat)

40X / 1.3 oil DIC objective (Zeiss, Plan-Apochromat)

63X / 1.4 oil DIC objective (Zeiss, Plan-Apochromat)

For live cell Ca²⁺ imaging, 20X / 1.0 DIC objective (Zeiss, WPlan-Apochromat) was used.

3.2.9 Data analysis

3.2.9.1 Data analysis of immunostainings and immunoblots

Microsoft Excel 2010 software was used for creating bar graphs and statistical tests (for calculating standard error of the mean, p values, Student's t-test). Figures of immunostaining and immunoblotting experiments were prepared via Adobe Photoshop CS5.1 software. Bar graphs, diagrams, and figure assembly was finalised in Adobe Illustrator CS5.1 software.

Synapse numbers were counted by automated macros written for ImageJ / Fiji software. Co-localisation of Vamp2 / Syt immunostainings was analysed using MetaMorph® Microscopy Automation & Image Analysis software.

3.2.9.2 Data analysis of live cell Ca^{2+} signalling

To analyse Ca^{2+} events from movies of live cell Ca^{2+} imaging using GCaMP3 signal expressed exclusively in astrocytes, the ImageJ / Fiji plugin GECIquant was used (Srinivasan et al., 2015), which is a tool for semi-automatic detection and quantification of genetically encoded Ca^{2+} signals.

GECIquant was used to define soma, branchlet and microdomain regions within which Ca^{2+} fluctuations were quantified. A Matlab code was written and used to further define, quantify, and display events as described below. For every condition / event-type, all ROIs with greater than 10% total frames of 0 fluorescence (in at least two consecutive frames) were excluded from analysis. Ca^{2+} events within each region were detected from the absolute fluorescence values output by GECIquant, and plotted as dF/F .

For somatic events in MD and IP astrocytes (which were slow-rising and infrequent), the baseline fluorescence was calculated as the average of 15 frames before and 15 frames after the minimum fluorescence value (i.e. average of 30 frames total). An event was then defined as having at least 30 frames above $3.5 \times \text{RMS}$ (root mean square) noise. The event amplitude was calculated as the average of 30 frames around the maximum value. For somatic events in co-culture and NB+H astrocytes, the average of the 75th percentile (average of 75% of the total frames with the lowest fluorescence values) was used to calculate the baseline; an event was defined as fluorescence values above a threshold of $3.5 \times \text{RMS}$ noise, where single points above the threshold, or the maximum value of a cluster of points above the threshold were used to define amplitude and half-width.

Branchlet events were defined as for the soma in each condition. Except in co-culture and NB+H conditions, events were defined as being above the 91.5th percentile of all events (to exclude small “events” that looked like noise upon visual inspection).

The baseline for microdomain events was defined as the mean of all fluorescence values in each trace. (Because microdomain events were shorter-lived and lower in amplitude than somatic and branchlet events, the average of all fluorescence values best approximated baseline). Microdomain events were then defined as above for branchlet events. Peak half-width was defined as the duration of peak width at half maximal amplitude.

4. Results

4.1 Characterisation of different astrocyte cultures

4.1.1 Specific media alter astrocyte morphology, protein expression, and proliferation

To study vesicle characteristics of astrocytes in culture, we first tested different culturing methods: co-cultures (of neurones, astrocytes, and other glia) and astrocyte monocultures generated by the MD and IP methods (see Table 1).

Co-cultures are best generated from embryonic day 18-19 tissue, whereas MD astrocyte monocultures are usually derived from P0 to P3 tissue when astrogliogenesis peaks in the central nervous system (Freeman, 2010). In the spinal cord, astroglial precursors start to express glial fibrillary acidic protein (Gfap) and excitatory amino acid transporter 1 (EEAT1, also known as GLAST or SLC1A3) on embryonic day 14 (Deneen et al., 2006; Fan et al., 2005), whereas astrogliogenesis begins later in the prenatal cortex (He et al. 2005; Miller and Gauthier 2007; Ge et al. 2012). To obtain relatively mature astrocytes for monocultures but also prepare co-cultures from the same animals for comparison, we chose to dissect tissue from embryonic day 19 animals (i.e. shortly before birth) for co-cultures and MD astrocytes prepared from cortex. In contrast, we prepared IP astrocytes from one week-old rats as suggested by the authors of the IP method (Foo, 2013b; Foo et al., 2011).

As described in Table 1, astrocyte morphology and protein expression depend on the cell culture method. When we compared astrocytes from co-cultures (of neurones and glia) with MD and IP astrocytes, the morphology varied: While co-culture and IP astrocytes appeared stellate, similar to astrocytes *in vivo*, MD astrocytes were polygonal (Fig. 8). Apart from the protocols used, another difference between these cultures is the medium (co-cultures are grown in Neurobasal medium with B-27 and glutamax supplements (NB+), MD astrocytes are grown in DMEM including 10% FCS, (DMEM+) and IP astrocytes are grown in a mix of NB+ and DMEM including human epidermal EGF-like growth factor (HBEGF). Interestingly, the culture medium determines how embryonic stem cells proliferate and differentiate (Draper et al., 2004), and fibroblast cultures (with a morphology similar to MD astrocytes) can be directly trans-differentiated into epiblast stem cells via transcription factors

only in epiblast stem cell medium (Han et al., 2011). Therefore, we tested whether using different media would make MD astrocytes more similar to co-culture astrocytes by morphology (Fig. 8).

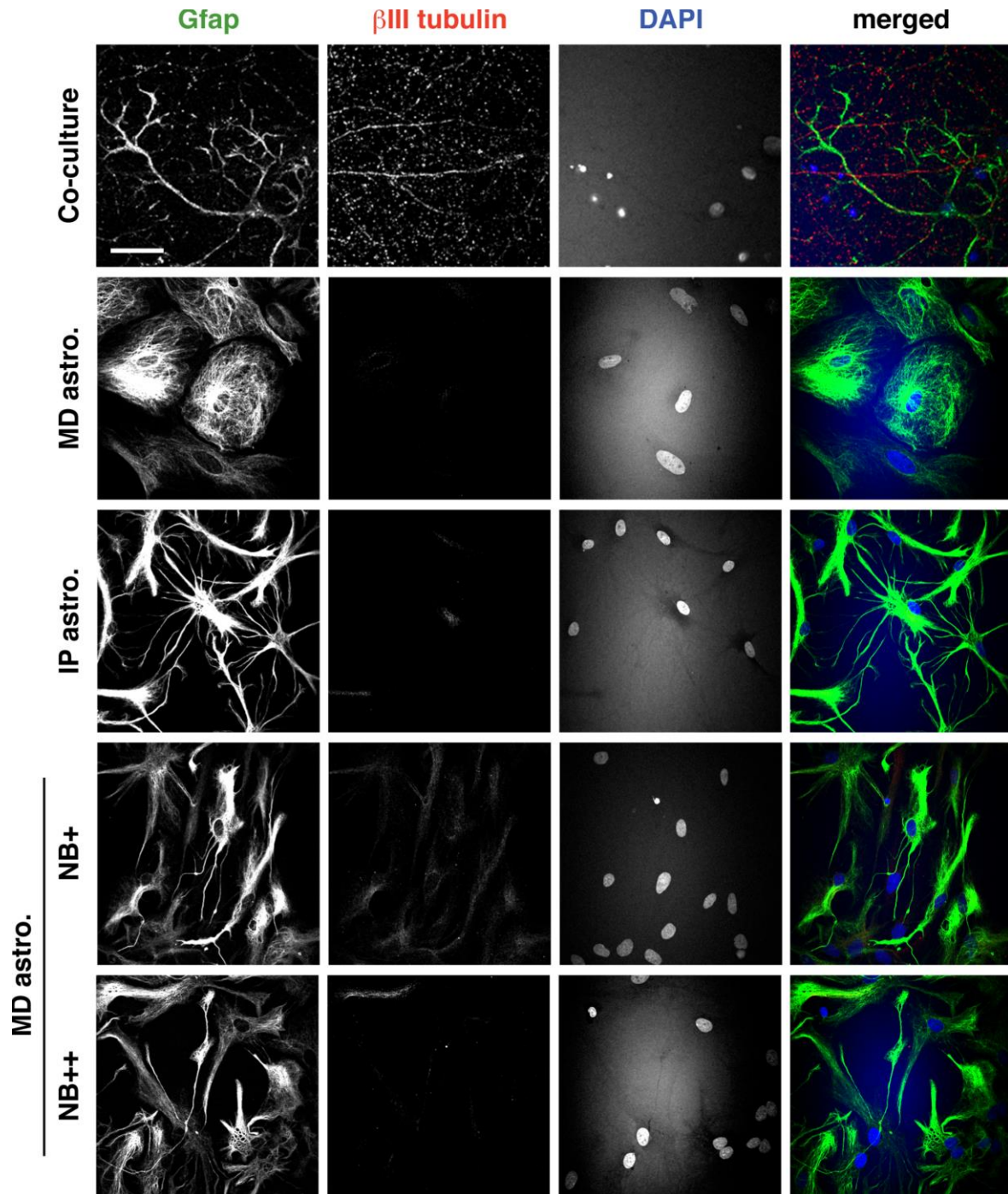


Fig. 8: Conditioned medium from co-cultures makes astrocytes more similar to co-culture and IP astrocytes by morphology

Immunocytochemistry of DIV14 co-cultures (neurons with glia) and DIV16 astrocyte monocultures: MD astrocytes grown in DMEM+, IP astrocytes, and MD astrocytes treated with Neurobasal medium including supplements (NB+) –like co-cultures– or with conditioned medium from co-cultures (NB++), are shown. Gfap labels astrocytes, β III tubulin labels neurones, and DAPI labels cell nuclei. Secondary antibody controls are provided in Fig. 9. Similar morphology was observed in n=7 (co-cultures, IP, NB++) and n=3 (MD, NB+) culture preparations. Scalebar = 50 μ m.

Growing MD astrocytes in NB+ changed astrocyte morphology from polygonal to bipolar and often stellate. However, cell survival was low, so these astrocytes were plated at a higher density than MD astrocytes grown in DMEM+, for comparison of different culture methods (discussed later in this chapter, see Fig. 11). In contrast to MD astrocytes grown in NB+, astrocytes in co-cultures are also exposed to neuronal secreted factors that may influence astrocyte morphology, protein expression, and proliferation. Indeed, when conditioned medium from day *in vitro* (DIV) 7 co-cultures (NB++) was transferred to DIV7 MD astrocytes, their morphology became bipolar to stellate as in the NB+-treated MD astrocytes. In addition, cell survival of conditioned medium-treated astrocytes was similar to that of MD and IP astrocytes (data not shown). Thus, adding conditioned NB++ to MD astrocytes on DIV7 proved an easier and faster protocol than generating IP astrocytes, while providing more stellate astrocyte morphology than the traditional MD astrocyte protocol.

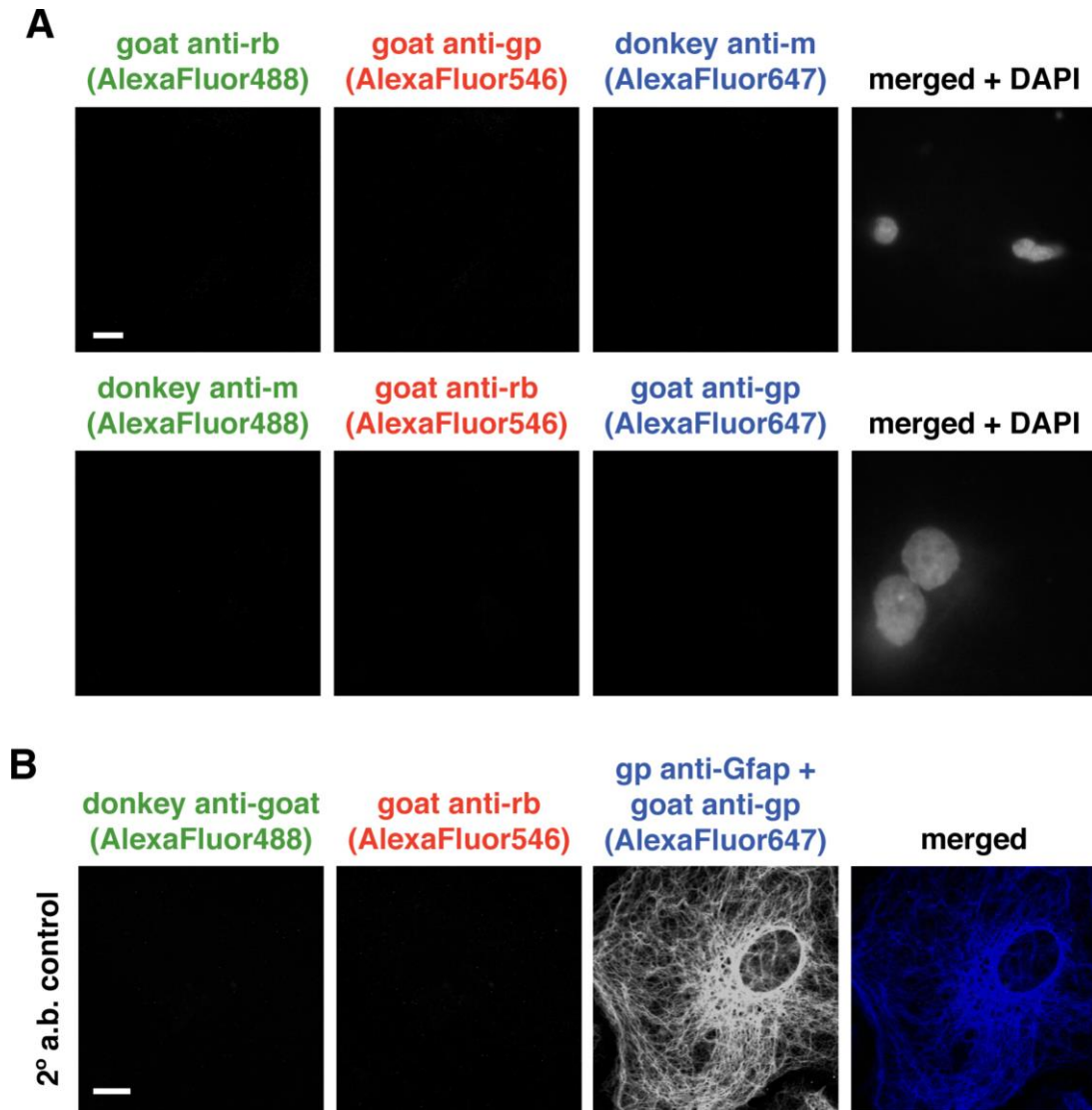


Fig. 9: Secondary antibody controls for immunocytochemistry

Control immunocytochemistry with secondary antibodies (2° a.b.) and DAPI or Gfap primary antibody. **A** DIV14 co-cultures (top panel) and DIV16 MD astrocytes (bottom panel) treated with the indicated combinations of 2° a.b. and DAPI. 2° a.b. against rabbit (rb), guinea pig (gp), and mouse (m) were used. **B** DIV16 MD astrocytes treated with a primary a.b. against Gfap and then a donkey anti-goat 2° a.b. followed by a goat anti-rb 2° a.b. applied individually and consecutively to avoid donkey anti-goat 2° a.b. binding to goat anti-rb 2° a.b. (as a control for later figures, i.e. Fig. 23B), n=5 (**A**), and n=4 (**B**) individual immunostains yielded similar results. Scalebar = 10 µm.

While this quick and simple method saved time and effort, an extra set of co-cultures had to be prepared for each set of MD astrocyte monocultures to be used to generate NB++ medium, and potential batch variation was an issue. Thus, we decided to test which medium composition causes the most “*in vivo*-like” astrocyte morphology, with a goal to develop chemically defined media rather than preparing extra co-cultures that produce media with unknown constituents.

We found that astrocytes develop a stellate morphology when grown in Neurobasal medium with HBEGF (NB+H), regardless of whether they were prepared by the MD or IP method (Fig. 10A). NB+H mixed with DMEM (i.e. IPm – the medium used for IP astrocyte cultures by Foo et al.) also yielded stellate astrocytes, but with slightly fewer thin processes. However, growing astrocytes in DMEM+ alone (with or without HBEGF) made astrocytes polygonal, even when the cells were generated by immunopanning. Therefore, HBEGF supported stellate morphology in MD astrocytes, but only when combined with Neurobasal medium. As a result, we selected this simple and fast protocol for further analysing astrocytes in culture (i.e. incorporating the MD method of shaking astrocytes on DIV7, but then growing them in NB+H); monocultures generated in this way will be referred to as NB+H astrocytes from here onwards.

Next, we compared MD, IP, and NB+H astrocytes with co-cultures and whole brain lysate by Western blot analysis (Fig. 10C). Notably, the cell yield of IP astrocytes was much lower than for other cultures, so that loading enough IP astrocyte lysate onto Western blot gels for multiple antibody analysis was challenging, demonstrating a disadvantage of this protocol over MD and NB+H astrocytes.

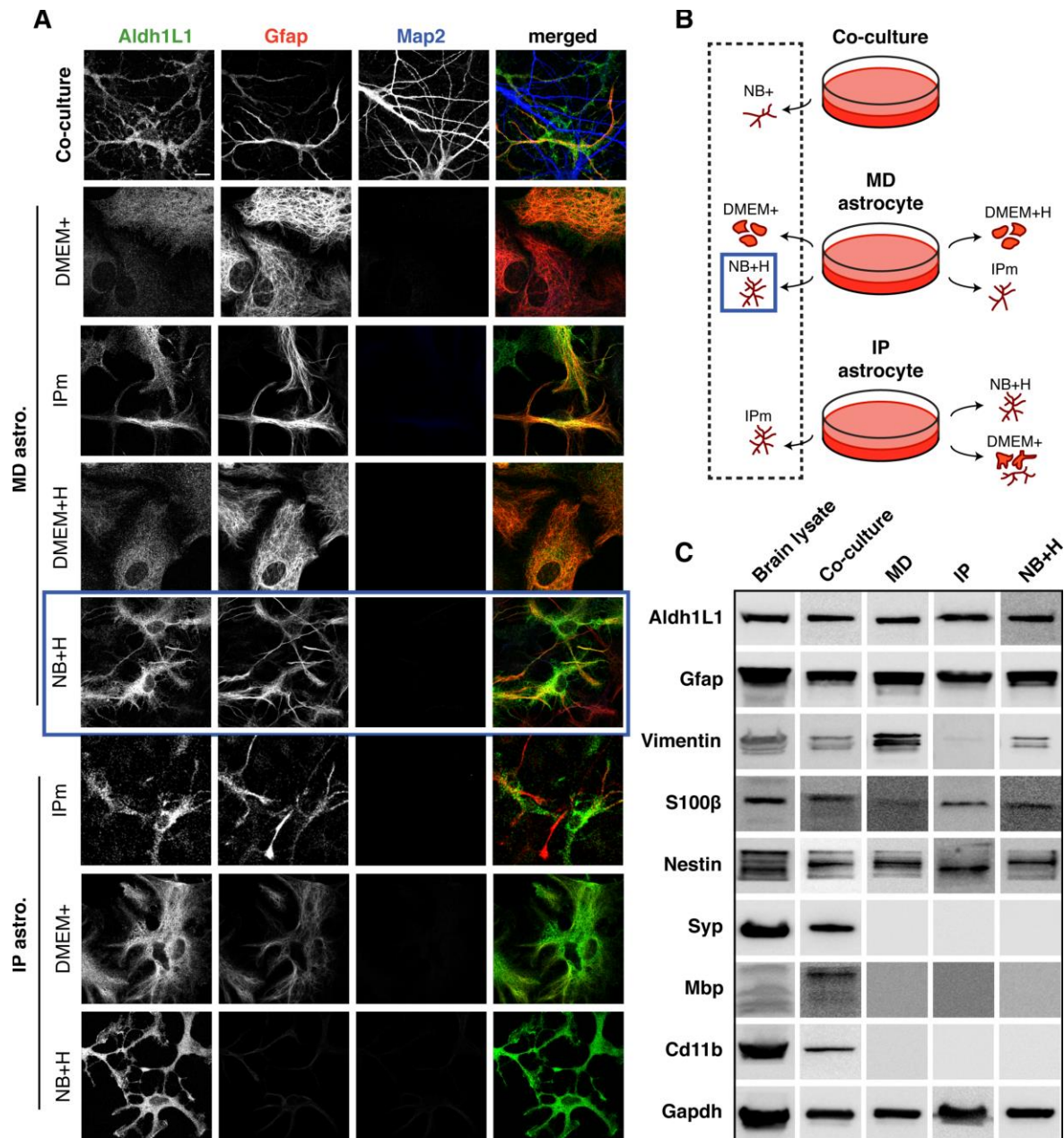


Fig. 10: Different media yield morphologically different astrocytes

A Immunocytochemistry of DIV14 co-cultures and the indicated types of DIV16 astrocyte monocultures. Aldh1L1 and Gfap label astrocytes and Map2 labels neuronal processes. MD and IP astrocyte preparations were grown in different media as explained in **B**: Co-cultures were directly plated in NB+, whereas MD astrocyte monocultures were shaken on DIV7 and then grown in either DMEM with 10% fetal calf serum (DMEM+) for classical MD astrocytes, NB+ with heparin-binding EGF-like growth factor (HBEGF) (NB+H), DMEM+ with HBEGF (DMEM+H), or the medium used in the Foo et al. IP astrocyte protocol (IPm), which is a 1:1 mix of DMEM and NB+H. IP astrocytes were generated as described by Foo et al. (2013) and grown in IPm, NB+H, or DMEM+. In **A** and **B**, the blue square marks MD cultures grown in NB+H (NB+H astrocytes), which we selected for further analysis due to the stellate morphology and ease of production. **C** Western blot analysis of adult rat brain lysate compared with DIV14 co-culture, MD, IP, or NB+H astrocyte lysate. Different antibodies against proteins that mark astrocytes (Aldh1L1, Gfap), immature or reactive astrocytes (Vimentin, Gfap), mature astrocytes (S100β), neurones (synaptophysin (Syp)), oligodendrocytes (myelin basic protein (Mbp)), and microglia (Cd11b) were used; Gapdh serves as a loading control. Western blots were prepared by Dr. Saheeb Ahmed (European Neuroscience Institute, Göttingen). From top to bottom, immunostains yielded similar results in n=6, 4, 8, 4, 8, 5, 4, 6 for each panel in **A**. Scalebar = 10 μm.

All samples included astrocytic proteins, e.g. aldehyde dehydrogenase 1 family member L1 (Aldh1L1) and glial fibrillary acidic protein (Gfap). Similarly, all samples expressed Vimentin and Nestin, which are markers of immature and reactive astrocytes (Dahl et al., 1981; Pixley and de Vellis, 1984; Schiffer et al., 1986). We found the highest Vimentin levels in MD astrocytes, and the lowest in IP astrocytes, indicating that IP astrocytes are more mature than MD astrocytes. While Nestin expression was similar in all samples, S100 β expression was opposite to Vimentin expression (highest in IP astrocytes and lowest in MD astrocytes); S100 β is expressed by mature astrocytes that have lost their stem cell potential (Raponi et al., 2007), again indicating that IP astrocytes are more mature than MD astrocytes.

Proteins characteristic of other, non-astrocytic cell types were only found in brain lysate and co-cultures, i.e. synaptophysin (marking neurones), myelin basic protein (marking oligodendrocytes), and Cd11b (marking microglia). Thus, MD, IP, and NB+H monocultures were free of any other cell types than astrocytes.

Both IP and NB+H astrocytes were stellate and expressed low Vimentin levels compared with MD astrocytes. Foo et al. (2011) reported that HBEGF is essential for IP astrocyte survival. However, in Fig. 8 we show that astrocytes grown in NB+ without HBEGF do survive (although astrocytes need to be plated at a higher density to survive). To test whether IP astrocytes undergo apoptosis without HBEGF, or whether plating IP astrocytes at a higher density can rescue cell survival as in NB+H astrocytes grown without HBEGF (see Fig. 8), we compared IP and NB+H astrocytes grown with or without HBEGF.

After growing IP and NB+H astrocytes with or without HBEGF for 14 days, we labelled apoptotic cells using the Apoptag® Fluorescein kit, and used DAPI to detect all cell nuclei (Fig. 11A). IP astrocytes plated at both low and high densities survived in HBEGF-free media. Although this growth factor was not required for IP astrocyte survival, the cell number after 14 days was significantly higher in IP astrocytes grown in HBEGF-containing medium (Fig. 11B). The same was true for NB+H astrocytes, which showed a dramatic decrease in cell number in the absence of HBEGF. However, assessing the relative proportion of apoptotic cells revealed that more than half of all cells counted by DAPI staining were alive in any HBEGF-free condition (Fig. 11C). Although both NB+H and IP astrocytes survived without HBEGF, HBEGF contributed significantly to cell proliferation. Therefore, we included HBEGF in IP and NB+H astrocyte media for further experiments.

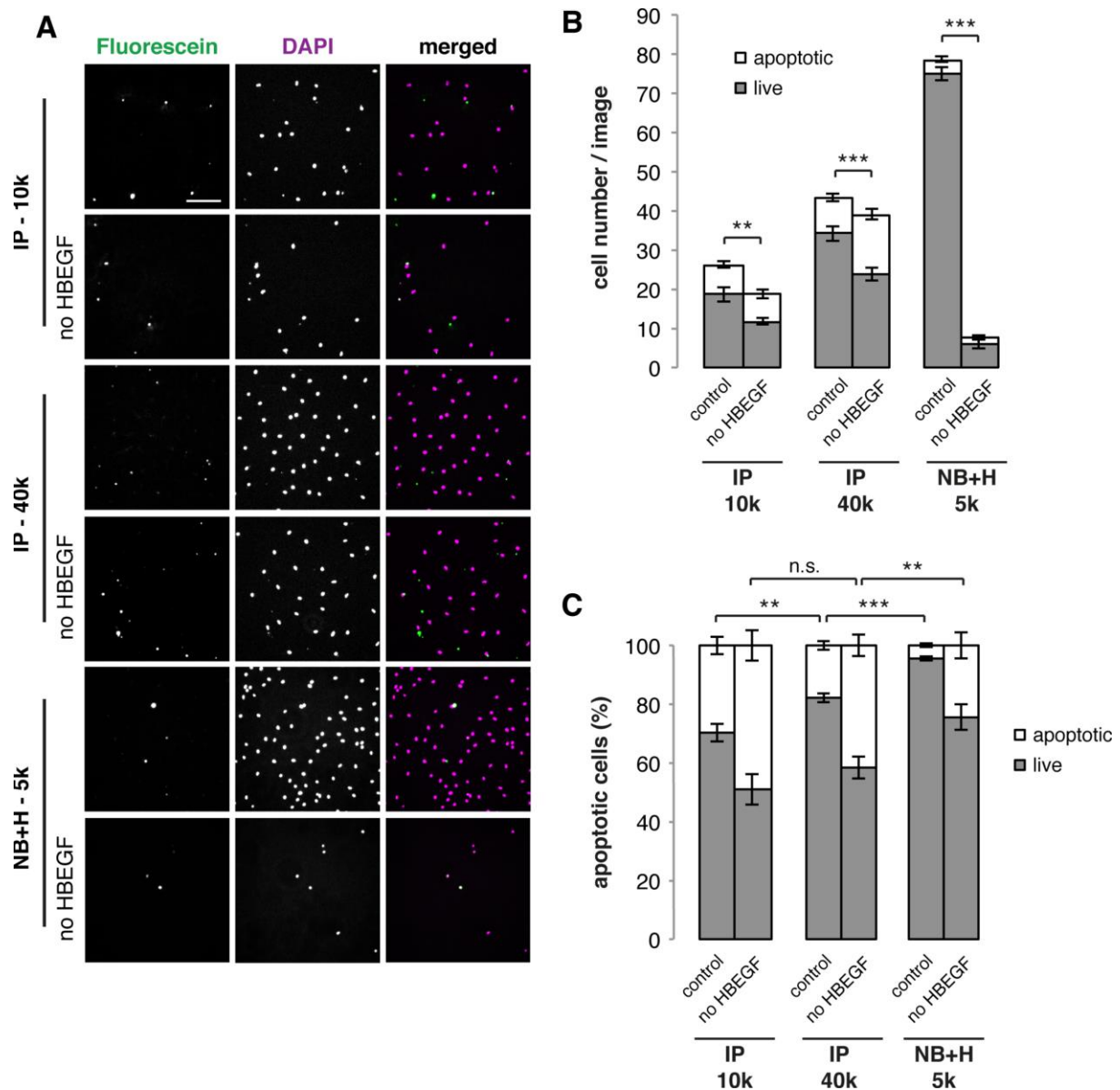


Fig. 11: HBEGF promotes astrocyte proliferation

A Immunocytochemistry of DIV14 IP and NB+H astrocytes plated at 10,000 or 40,000 and 5,000 cells / 24-well coverslip, respectively. Fluorescein marks apoptotic cells and DAPI marks all cell nuclei. For each condition, cell number in media with or without HBEGF was compared and quantified in **B** as absolute numbers and in **C** as relative numbers. $n=12$ for images from 4 cultures. Error bars: SEM, $**=p < 0.01$, $***=p < 0.001$, $n.s.=p > 0.05$ by an unpaired two-tailed Student's t-test. Scalebar = 100 μ m.

Another difference between IP and NB+H astrocytes is the tissue age the cells are generated from. One advantage of the IP protocol is that it allows isolating astrocytes from older animals (up to postnatal day (P) 14 according to (Foo et al., 2011)). Thus, we tested if IP astrocytes derived from younger tissue like NB+H astrocytes (P0) change by morphology, and conversely, if NB+H astrocytes derived from older tissue (P7, as Foo et al. recommend for IP astrocytes) change by morphology.

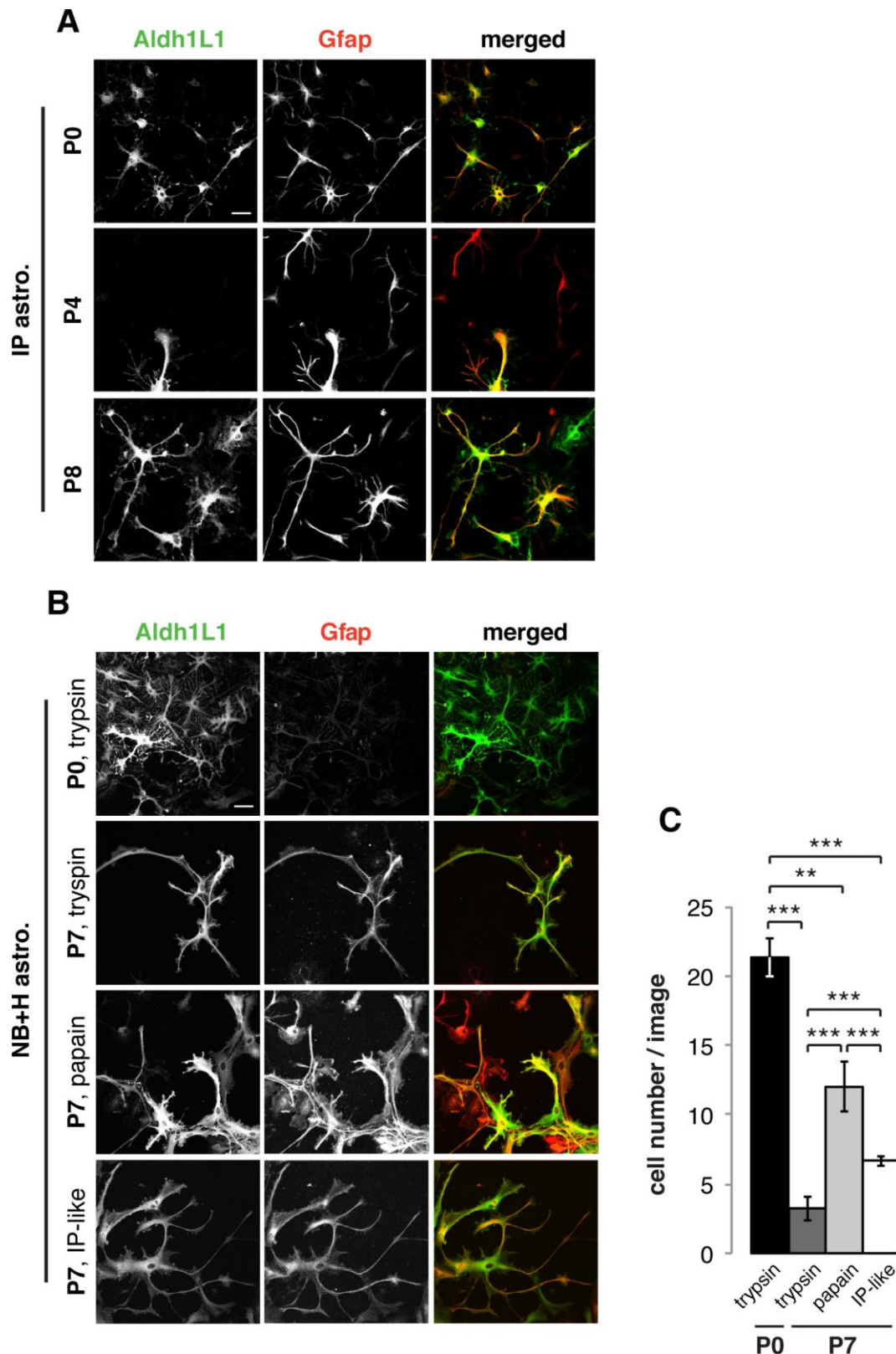


Fig. 12: Older tissue yields fewer but viable astrocytes

A Immunocytochemistry of DIV14 IP astrocytes derived from P0, P4, or P8 rats, where Aldh1L1 and Gfap depict astrocyte morphology. **B** Immunocytochemistry of DIV14 NB+H astrocytes derived from P0 or P7 rats, and dissociated with trypsin, papain, or as described in Foo et al. (2013) but without immunopanning before plating cells. As in **A**, Aldh1L1 and Gfap depict astrocyte morphology. **C** Quantification of cells counted per image in the indicated conditions. Images per experiment: $n=12$ (P0) and 11 (P4 and P8) in **A**, and $n=6$ (P0), $n=8$ (P7, trypsin), $n=6$ (P7, papain), and $n=16$ (IP-like) in **B**. Error bars: SEM, $**= p < 0.01$, $***= p < 0.001$ by unpaired two-tailed Student's *t* test. Scalebar = 25 μm **A** and 50 μm **B**.

Fig. 12A shows that IP astrocyte morphology was stellate no matter if cells were derived from P0, P4, or P8 tissue. However, P8-derived IP astrocytes showed the most refined processes. In the IP protocol, tissue is digested with papain, while tissue for generating NB+H astrocytes from perinatal tissue is digested with trypsin, which may be more harsh to cells (Kaiser et al., 2013). Astrocytes in older tissue have more refined, intermingled processes, so that using papain may be important for maintaining cell health when digesting older tissue. Consequently, we tested protocols in which we digested P7 tissue for NB+H astrocyte monocultures with trypsin, but also tested papain, and the entire IP protocol (minus the immunopanning steps) (IP-like). As IP astrocytes, NB+H astrocytes could be generated from older tissue (P7), but NB+H astrocyte morphology was equally stellate amongst P0- and P7-derived cultures (Fig. 12B). Subsequently, we compared NB+H astrocyte numbers following trypsin, papain, or IP-like tissue preparations (Fig. 12C). We achieved the greatest cell yield from P0-derived astrocytes, but among older NB+H astrocytes, cell numbers were highest when using papain. In conclusion, both IP and NB+H astrocytes can be generated from perinatal and older postnatal tissue, where tissue digestion with papain yields the most cells.

4.1.2 Ca²⁺ signalling profiles in different astrocyte cultures

Unlike neurones, astrocytes are electrically silent, but they employ another inter- and intracellular signalling method: Ca²⁺ signalling (Khakh and McCarthy, 2015; Scemes and Giaume, 2006). To compare Ca²⁺ signalling parameters of the different astrocyte cultures, we transduced astrocytes of co-cultures and monocultures with adeno-associated viral particles carrying GCaMP3 (a genetically encoded Ca²⁺ indicator). By using the astrocyte-specific Gfap promoter, we ruled out that neurones expressed GCaMP3 in co-cultures. Further, GCaMP3 was fused to the membrane-tethering Lck domain. Lck-GCaMP3 reports Ca²⁺ events even in fine astrocyte processes, and is thereby superior to conventional GCaMPs without the membrane-tethering domain (Shigetomi et al., 2010b).

Using semi-automated GECIquant analysis (Srinivasan et al., 2015), Ca²⁺ signals were first categorised by defining three domains in infected astrocytes: somata (area $\geq 30 \mu\text{m}^2$), branchlets (after subtracting somata: area of 5 - 2000 μm^2), and microdomains (area of 0.5 - 4 μm^2). Subsequently, we compared fluorescence intensity of Ca²⁺ events occurring in these three domains from all cultures. Example traces illustrate that astrocytes from co-cultures and NB+H cultures showed Ca²⁺ events distinct from MD and IP astrocytes (Fig. 1A): While clearly distinguishable Ca²⁺ events appeared in traces from co-cultured and NB+H astrocytes, MD and IP astrocytes exhibited mostly wave-like fluorescence intensity changes which often persisted even after the end of the experiment (e.g. Fig. 1A, MD astrocytes, second somatic trace from the top). In addition, viral transduction was only successful half the time for IP astrocytes, which were also prone to apoptosis.

To compare Ca²⁺ signalling parameters in more detail, we analysed event frequency, amplitude, and duration for all cultures (Fig. 1B). Event frequency in somata was similar between co-culture and NB+H astrocytes, and between MD to IP astrocytes. In addition, the frequency of branchlet events was also similar in co-cultures and NB+H astrocytes, and much higher than in MD and IP astrocytes types. Thus, Ca²⁺ event frequency was much higher in both somata and branchlets of co-cultures and NB+H compared with MD and IP astrocytes. In microdomains, Ca²⁺ event frequency was the same across all cultures (although IP astrocytes showed a trend toward a decrease in frequency, with high error, given that many IP astrocytes did not survive transduction).

Concerning Ca²⁺ event amplitude, microdomains of co-cultures showed significantly lower amplitude than microdomains in astrocyte monocultures. In contrast, Ca²⁺ event

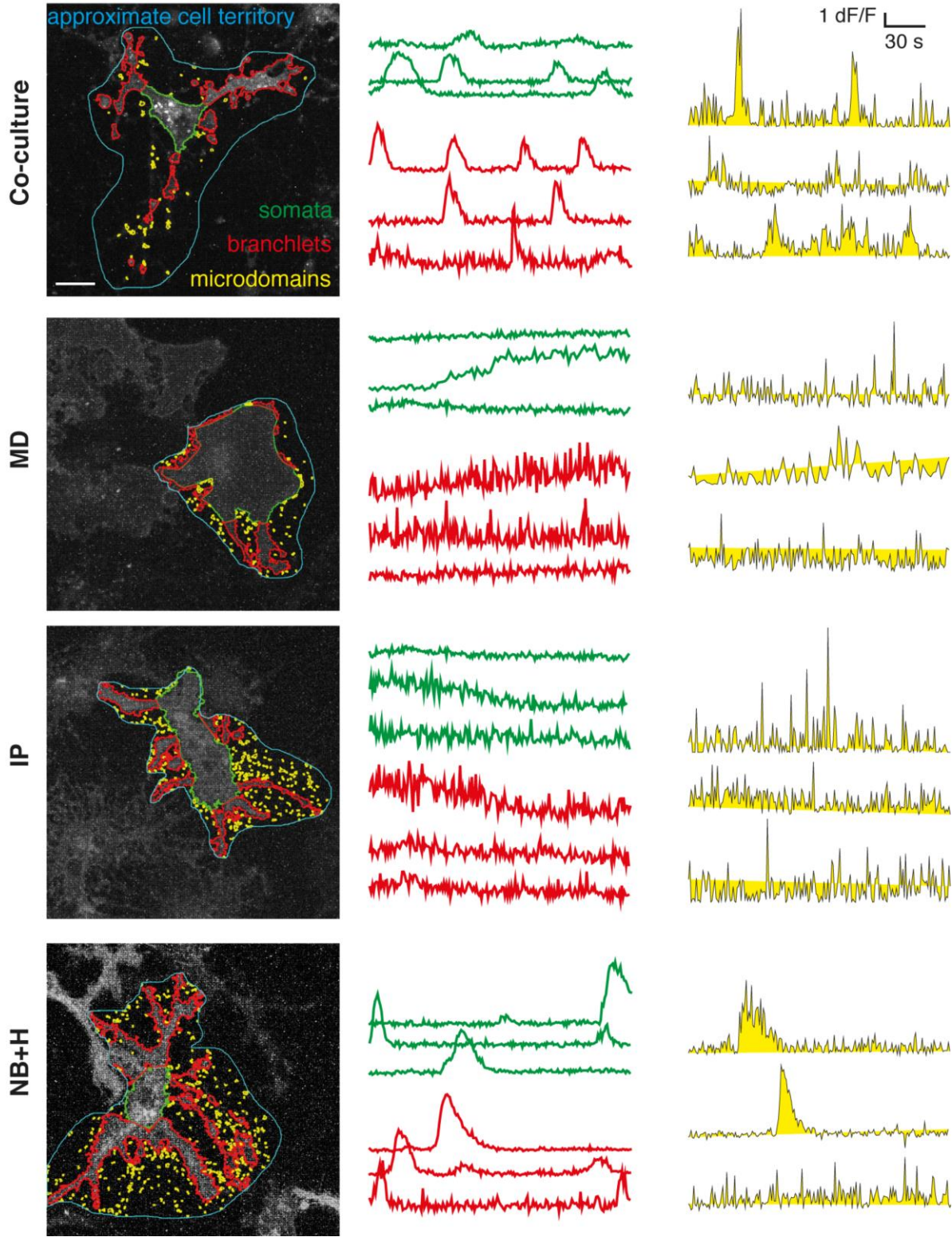
amplitude was the same in somata and branchlets of all culture types (except for amplitude in MD branchlets, which was significantly higher than in co-cultures and NB+H astrocytes).

In terms of Ca²⁺ event duration (plotted as event half-width), we found no difference in any domains between MD and IP astrocytes. In somata and branchlets, event duration was significantly longer in MD and IP astrocytes than in co-culture and NB+H astrocytes, but in microdomains, event duration was significantly shorter in MD and IP astrocytes than in co-culture and NB+H astrocytes. Co-culture or NB+H event duration in general were similar to each other, but differed from all other cultures.

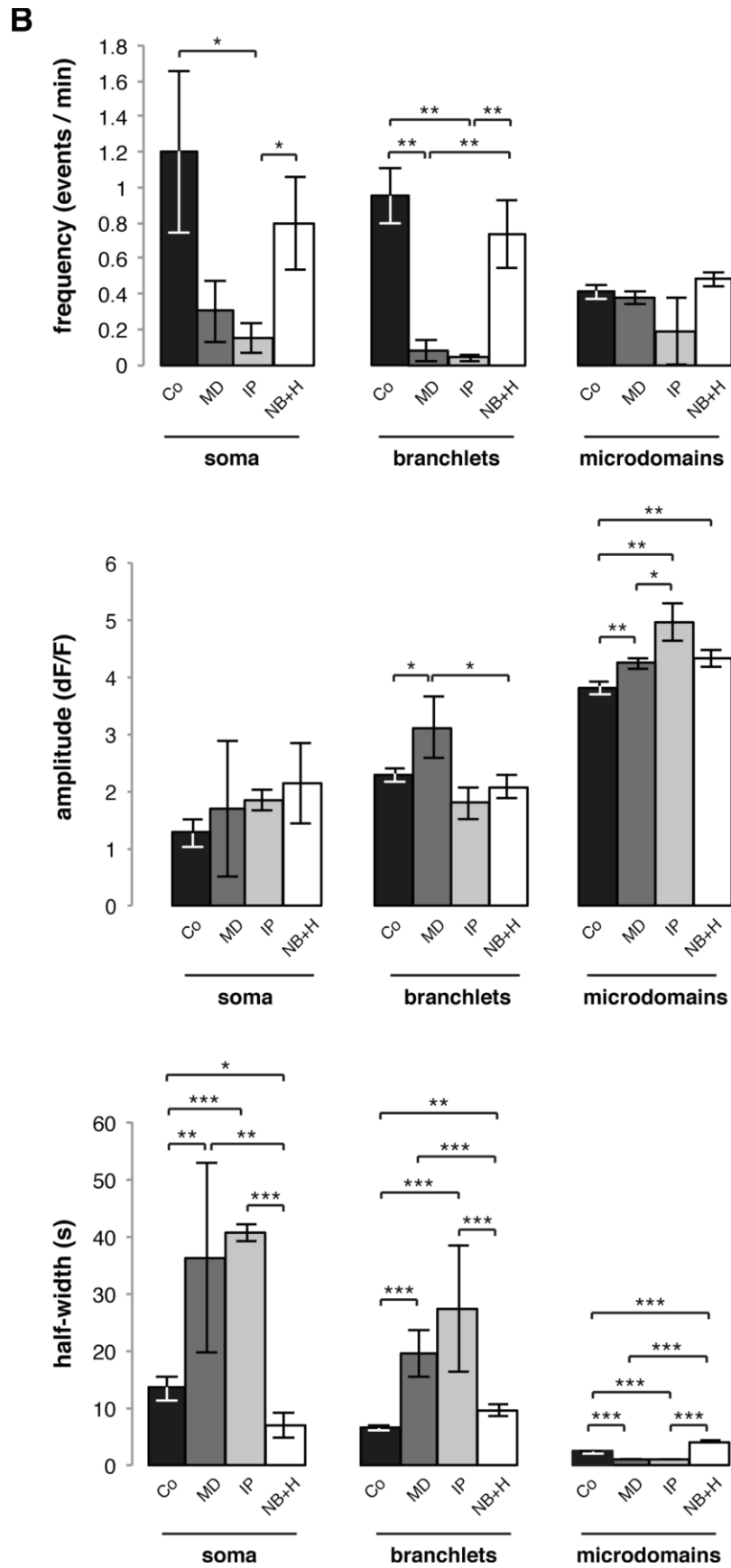
We next compared astrocytic Ca²⁺ signalling in somata, branchlets, and microdomains from within one culture type (Fig. 13C). In each culture type, the amplitude of Ca²⁺ events in microdomains was significantly higher than in branchlets or somata. Similarly, microdomain Ca²⁺ event duration was significantly shorter than branchlet and soma Ca²⁺ event duration. In co-cultures, soma and branchlet Ca²⁺ event amplitude and duration differed, but in astrocyte monocultures, soma and branchlet Ca²⁺ event amplitude and duration was the same. Thus, only co-cultures displayed distinct Ca²⁺ event amplitude and duration properties between all three domains (soma, branchlets, microdomains).

Ca²⁺ event frequency was comparable between the three domains of all astrocytes. Apart from frequency, astrocytes of all cultures had two things in common: (1) the Ca²⁺ event amplitude was significantly higher in microdomains than branchlets or somata, and (2) the Ca²⁺ event duration was significantly shorter in microdomains than branchlets or somata. Thus, microdomains shared similar characteristics in all culture conditions, i.e. short, high-amplitude Ca²⁺ events.

A



(see next page for Figure legend)



(see next page for Figure legend)

C

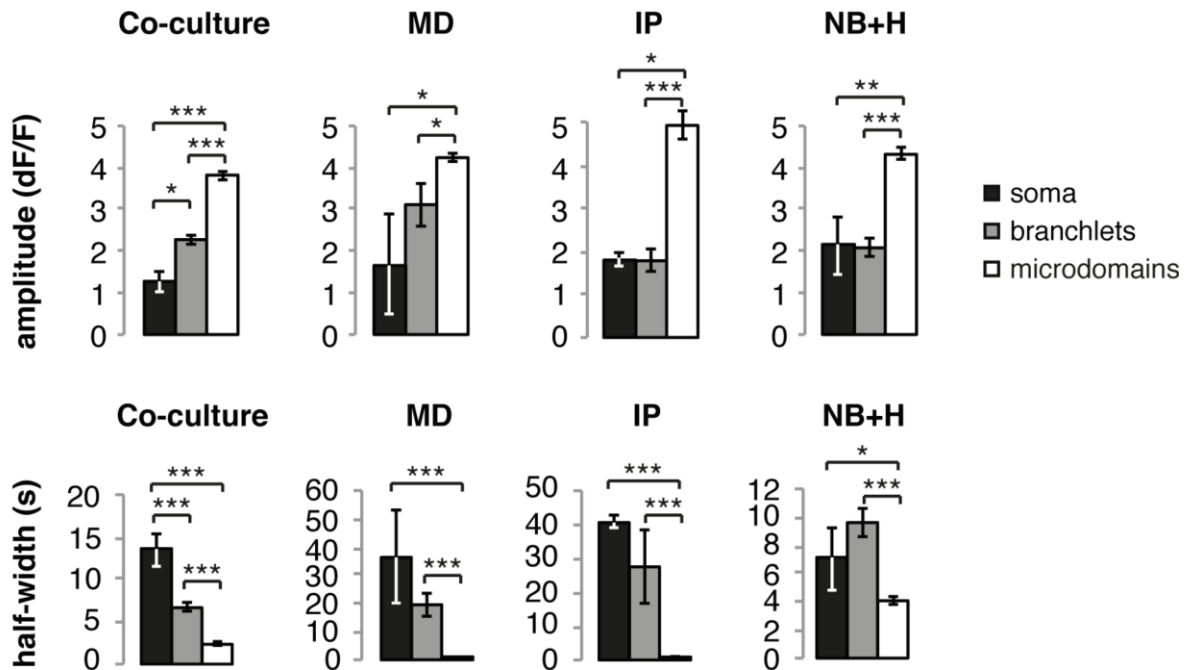


Fig. 13: Co-culture and NB+H astrocytes show Ca²⁺ events distinct from MD and IP cultures

Ca²⁺ signalling in DIV16 co-cultures, and MD, IP, and NB+H astrocyte monocultures, measured by Gfap promoter-driven Lck-GCaMP3 fluorescence changes in astrocytes. **A** Representative images of transduced astrocytes, where estimated territories (marked in blue) were analysed for Ca²⁺ events in the soma (green), branchlets (red), and microdomains (yellow). The approximate cell territory was used to define sub-domains using GECIquant. Example dF/F traces represent Ca²⁺ fluctuations from three regions of interest (ROIs) for each sub-domain as detected and quantified using the semi-automated software GECIquant. **B** Quantitation of event frequency, amplitude, and half-width for each sub-domain type for different culture types. **C** Quantitation of events as before, but comparing soma, branchlets, and microdomains within the same culture type. Note that the scale of y axes is different in frequency and event duration analyses for different culture types. MATLAB analysis was done by Ankit Awasthi (European Neuroscience Institute, Göttingen). Four culture types were analysed, where n=3 analysed videos per culture type with n=3 cells per culture type (i.e. 1 cell in each of 12 analysed videos); ROIs (somata): n=3 (co-culture, MD, NB+H), n=4 (IP); ROIs (branchlets): n=153 (co-culture), n=12 (MD), n=5 (IP), n=46 (NB+H); ROIs (microdomains): n=301 (co-culture), n=319 (MD), n=31 (IP), n=148 (NB+H). Error bars: SEM, *= $p < 0.05$, **= $p < 0.01$, ***= $p < 0.001$ by unpaired two-tailed Student's t test. Scalebar = 20 μ m.

In summary, Ca²⁺ events occurred in astrocytes of all culture types as identified by GCaMP3 signal. Co-culture and NB+H astrocyte Ca²⁺ signalling was distinct from MD and IP astrocyte Ca²⁺ signalling: (a) MD and IP astrocyte somata and branchlets had lower Ca²⁺ event frequency and longer event durations than co-culture and NB+H astrocytes (which had similar event frequencies); (b) MD and IP astrocytes showed the longest Ca²⁺ events in somata and branchlets, but the shortest Ca²⁺ events in microdomains (the opposite was true

for co-culture and NB+H astrocytes). Further differences included that in all three domains –soma, branchlets, microdomains– the Ca²⁺ event duration varied significantly across cultures (but was the same for MD and IP astrocytes).

Despite these dissimilarities, all infected astrocytes had in common that microdomains showed similar Ca²⁺ event frequency and somata showed similar Ca²⁺ event amplitude. Apart from MD astrocytes, all cultures also showed similar Ca²⁺ event amplitude in branchlets. Lastly, microdomains shared similar characteristics in all culture conditions, i.e. short, high-amplitude Ca²⁺ events that differed significantly from those in somata and branchlets.

Because NB+H astrocytes were most similar to astrocytes grown in more “*in vivo*-like” conditions in co-cultures with neurones –by morphology, markers of cell maturity, and Ca²⁺ signalling– we concluded that NB+H astrocytes generated using our novel protocol were superior to other astrocyte monoculture methods.

4.2 Evidence for vesicles in astrocytes

4.2.1 Astrocytes contain vesicular organelles

Ultrastructural and structured illumination microscopic analysis has previously revealed that astrocytes contain (possibly exocytotic) vesicles of approximately 30 nm in diameter (Bezzi et al., 2004; Martineau et al., 2013) or up to 300 nm (Singh et al., 2014). Here, we compared co-cultures with MD, IP, and NB+H astrocyte monocultures by electron microscopy to assess if these cultures contain vesicles (Fig. 14). Apart from MD astrocytes, all cultures featured clathrin-coated vesicles. We also found late endosomal multivesicular bodies in MD astrocytes (data not shown), while the IP astrocyte shown contained a lysosome (Fig. 1). However, electron microscopy of cell cultures is difficult because the extracellular space is greater than *in vivo*, making samples prone to damage during preparation, which can lead to artefacts and difficulties in identification of true vesicular structures and organelles. We therefore decided instead to focus our efforts on identification of vesicle-associated proteins and functional recycling of these proteins in astrocytes in response to stimulation, as shown in later figures. In summary, by electron microscopy, all culture types contained vesicular organelles, although such a general statement can be made for any cell.

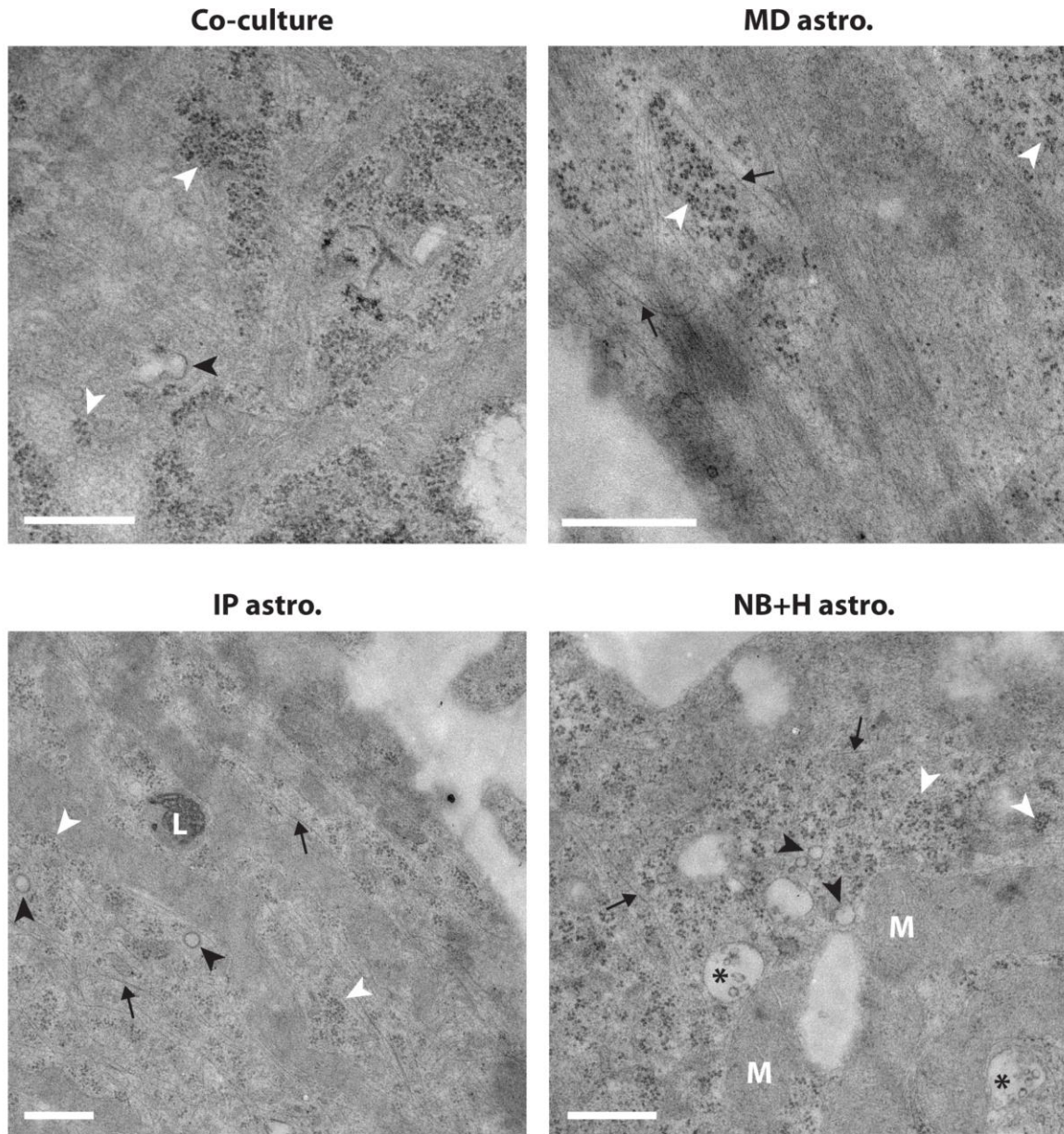


Fig. 14: Cultured astrocytes contain different vesicular organelles

Electron microscopy of DIV14 co-cultures, and MD, IP, and NB+H astrocytes. All images show ribosomes (white arrowheads). Mitochondria (M) appear in the NB+H culture, and all astrocytes feature cytoskeletal filaments (black arrows). Apart from MD astrocytes, all cultures also feature clathrin-coated vesicles (black arrowheads). The IP culture contains a lysosome (L) and the NB+H culture contains multivesicular bodies (asterisks). Pictures were prepared by Dr. Wiebke Möbius and Torben Ruhwedel (MPI for Experimental Medicine, Göttingen). n=7 (co-culture), 6 (MD), 14 (IP), and 12 (NB+H) images for each condition were collected, and showed similar characteristics. Scalebar = 500 nm.

4.2.2 Astrocytes express vesicle-associated proteins

To assess the presence of vesicle-associated proteins in astrocytes, we compared adult rat brain and co-culture lysate to MD, IP, and NB+H astrocyte lysate by Western blot analysis (Fig. 15). Some proteins that form the SNARE complex for vesicle fusion in neurones also appeared in MD, IP, and NB+H astrocyte samples: syntaxin1, a SNARE protein associated with the neuronal plasma membrane, and Vamp2, a synaptic vesicle-associated SNARE protein important for controlled vesicle exocytosis (Schoch et al., 2001). In contrast, Snap25 and Rab3a were only expressed in samples that contained neurones.

In neurones, vesicular glutamate transporters (vGluTs) load synaptic vesicles with the neurotransmitter glutamate; here, vGluT isoforms 1 and 2 were absent from astrocyte monocultures, whereas vGluT3 was expressed in all samples.

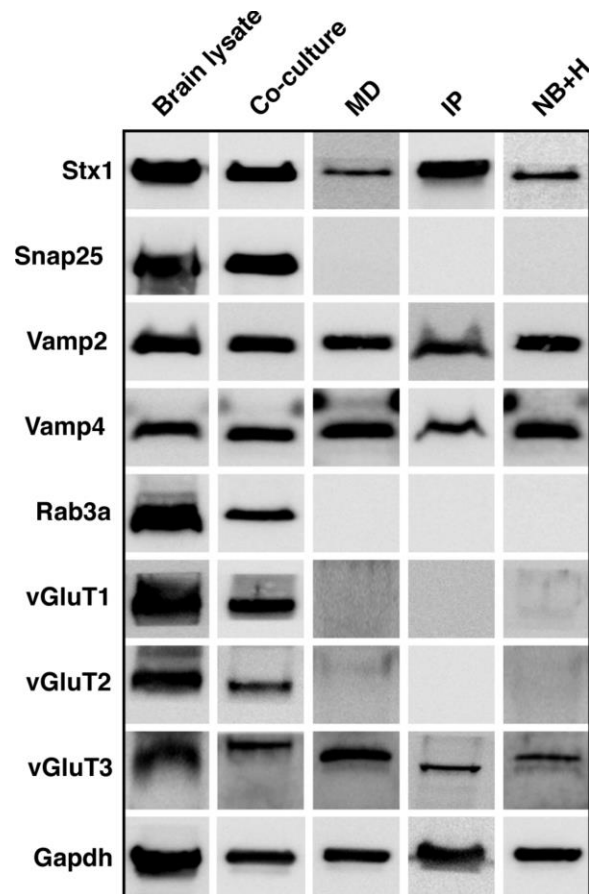


Fig. 15: Astrocytes express vesicle-associated proteins

Western blot analysis of adult rat brain lysate compared with DIV 14 co-culture, and MD, IP, and NB+H astrocyte monoculture lysates. Proteins that form the SNARE complex in neuronal vesicle fusion, syntaxin1 (Stx1) and Vamp2 both appear in all samples, whereas Snap25 is absent from astrocyte monocultures. Vamp4 and vesicular glutamate transporter (vGluT) 3 are expressed in all samples, while Rab3a and vGluT1 and 2 are not expressed in astrocyte monocultures. Gapdh serves as a loading control (note that the same Gapdh blot appears in Fig. 10), where samples were processed together. Western blots were prepared by Dr. Saheeb Ahmed (European Neuroscience Institute, Göttingen).

Several publications have reported that astrocytes express Vamp2 (Bezzi et al., 2004; Crippa et al., 2006). These findings were recently challenged by a report that astrocytes were devoid of Vamp2, but this was only found in MD cultures (Li et al., 2015). In brain slices, Vamp2 co-localises with Gfap by 3D reconstruction methods (Bergami et al., 2008). Since co-cultures and astrocyte monocultures all expressed Vamp2 in our Western blots and immunostainings, we next focused on Vamp2 distribution and function.

4.2.3 Vamp2-harboured vesicles: Localisation and recycling

To analyse Vamp2 localisation in astrocytes, we stained co-cultures and astrocyte monocultures for Vamp2 by immunocytochemistry (Fig. 16). Vamp2 signal was apparent in all cultures, as expected given the detection of Vamp2 in Western blots (Fig. 15), and Vamp2 staining appeared punctate.

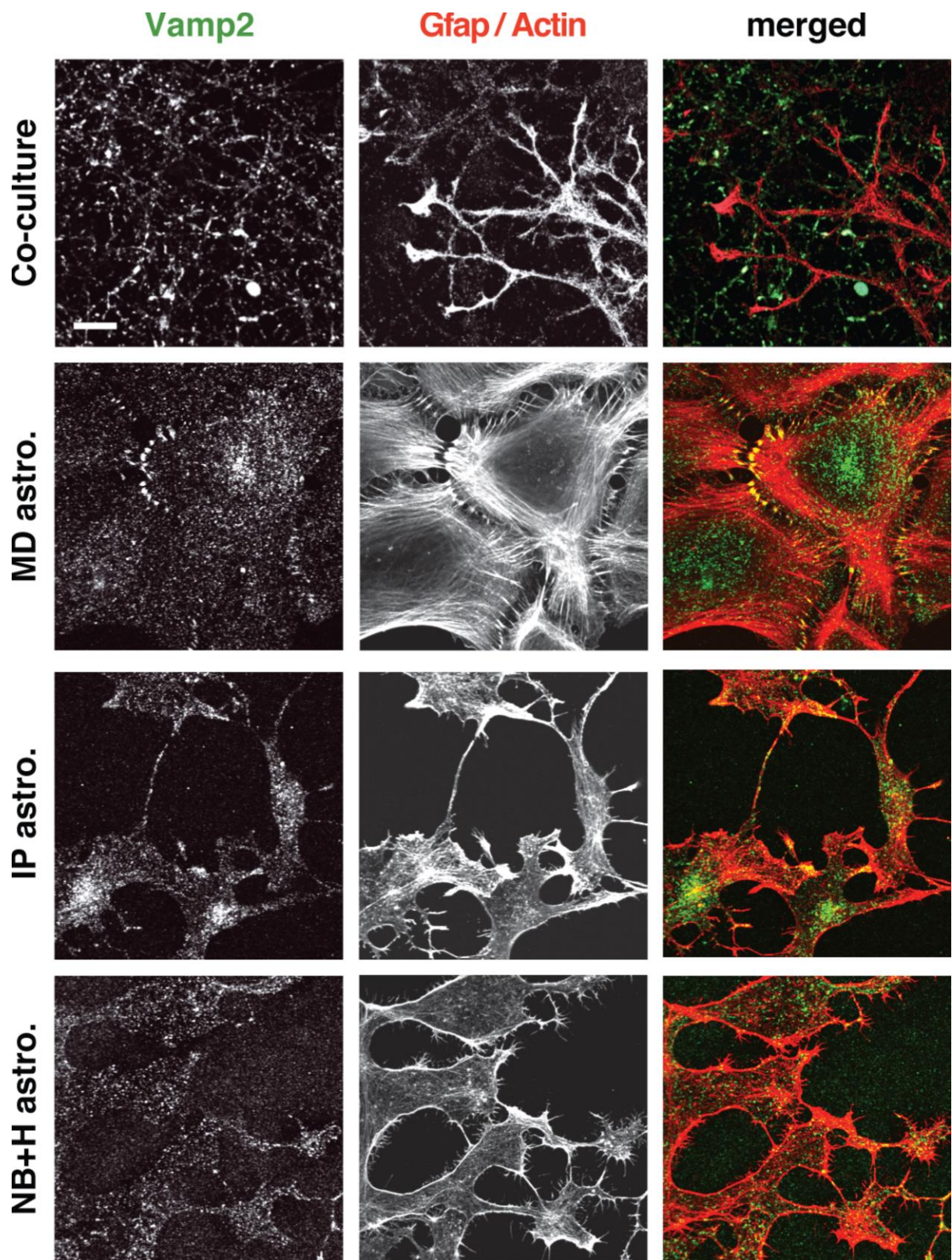


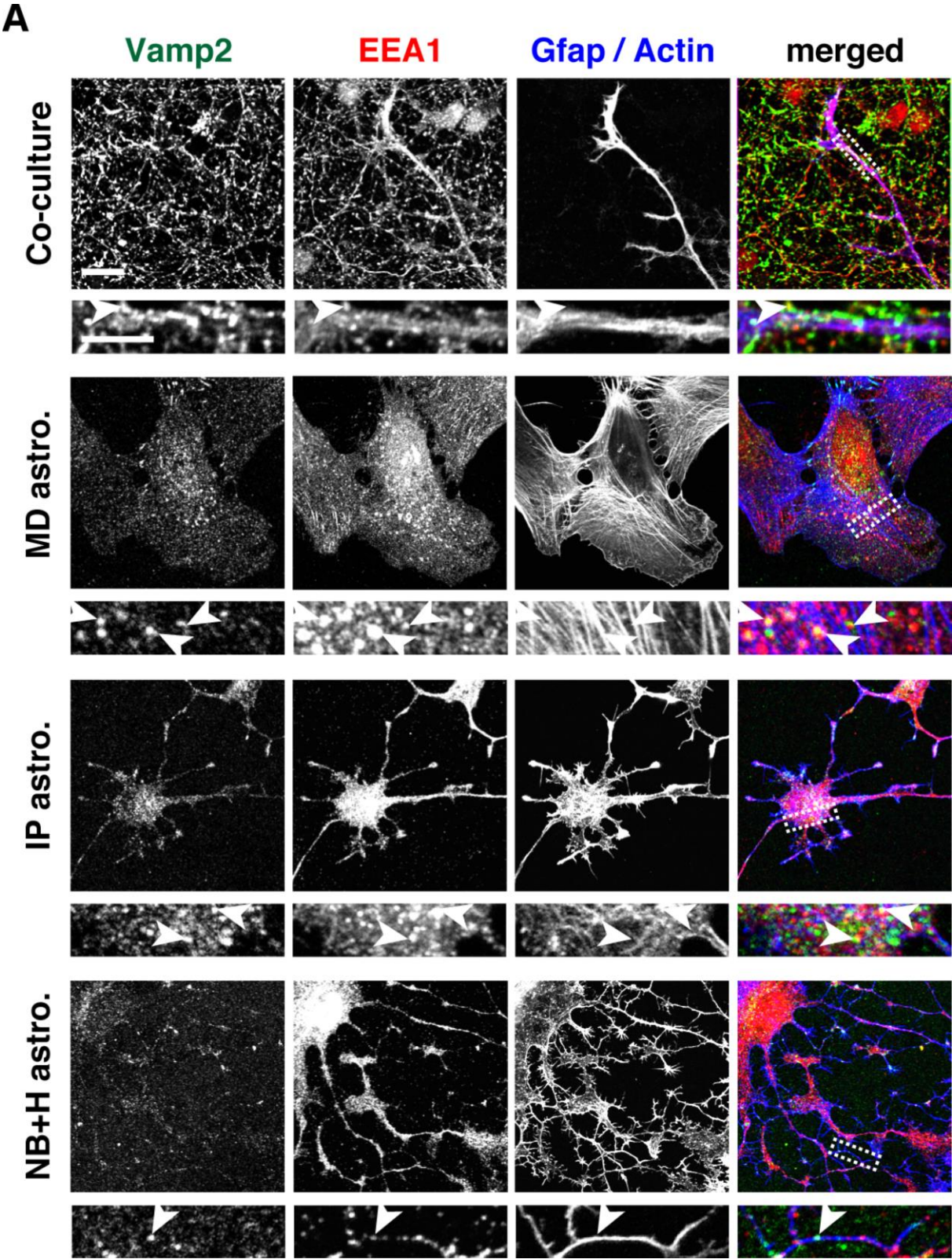
Fig. 16: Endogenous Vamp2 is distributed sparsely in astrocyte monocultures

Immunocytochemistry of DIV14 co-cultures and DIV16 MD, IP, and NB+H astrocytes comparing Vamp2 distribution, where Gfap labels astrocytes in co-cultures, and Actin labels all cells in astrocyte monocultures. In co-cultures, Vamp2 is also expressed by other cells (presumably neurones) surrounding astrocytes. Images per experiment: n=5 for all conditions. Scalebar = 10 μ m.

In neurones, Vamp2 is involved in exocytotic vesicle release (Schoch et al., 2001). Since regulated vesicle-mediated exocytosis is under debate in astrocytes, and only little evidence for specific exocytotic marker proteins in astrocytes exists (Fiacco et al., 2009), we first tested if Vamp2 is found on vesicles that recycle via exo- and endocytosis in astrocytes.

In neurones and HeLa cells, Vamp2 co-localises with endocytotic / recycling vesicles (Bonanomi et al., 2007; Koo et al., 2011; Zylbersztejn et al., 2012). Consistent with this, Vamp2 regulates endosomal vesicle fusion in rat kidney cells (Jo et al., 1995). Our co-immunostains of Vamp2 and the early endosomal protein EEA1 (a Vamp2-negative organelle) showed that co-cultures and astrocyte monocultures expressed both of these proteins (Fig. 17A). In co-cultures as well as IP and NB+H astrocytes, Vamp2 and EEA1 rarely co-localised. However, MD astrocytes showed several puncta positive for both Vamp2 and EEA1. The same was true in co-stains of Vamp2 and the late endosomal protein Rab7 (Fig. 17B), which co-localised in several puncta in MD astrocytes, but only rarely in co-cultures, IP, and NB+H astrocytes. This indicates that MD astrocytes differ from astrocytes cultured by other means in that Vamp2 was often found on (or very close to) endosomal vesicles in MD astrocytes.

In addition, all astrocyte culture types had more EEA1- and Rab7-positive puncta than Vamp2-positive puncta. Thus, only a small population of total EEA1- and Rab7-harboured endosomes co-localised with Vamp2.



(see next page for Figure legend)

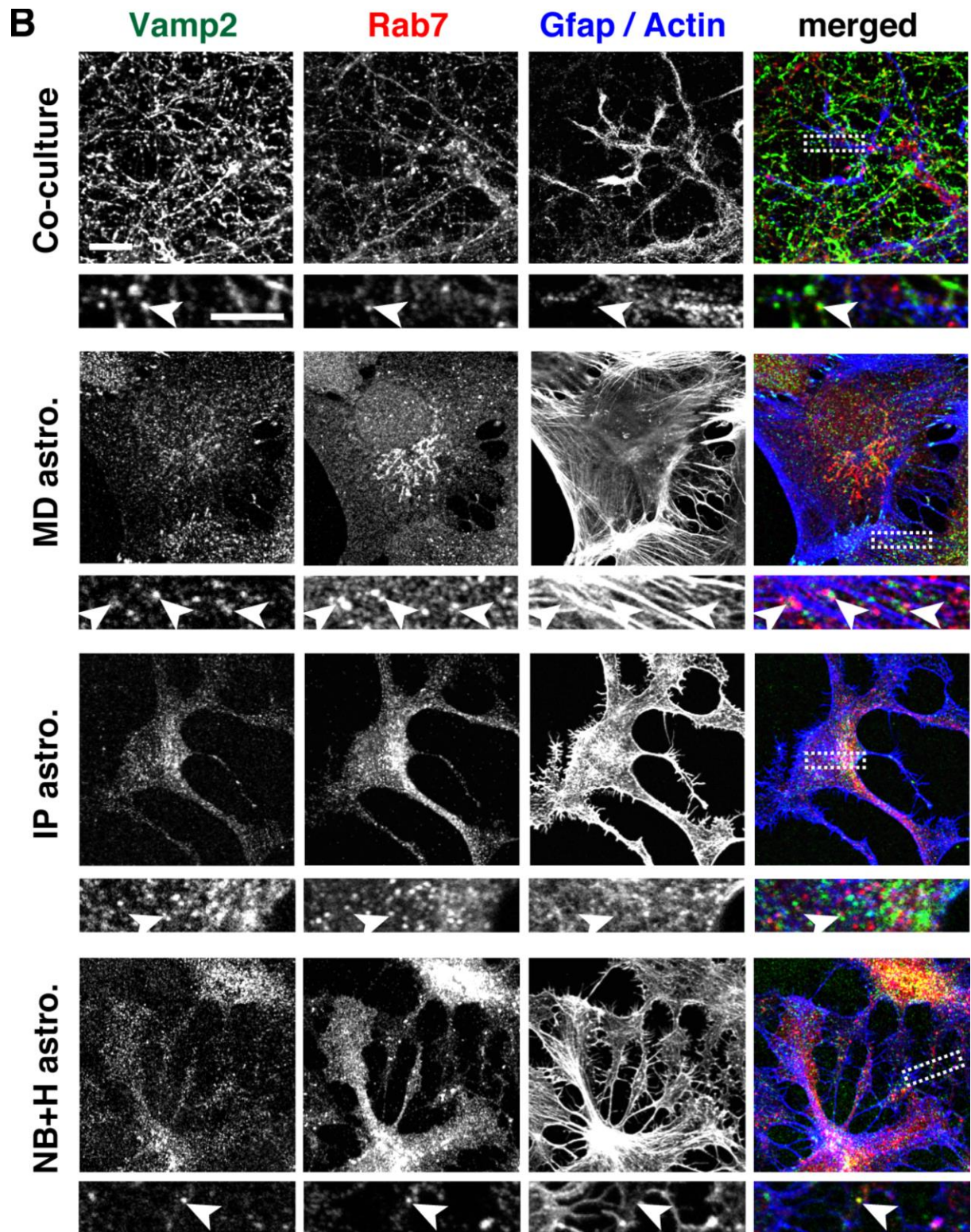


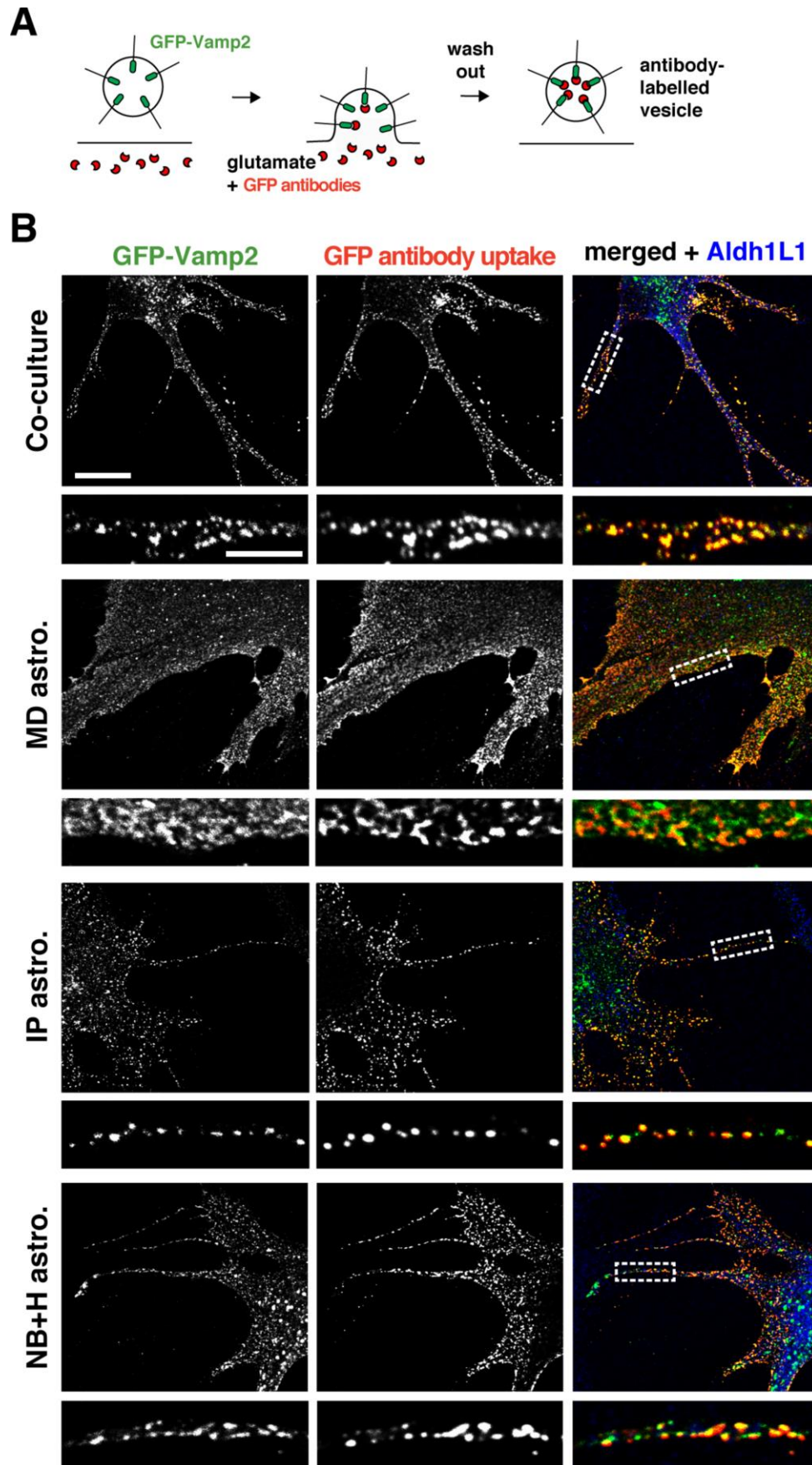
Fig. 17: Vamp2 partly co-localises with endosomal proteins in MD astrocytes

Immunocytochemistry of DIV14 co-cultures and DIV16 MD, IP, and NB+H astrocytes, where Vamp2, EEA1, and Rab7 antibodies label vesicle-associated proteins, early endosomes, and late endosomes, respectively, Gfap labels astrocytes in co-cultures, and Actin labels all cells in astrocyte monocultures. **A** Vamp2 co-localises with the early endosomal protein EEA1 and **B** the late endosomal protein Rab7 (arrowheads) in several areas of MD astrocytes, but only rarely in co-culture, IP, or NB+H astrocytes. Images per experiment: n=6 (co-culture), n=10 (MD, IP), n=11 (NB+H). Scalebar = 10 µm, 5 µm for zoom-ins.

To investigate Vamp2 function in astrocytes, we next performed an internalisation assay on astrocytes, by which recycling Vamp2-harboured vesicles can be identified. We transfected co-cultures, MD, IP, and NB+H astrocytes with GFP coupled to the luminal domain of Vamp2. Astrocytes expressing GFP-Vamp2 were stimulated by placing them in 50 μ M glutamate solution for 10 minutes to initiate vesicle fusion (as described in Bittner et al. (2011)). Anti-GFP antibodies present in the stimulation solution label GFP-Vamp2-harboured vesicles that recycle – where the GFP on the luminal domain of Vamp2 is exposed to the extracellular solution allowing GFP antibodies to bind before vesicles are endocytosed (as explained in Fig. 18A).

In all astrocyte culture preparations, the somata contained several puncta with transfected GFP-Vamp2 that showed no anti-GFP antibody uptake (Fig. 18B) as expected, since vesicle recycling occurs at the cell membrane. In astrocytic processes, however, most GFP-Vamp2-positive puncta were also labelled by anti-GFP antibodies, indicating antibody uptake via vesicle recycling. Notably, MD astrocytes featured no fine processes, and antibody uptake was less profound in the outer edges of MD astrocytes compared with thin astrocytic processes in other culture preparations.

We also performed a parallel experiment, in which we kept astrocytes in basal 2 mM KCl solution without stimulating them (Dallwig et al., 2000; Härtel et al., 2007). However, the staining pattern was similar to that following stimulation of astrocytes with 50 μ M glutamate (data not shown), suggesting that astrocytes constitutively recycle Vamp2-harboured vesicles. We next tested if antibody uptake in astrocytes of co-cultures would be inhibited at 4 °C, when vesicle recycling should be stalled. Compared with co-cultures at 37 °C, there was less co-localisation of total GFP-Vamp2 with anti-GFP antibodies at 4 °C, but a considerable amount of GFP antibody signal was still detected on cells at 4 °C (Fig. 18C). We also tested if anti-GFP antibodies label GFP-Vamp2 protein that remained at the cell surface at 37 °C by fixing –but not permeabilising– cells after the internalisation assay, and then adding a second anti-GFP antibody to label only extracellular GFP-Vamp2 domains (explained in Fig. 18D). However, only little GFP-Vamp2 was exposed to the extracellular space (Fig. 18E), so that much of the anti-GFP antibody uptake resulted from vesicle recycling or endocytosis.



(see next page for Figure legend)

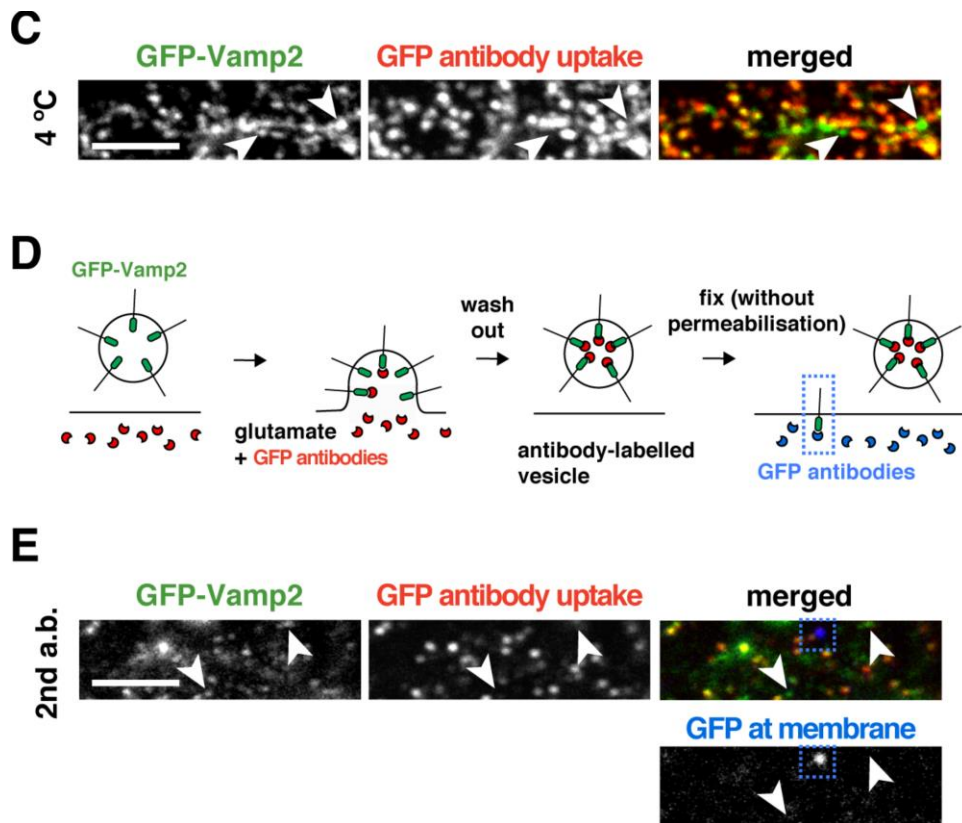


Fig. 18: Astrocytes recycle Vamp2-harboured vesicles in cell cultures

Internalisation assays show anti-GFP antibody uptake by astrocytes transfected with GFP-Vamp2 two days before the assay. **A** Schematic explaining the internalisation assay: GFP-Vamp2-harboured vesicles in live astrocytes that fuse with the cell membrane upon stimulation with 50 μ M glutamate solution expose their lumenally tagged GFP to the extracellular solution which contains anti-GFP antibodies that target GFP-Vamp2. These antibodies are then internalised in vesicles via endocytosis. **B** Immunocytochemistry of DIV14 co-cultures and DIV16 MD, IP, and NB+H astrocytes (identified by Aldh1L1) shows that transfected GFP-Vamp2 and anti-GFP antibodies that have been taken up by recycling GFP-Vamp2 vesicles are often distinct in the soma but co-localise in astrocytic processes. **C** Immunocytochemistry of the same experiment performed in DIV14 co-cultures at 4 °C shows slightly less uptake than at 37 °C (**A**); only few punctate regions stained positive for GFP-Vamp2 but negative for anti-GFP antibody uptake (white arrowheads). **D** Schematic explaining how in **E**, DIV14 co-cultures were fixed without permeabilising the membrane, so that a second antibody (2nd a.b.) labelled only GFP-Vamp2 at the membrane. In this assay, very little GFP-Vamp2 was found at the membrane (blue dashed square), and only few puncta stained positive for GFP-Vamp2 but negative for anti-GFP antibody uptake (white arrowheads). Images per experiment: n=6 for all conditions. Scalebar = 10 μ m, 5 μ m for zoom-ins.

We next tested if vesicle recycling was blocked by cleaving Vamp2 with tetanus toxin. We treated cultures with tetanus toxin light chain peptides (TeNT) to cleave Vamp2, which results in blockade of vesicle recycling via the SNARE proteins (Schiavo et al., 2000), but does not cleave the luminal GFP domain coupled to Vamp2-harboured vesicles (explained in Fig. 19A). We initially set up co-cultures, MD, IP, and NB+H astrocytes for this experiment, but IP astrocytes did not survive the transfection and TeNT treatment.

When TeNT was applied to cultures, astrocytes showed a drastic decrease in anti-GFP antibody uptake (Fig. 19B): Co-culture, MD, and NB+H astrocytes still expressed puncta positive for transfected GFP-Vamp2, but showed only little or (as in the case of MD astrocytes) no antibody uptake at all. Therefore, TeNT blocked the function of transfected Vamp2 in astrocytes.

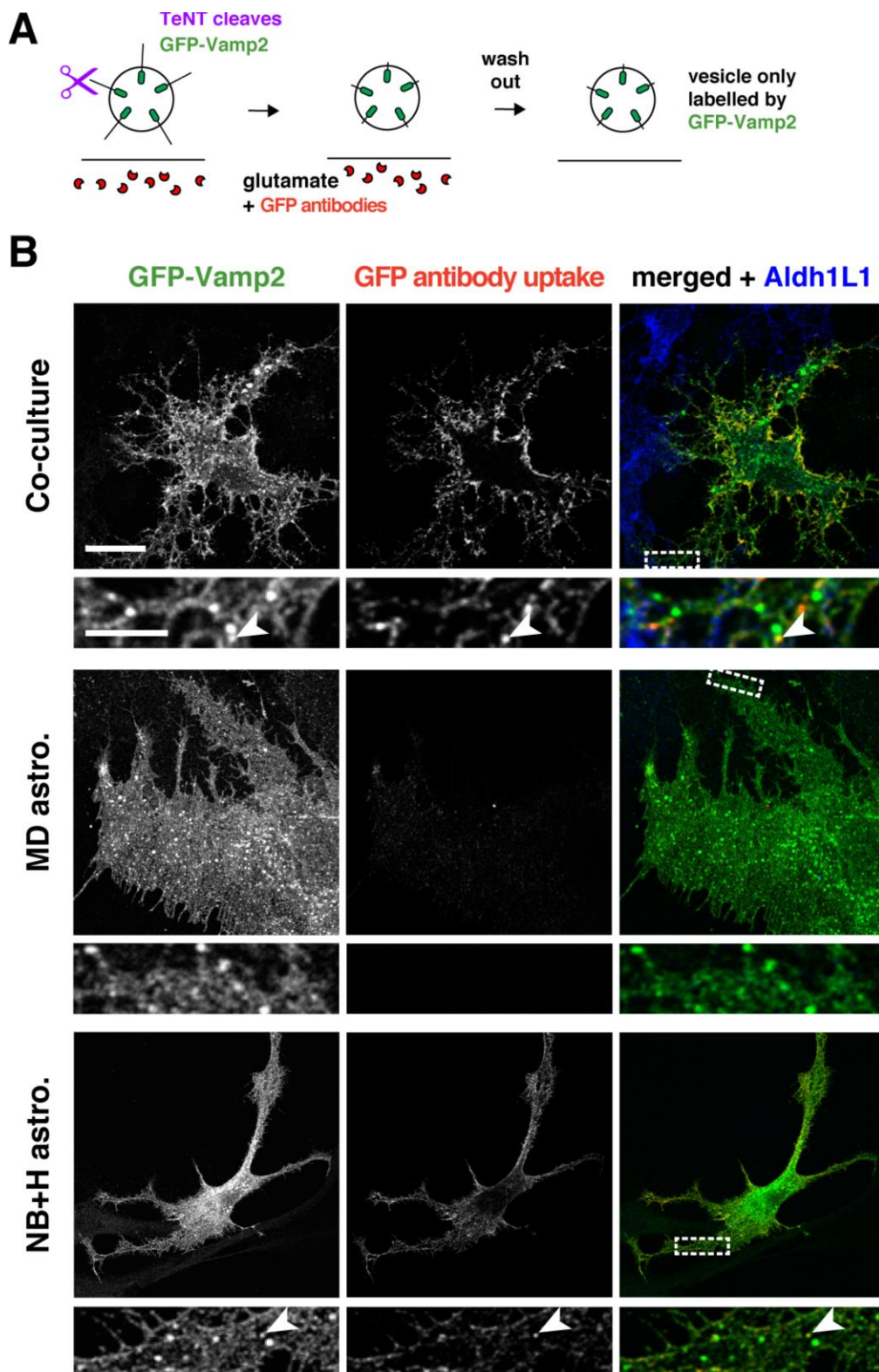


Fig. 19: TeNT blocks GFP-Vamp2 vesicle recycling in astrocytes in vivo

Internalisation assay showing almost no antibody uptake by astrocytes transfected with GFP-Vamp2 and tetanus toxin light chain peptides (TeNT). **A** Schematic explaining how Vamp2 in GFP-Vamp2-harboured vesicles is cleaved by TeNT in live astrocytes. Vesicles can then no longer fuse with the cell membrane. **B** Immunocytochemistry of DIV14 co-cultures and DIV16 MD, and NB+H astrocytes (as identified by Aldh1L1) shows that transfected GFP-Vamp2 and GFP antibody uptake only rarely co-localise (arrowheads) in astrocyte processes. Images per experiment: n=8 (co-culture), 19 (MD), 17 (NB+H). Scalebar = 10 μ m, 5 μ m for zoom-ins.

4.2.4 Syt-harboured vesicles: Localisation and recycling

The structure of a synapse shows how closely astrocytes are associated with neurones: Fine astrocytic processes engulf neuronal synapses, where astrocytes take up excess neurotransmitter, but also release glial factors (Hamilton and Attwell, 2010; Parpura and Zorec, 2010). We found that our “*in vivo*-like” cultured astrocytes not only developed fine processes, but also exhibited distinct Ca^{2+} events in those processes (Fig. 13).

On a molecular level, we found that astrocytes expressed the vesicle-associated proteins syntaxin1 and Vamp2, which were previously suggested to form SNARE complexes for regulated vesicle release in astrocytes (Maienschein et al., 1999). In agreement with these observations, we found that Vamp2-harboured vesicles were recycled in fine astrocyte processes, and this recycling was blocked when TeNT cleaved Vamp2. In neurones, the SNARE complex initiates vesicle fusion in response to a local $[\text{Ca}^{2+}]$ rise (Jahn and Fasshauer, 2012), which is detected by Syt1 and 2. Since astrocytes express mRNA of different Syt isoforms *in vivo* (Mittelsteadt et al., 2009), we next investigated whether cultured astrocytes express Syt protein.

First, we tested if astrocytes express Syt isoforms for which mRNA was previously found in astrocytes by Mittelsteadt et al. (2009): The authors found that astrocytes express Syt4, 7, and 11; we further assessed Syt17 as a previously untested candidate. Indeed, we found Syt4, 7, 11, and also Syt17 protein in astrocyte monocultures, but not Syt1, 3, or 5 by Western blot analysis (Fig. 20). Syt7 antibodies detected multiple bands, consistent with multiple Syt7 splice isoforms as reported by Fukuda et al. (2002).

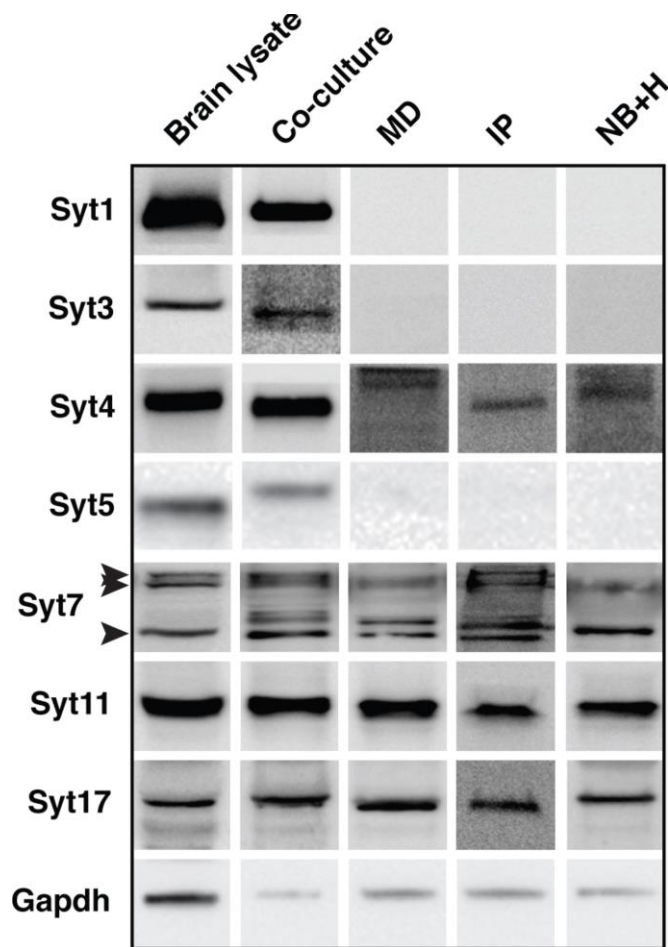


Fig. 20: Astrocytes express several synaptotagmin isoforms

Western blot analysis of adult rat brain lysate compared with DIV14 co-culture, MD, IP, or NB+H astrocyte monoculture lysates. Several synaptotagmin (Syt) isoforms appear in astrocyte monocultures, i.e. Syt4, 7, 11, and 17, but not Syt1, 3, or 5. As previously reported by Fukuda et al. (2002), Syt7 has multiple splice isoforms, here at 46, 70, and \approx 80 kDa (arrowheads). Gapdh is used as a loading control.

Next, we focused on Syt subcellular distribution in astrocytes, for which we compared two anti-Syt7 antibodies by immunocytochemistry and Western blot analysis of wild-type (Wt) and *Syt7*^{-/-} samples (Fig. 21). Only one of the antibodies (raised in rabbit) targeted proteins in a punctate pattern both in neurones and astrocytes from co-cultures (Fig. 21A). When applying the same antibody to Wt or *Syt7*^{-/-} co-cultures, a punctate staining pattern appeared only in Wt cultures (Fig. 21B). Similarly, the same antibody detected Syt7 protein in *Syt7*^{+/+} and *Syt7*^{+/-}, but not *Syt7*^{-/-} mouse brain lysate (Fig. 21C). One band of low signal intensity appeared in all brain lysate samples, but this was below 45 kDa, at which Syt7 bands have not been reported. In summary, the Syt7 antibody raised in rabbit recognized Syt7 protein specifically both in immunostainings and Western blots.

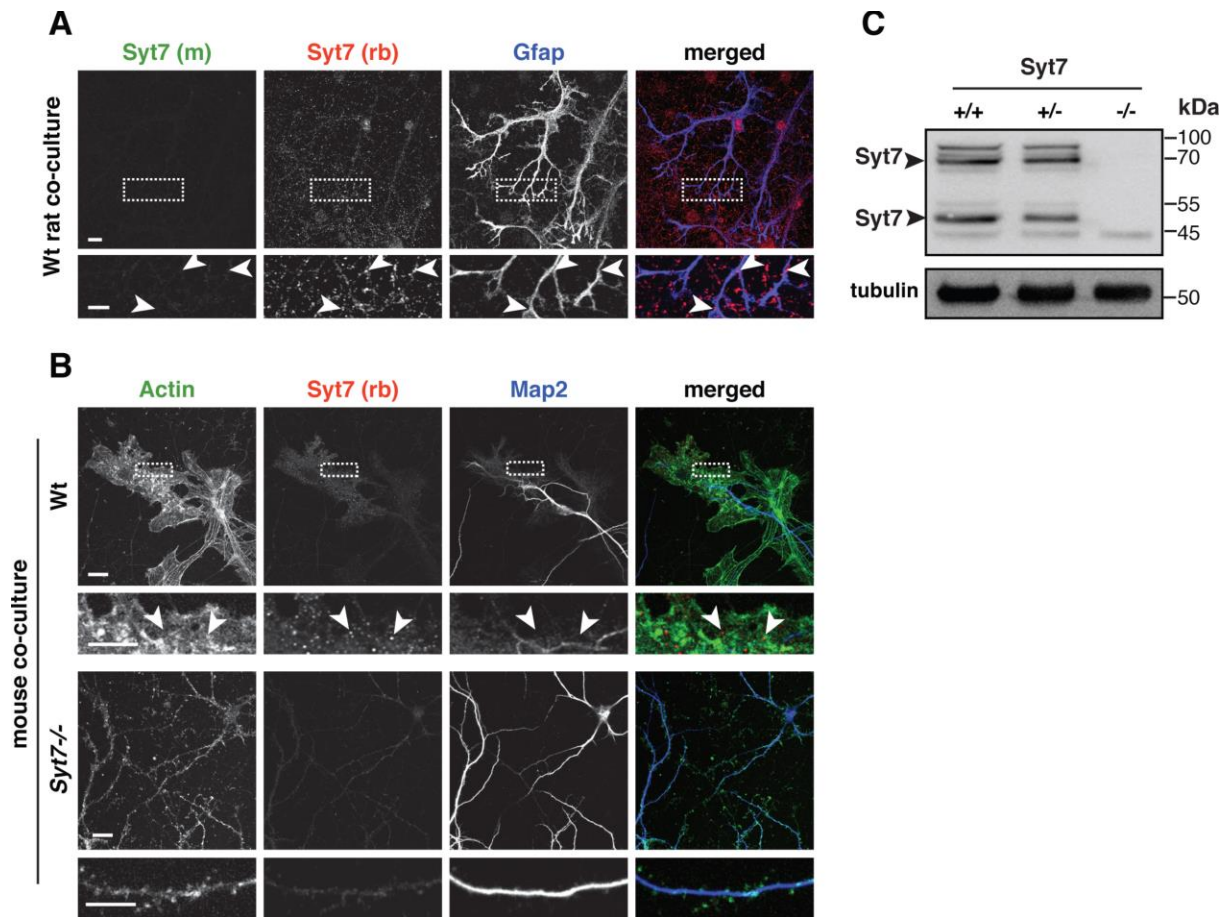


Fig. 21: Testing Syt7 antibodies on Wt and Syt7^{-/-} samples

A Immunocytochemistry of DIV14 rat wild-type (Wt) co-cultures stained for Syt7 using mouse monoclonal (m) and rabbit polyclonal (rb) antibodies, and Gfap. In zoomed-in images, punctate Syt7 (rb) staining co-localises with Gfap staining (arrowheads) but also appears in neighbouring, unlabelled neuronal processes; no structures are stained by the Syt7 (m) antibody. **B** Immunocytochemistry of DIV14 mouse Wt versus Syt7^{-/-} co-cultures stained for Actin, Syt7 (rb), and the neuronal marker Map2. The Syt7 (rb) antibody labels punctate structures in Wt (arrowheads) but not Syt7^{-/-} cells. **C** Western blot showing multiple Syt7 splice isoforms in adult brain lysate of Syt7^{+/+} and Syt7^{+/-} but not Syt7^{-/-}, where tubulin serves as a loading control. Images per experiment: n=5 (**A**), 13 (**B**, Wt), 12 (**B**, Syt7^{-/-}). Scalebar = 10 µm, 5 µm for zoom-ins.

To test if Syts can be localised in astrocytes *in vivo*, we first tested a negative control using Syt1 (which is not expressed by astrocytes). However, in brain slices from perfused Wt mice (Fig. 22), Syt1 puncta seemingly co-localised with astrocytic processes, illustrating that this approach created false positive signals. Due to these methodological limitations, we did not pursue immunohistological stainings for other Syt isoforms and used our newly developed “*in vivo-like*” astrocyte culture method to test Syt localisation in cultured astrocytes instead.

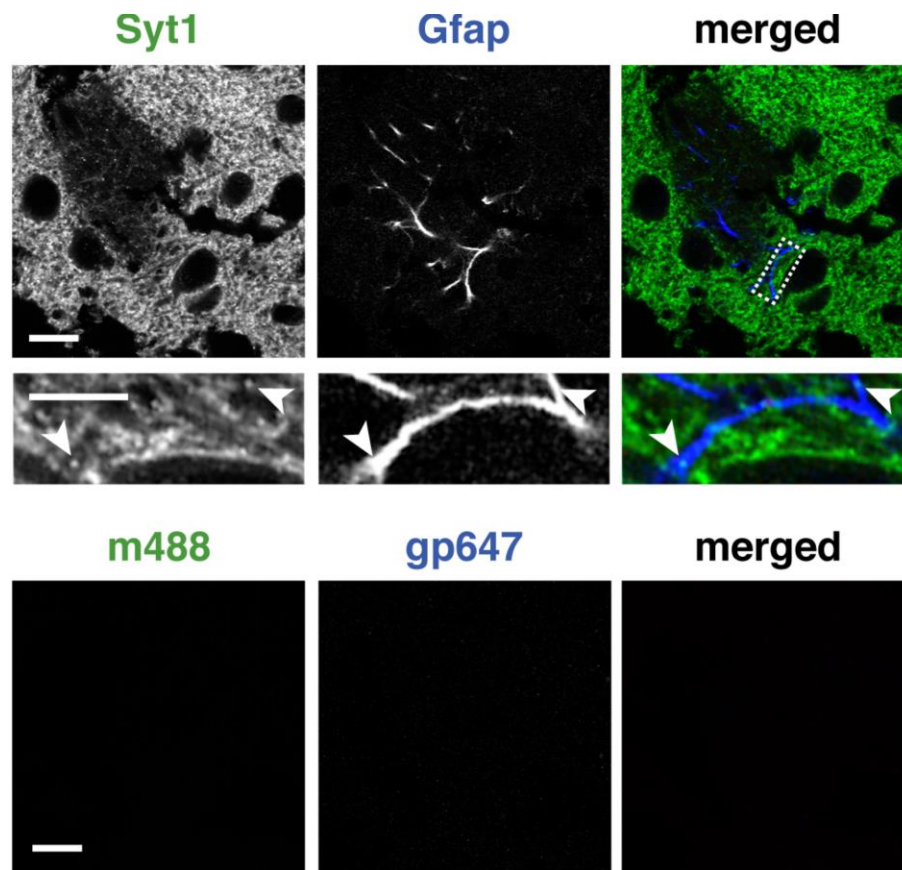


Fig. 22: Syt1 expression near astrocytes *in vivo*

Immunohistochemistry of coronal cortical sections from perfused adult Wt mice showing Syt1 and Gfap distribution. In the zoomed-in images, Syt1 puncta appear to co-localise with the astrocyte-specific Gfap (arrowheads). Control immunohistochemistry of goat anti-mouse AlexaFluor488-conjugated (m488) or goat anti-guinea pig AlexaFluor647-conjugated (gp647) secondary antibodies. Images per experiment: n=5 for all conditions. Scalebar = 20 μ m, 10 μ m for zoom-ins.

According to the Western blot in Fig. 20, astrocytes express Syt4, 7, 11, and 17. We therefore analysed the distribution of these four Syt isoforms via immunocytochemistry in co-culture and NB+H astrocytes, which developed fine processes in culture and showed similar Ca^{2+} signalling profiles (Fig. 13). For all four Syt isoforms, we found punctate staining patterns (Fig. 23). In co-cultures, astrocytes and neurones both expressed these Syt isoforms, where Syt17 staining was more prominent in astrocytes than in neurones. In addition, a subset of astrocytes (about one third of all astrocytes) expressed high levels of Syt4, 7, and 11 in both culture types, whereas Syt17 was ubiquitously expressed amongst all astrocytes (personal observation). These data confirm the Western blot analysis in Fig. 20, i.e. astrocytes express at least four different Syt isoforms in cell cultures.

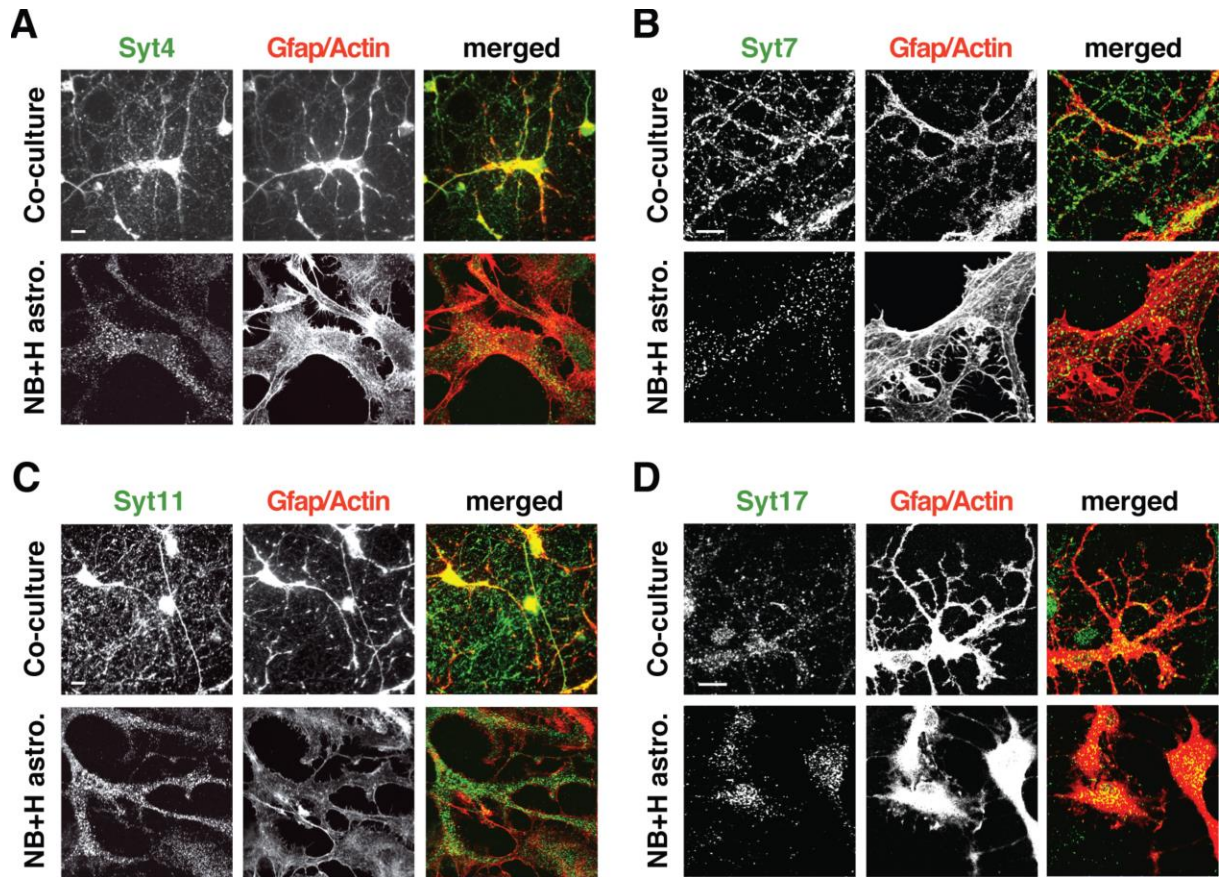


Fig. 23: Syt staining appears punctate in co-culture and NB+H astrocytes

Immunocytochemistry of Syt isoforms with Gfap (to label astrocytes in DIV14 co-cultures) or Actin (to label all cells in DIV16 NB+H astrocyte monocultures). Punctate staining for Syt4 (A), Syt7 (B), Syt11 (C), and Syt17 (D) appears in astrocytes of all cultures. Images per experiment: n=3 (co-cultures in A, C, D), 6 (co-culture in B), 5 (NB+H in A, D), 3 (NB+H in B, C). Scalebar = 10 µm.

Since the staining patterns of all four Syt isoforms were punctate just like the staining pattern of Vamp2, and both protein classes are involved in vesicle fusion (Lang and Jahn, 2008; Südhof, 2002), we next tested if Syts and Vamp2 co-localise in astrocytes. In co-stainings of Syt4, 7, 11, or 17 with Vamp2, we found that these Syts and Vamp2 do not localise to the same vesicles (puncta) in astrocytes (Fig. 24A). In co-cultures, Syt1 co-localised with Vamp2 in neurones, but not with Aldh1L1 that marked astrocytic processes. To test if even a small subpopulation of Vamp2-harboured vesicles contained any Syt isoforms in addition, we analysed the images using MetaMorph co-localisation analysis software (Fig. 24B). This co-localisation analysis confirmed our observations, i.e. Vamp2 did not co-localise with Syt4, 7, 11, or 17 in astrocytes (but did colocalise with Syt1 in neurones). This implies that Vamp2 and Syts are found on distinct vesicles / organelles in astrocytes.

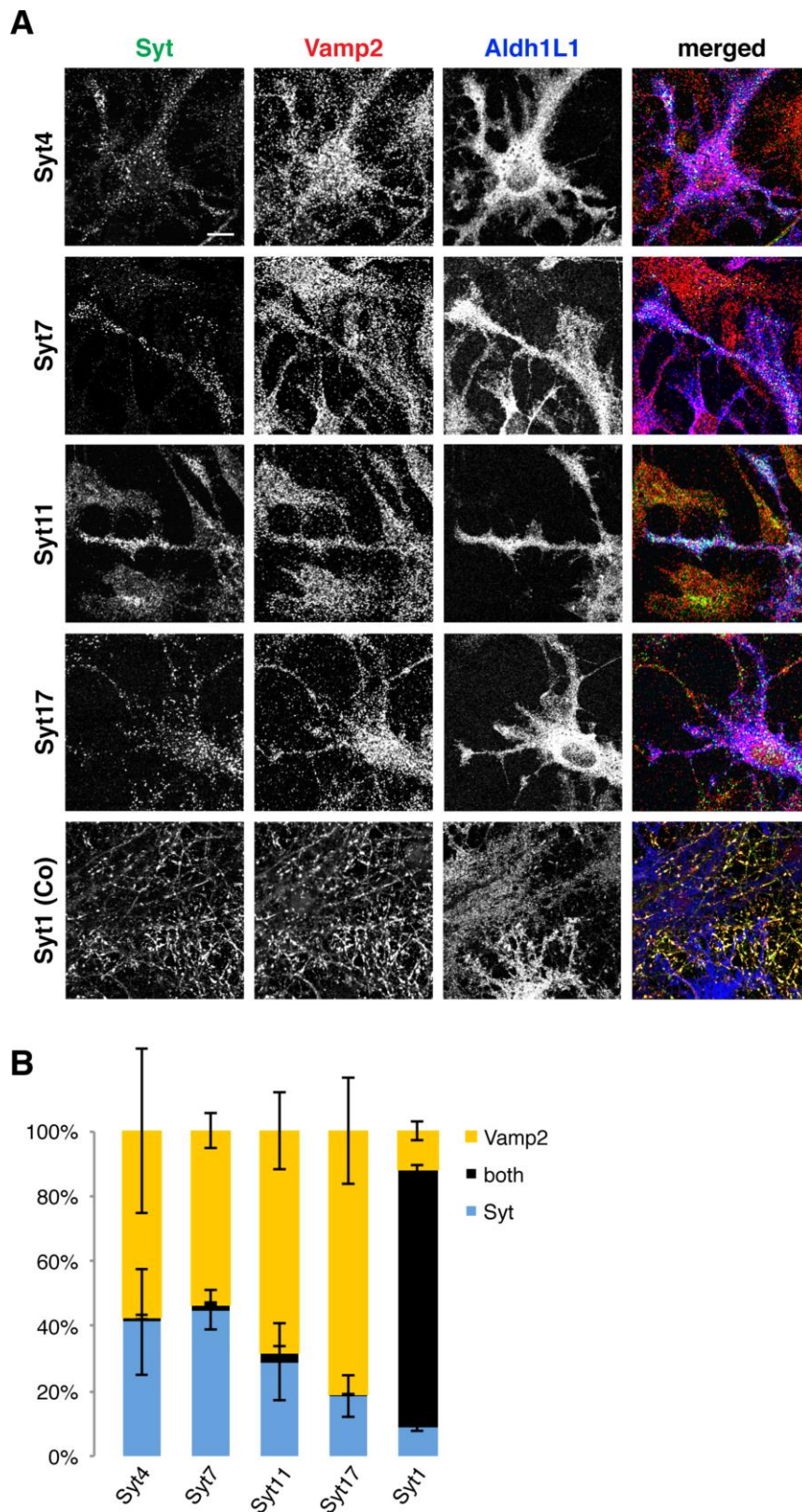


Fig. 24: Syts do not co-localise with Vamp2 in NB+H astrocytes

A Immunocytochemistry to detect if Syt isoforms co-localise with Vamp2 in DIV16 NB+H astrocytes, where staining for Syt1 and Vamp2 in DIV14 co-cultures serves as a positive control; Aldh1L1 labels astrocytes. In NB+H astrocytes, there is almost no co-localisation of Syt4, 7, 11, or 17 with Vamp2, whereas most Syt1 puncta in co-cultures co-localise with Vamp2. **B** Bar graphs represent percentages of Syt puncta, Vamp2 puncta, and puncta positive for both as found by co-localisation analysis using MetaMorph software. Images per experiment: n=7 (Syt4), 8 (Syt7), 6 (Syt11), 7 (Syt17), 4 (Syt1). Scalebar = 10 μ m.

Unlike Vamp2, several Syt isoforms are considered Ca^{2+} sensors, including Syt7 and 17 (Bhalla et al., 2005, 2008). If any Syts are involved in Ca^{2+} -dependent exocytosis in astrocytes, they may be located on small exocytotic vesicles as in neurones, or on lysosomes: Previous work reported lysosomes as the main vesicular organelle involved in astrocytic exocytosis (Li et al., 2008). Moreover, studies in rat kidney cells and mouse embryonic fibroblasts revealed Syt7 as a crucial regulator of Ca^{2+} -dependent lysosomal exocytosis (Jaiswal et al., 2004; Rao et al., 2004). To assess if Syt7 also mediates lysosomal exocytosis in astrocytes, we tested whether Syt7 co-localises with lysosome-associated membrane glycoprotein 1 (Lamp1) (Fig. 25). However, Syt7 and Lamp1 did not co-localise. Thus, we considered the possibility that Syt7 is associated with small exocytotic vesicles in astrocytes.

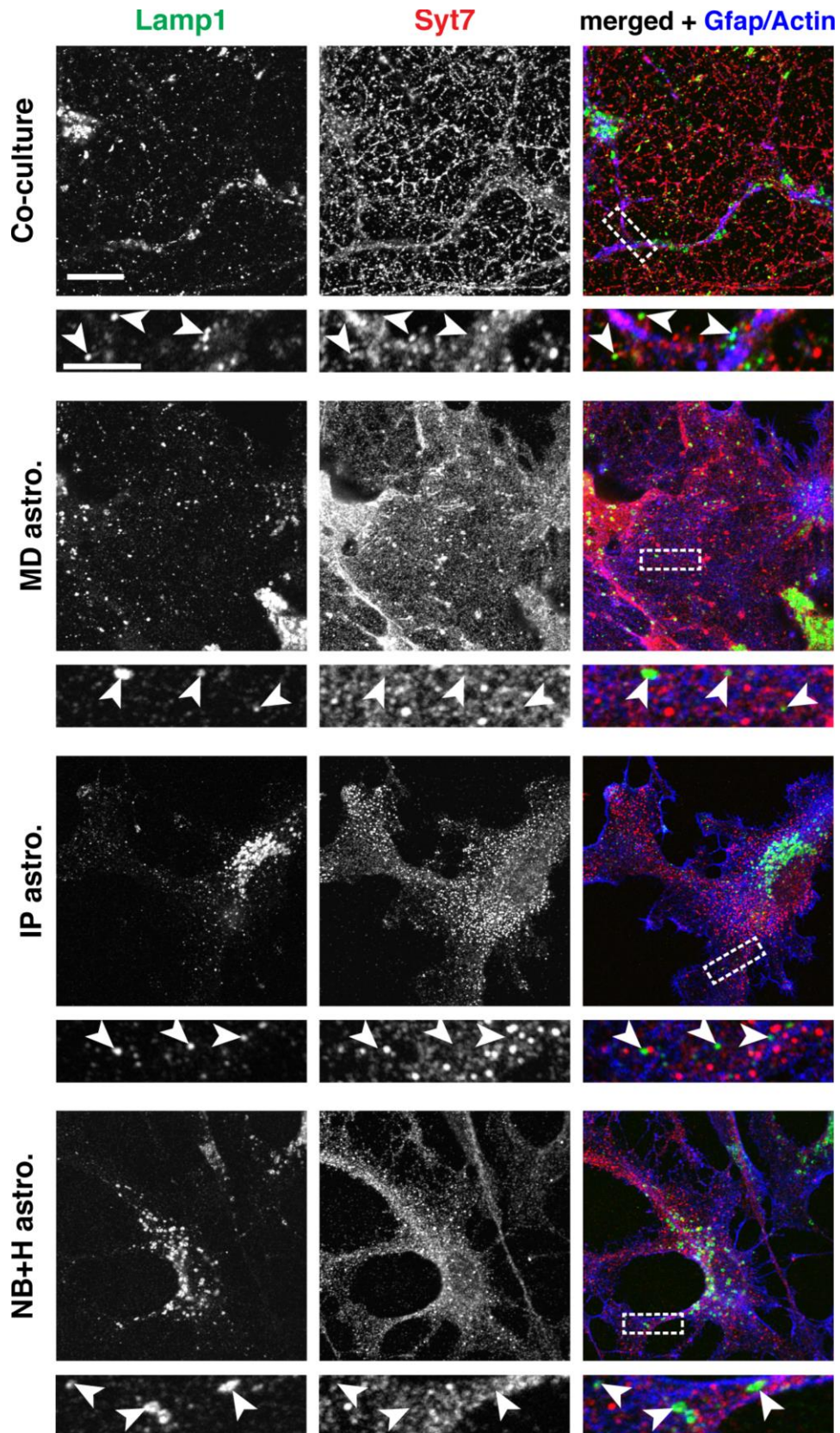


Fig. 25: Syt7 and Lamp1 do not co-localise in astrocytes

Immunocytochemistry of DIV14 co-cultures and DIV16 MD, IP, and NB+H astrocytes to detect if Syt7 co-localises with the lysosomal protein Lamp1 in astrocytes; Aldh1L1 labels astrocytes in co-cultures, Actin labels all cells in astrocyte monocultures. Syt7 and Lamp1 do not co-localise (arrowheads). Images per experiment: n=6 for all conditions. Scalebar = 10 μ m, 5 μ m for zoom-ins.

4.2.4.1 *Syt7 vesicle recycling*

In endocrine cells, Syt7 was reported to act as a high-affinity Ca^{2+} sensor, and was found on large dense core vesicles (and lysosomes) (Wang et al., 2005). In neuroendocrine cells, Syt7 was found to regulate the dynamics of vesicle fusion pores that open and expand during exocytosis (Segovia et al., 2010), thus affecting the stability of fusion pores and if vesicles undergo transient or full fusion. To test recycling of Syt7-harboured vesicles, we performed antibody internalisation assays as before (Fig. 18) by stimulating astrocytes transfected with GFP-Syt7 (Fig. 26) in the presence of extracellular solution containing GFP antibodies.

In response to 50 μM glutamate solution, GFP-Syt7-transfected astrocytes showed anti-GFP antibody uptake, with the same uptake pattern under unstimulated conditions (data not shown). Compared to previous internalisation assays, GFP-Syt7-transfected astrocytes displayed slightly less anti-GFP antibody uptake (i.e. vesicle recycling) than GFP-Vamp2-transfected astrocytes (Fig. 18).

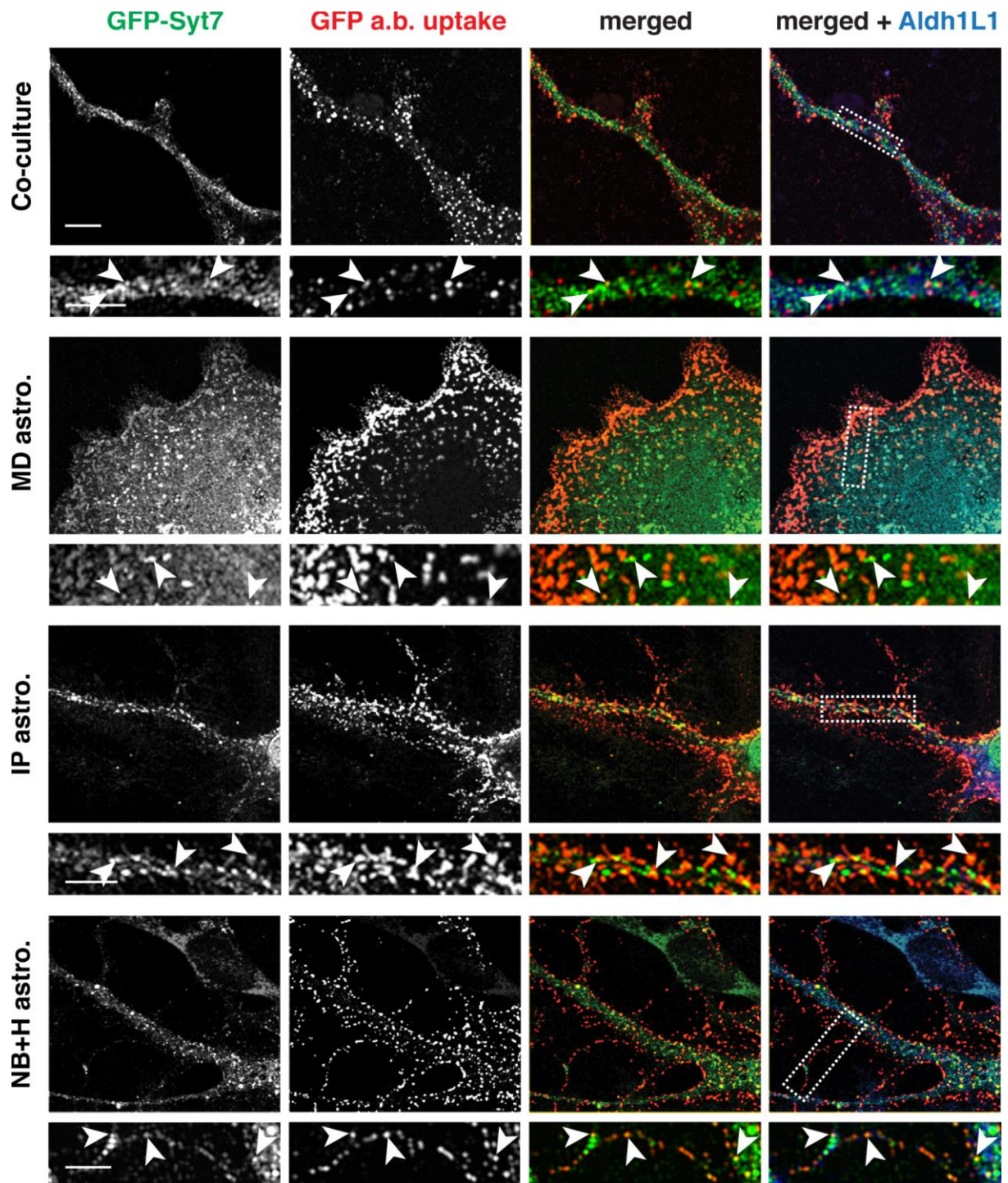


Fig. 26: Astrocytes recycle some Syt7-harboring vesicles

Internalisation assay showing antibody uptake by astrocytes transfected with GFP-Syt7 when stimulated with 50 μ M glutamate solution (see schematic in Fig. 11A). Immunocytochemistry of DIV14 co-cultures and DIV16 MD, IP, and NB+H astrocytes (as identified by Aldh1L1) shows that some puncta positive for GFP-Syt7 co-localise with antibody uptake staining (arrowheads). MD astrocytes show anti-GFP antibody uptake in the cell periphery, whereas co-culture, IP, and NB+H astrocytes possess thin processes in which anti-GFP antibody was taken up. Images per experiment: n=8 (co-culture), 6 (MD), 3 (IP), 7 (NB+H). Scalebar = 10 μ m, 5 μ m for zoom-ins.

To exclude that anti-GFP antibody is taken up by endosomes without being bound to its GFP antigen, we also transfected astrocytes with GFP-Syt17 (Fig. 27) – since Syt17 lacks a transmembrane domain, this GFP-Syt17 fusion protein is not exposed to the lumen of vesicles (although it is membrane-associated (Craxton, 2010)). Thus, anti-GFP antibodies would have no access to GFP antigens on GFP-Syt17 protein. Indeed, we found no co-localisation of GFP-Syt17 with anti-GFP antibodies following the internalisation assay in stimulated (Fig. 27) or unstimulated conditions (data not shown).

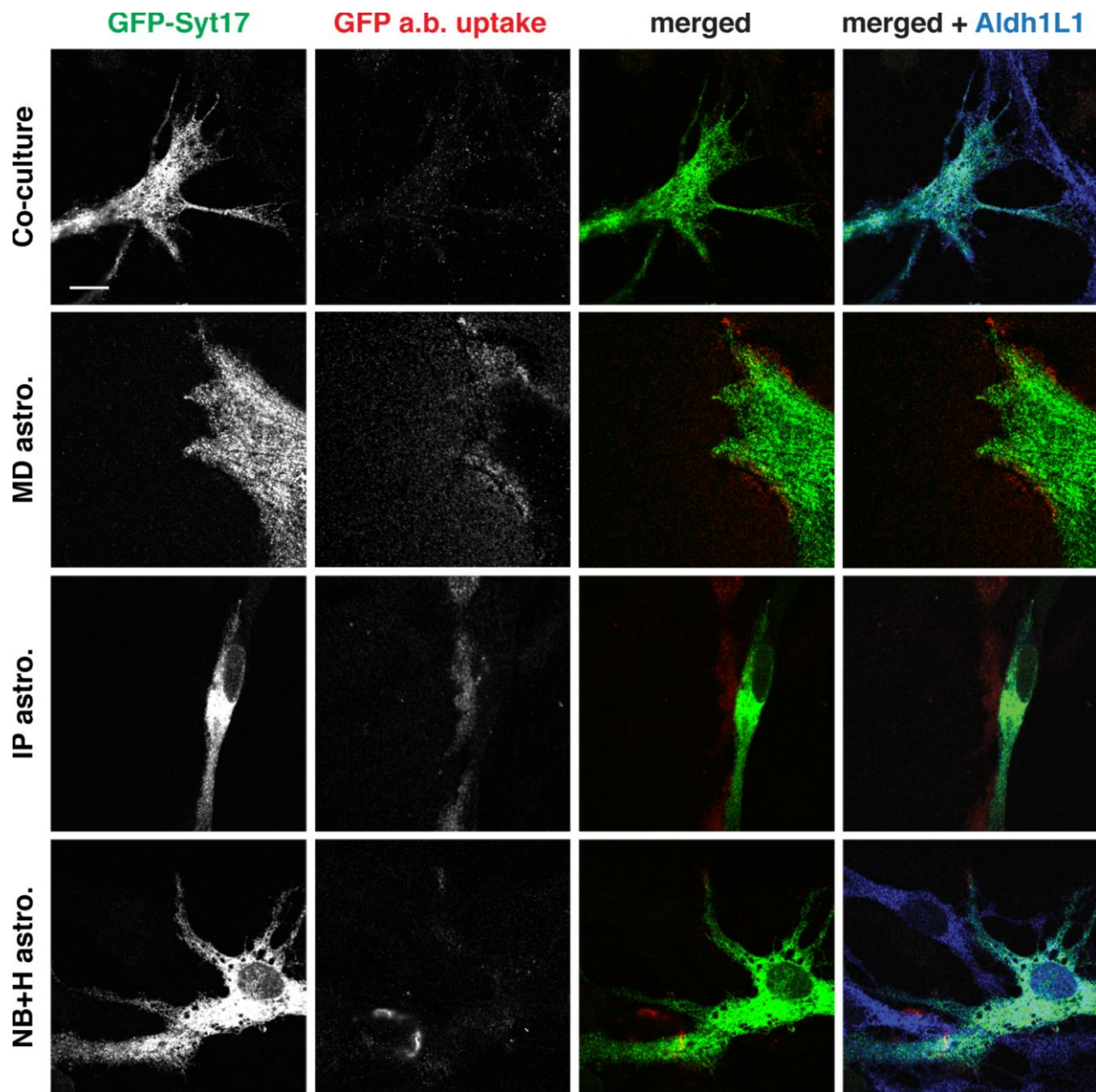


Fig. 27: Astrocytes do not take up anti-GFP antibodies via GFP-Syt17-harboured vesicles

Internalisation assay to test for GFP antibody uptake by astrocytes transfected with GFP-Syt17 when stimulated with 50 μ M glutamate solution (see schematic in Fig. 11A). Immunocytochemistry of DIV14 co-cultures and DIV16 MD, IP, and NB+H astrocytes (as identified by Aldh1L1) shows no GFP antibody uptake, as Syt17 lacks a transmembrane domain and GFP-Syt17 can therefore not be incorporated as an integral vesicle membrane protein (with GFP in the lumen) like Syt7 (Fig. 26). Images per experiment: n=4 (co-culture), 6 (MD), 3 (IP), 6 (NB+H). Scalebar = 10 μ m.

4.3 Syt7 in development and synaptogenesis

4.3.1 Syt7 is developmentally regulated in astrocytes

In Syt7 immunostainings, we noticed that 3-week-old astrocytes contained fewer Syt7 puncta than 2-week-old astrocytes (Fig. 23). To follow up this observation, we compared Syt7 staining in DIV16 and DIV21 IP and NB+H astrocyte monocultures, since these were morphologically closer to astrocytes *in vivo* than MD astrocytes, but lacked neurones that also express Syt7. As observed in preliminary tests, astrocytes expressed more Syt7 on DIV14 than on DIV21 in immunostains of both IP and NB+H astrocytes (Fig. 28A). Quantification revealed that Syt7 puncta were significantly more numerous in DIV14 astrocytes than DIV21 (Fig. 28B). To test whether this reflected a decrease in Syt7 protein levels during development, we analysed NB+H astrocytes grown in culture for 9, 14, and 21 days by Western blot (Fig. 28C). Here, DIV14 astrocytes expressed the highest levels of the Syt7 isoform of 46 kDa (matching the predicted molecular weight of Syt7 (Uniprot Consortium, 2012)), whereas the Syt7 levels of isoform 46 were decreased in DIV9 and DIV21 astrocytes.

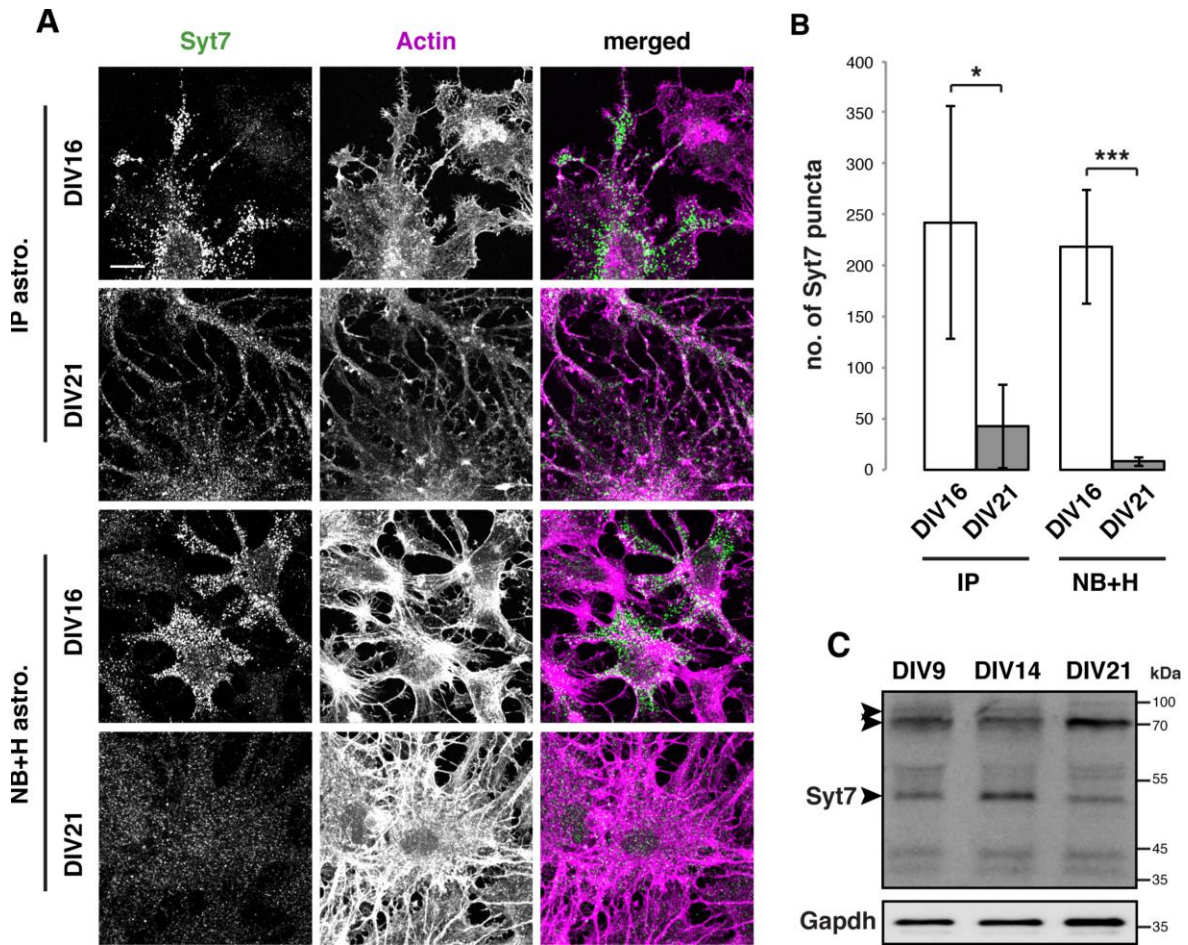


Fig. 28: Syt7 is developmentally regulated in astrocytes

Comparing Syt7 expression in IP and NB+H astrocytes on DIV16 versus DIV21. **A** Immunocytochemistry showing Syt7 and Actin staining, where Syt7 is punctate and expressed at higher levels on DIV16 than on DIV21. **B** Bar graph showing absolute numbers of Syt7 puncta in DIV16 versus DIV21 IP and NB+H astrocytes. **C** Western blot analysis of Syt7 expressed by NB+H astrocytes on DIV9, DIV14, and DIV21. As previously reported, multiple Syt7 splice isoforms appear, of which the 46 kDa isoform (which is missing in *Syt7*^{-/-} mice) is expressed at higher levels on DIV14. Images per experiment: n=4 (DIV16), 3 (DIV21). Error bars: SEM, * = $p < 0.05$, *** = $p < 0.001$ by unpaired two-tailed Student's t test. Scalebar = 10 μ m.

4.3.2 Synapse number decreases when astrocytes lack Syt7

Both immunocytochemistry and Western blot analysis showed that Syt7 expression was upregulated in astrocytes after two weeks in culture. In cultured neurones, synapses form and stabilise between DIV10 and DIV14 (Goslin et al., 1990), suggesting that Syt7 is expressed at the right time to be involved in synaptogenesis. To investigate a role of Syt7 in synapse formation, we plated Wt neurones on either Wt astrocytes or *Syt7^{-/-}* astrocytes (Fig. 29A). In contrast to Wt co-cultures, neurones grown on *Syt7^{-/-}* astrocytes showed fewer Syp puncta, which mark synapses. Quantification confirmed this, where synapse number significantly decreased by half depending on whether astrocytes expressed Syt7 (Fig. 29B).

To analyse if not only synapse number, but also synapse function was impaired in co-cultures with *Syt7^{-/-}* astrocytes, we stimulated co-cultures containing Wt astrocytes or containing *Syt7^{-/-}* astrocytes with 50 mM KCl solution that contained anti-Syt1 luminal domain antibodies. As in the previous internalisation assays, anti-Syt1 antibodies only bind to the luminal domain of Syt1 upon Syt1 vesicle fusion with the membrane, thus reporting Syt1 (synaptic) vesicle recycling. In both co-culture types, most Syp-positive puncta co-localised with anti-Syt1 antibodies (Fig. 29C). The number of Syp- and Syt1-positive puncta following the internalisation assay was significantly decreased in Wt neurones cultured on *Syt7^{-/-}* astrocytes, compared to Wt neurones on Wt astrocytes. Thus, neurones co-cultured with *Syt7^{-/-}* astrocytes featured fewer but functional synapses (as assessed by the internalisation assay) compared with neurones co-cultured with Wt astrocytes.

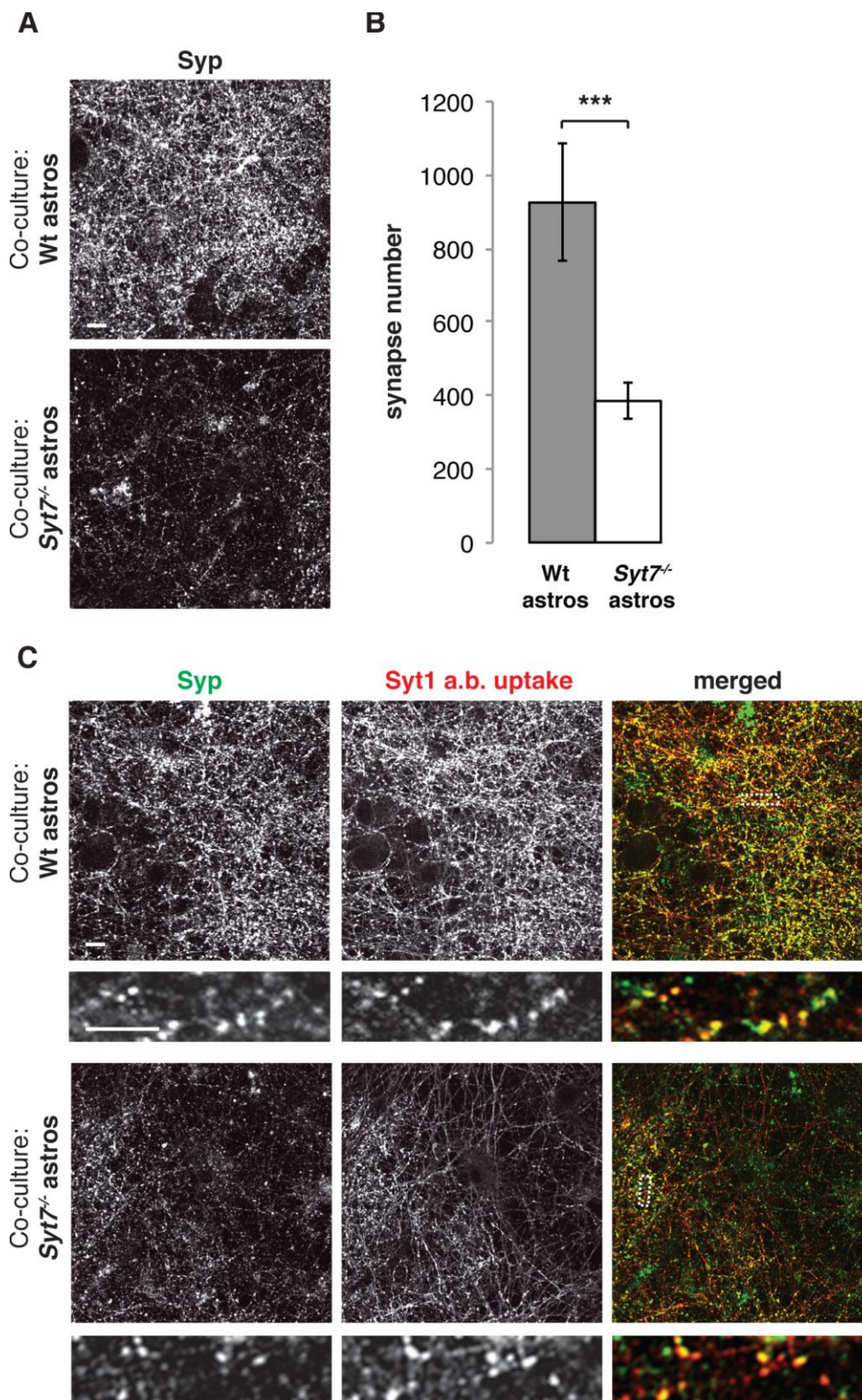


Fig. 29: Neurons have fewer synapses when grown on Syt7^{-/-} astrocytes

A Immunocytochemistry showing synapse distribution by synaptophysin (Syp) staining in DIV14 Wt neurones co-cultured with Wt or Syt7^{-/-} astrocytes. **B** Bar graph comparing absolute synapse numbers between the two conditions shown in **A**. **C** Internalisation assay showing Syt1 antibody uptake by DIV14 neurones grown on Wt or Syt7^{-/-} astrocytes when stimulated with 50 mM KCl solution. Syt1 antibody uptake co-localises with Syp staining (arrowheads). Images per experiment: n=10 for all conditions. Error bars: SEM, ***= $p < 0.001$ by unpaired two-tailed Student's t test. Scalebar = 10 μm , 5 μm for zoom-ins.

Here, astrocytic Syt7 affected neuronal synapse number, which points to the possibility of Syt7-mediated release of glial factors involved in synaptogenesis. Astrocytes express and release several synaptogenic factors that are important for synapse formation and refinement in early postnatal development, e.g. Hevin, thrombospondins (TSPs), or glypicans (Allen et al., 2012; Christopherson et al., 2005; Kucukdereli et al., 2011). However, how these synaptogenic factors are released from astrocytes is currently unknown.

Compared to the Syt7 expression pattern we found, TSP1 mRNA expression and Hevin protein expression in the mouse brain peak at similar timepoints (Iruela-Arispe et al., 1993; Kucukdereli et al., 2011). Therefore, we investigated if NB+H astrocytes also developmentally regulate synaptogenic factors that are released by astrocytes *in vivo*.

In Western blots of DIV9, 14, and 21 NB+H astrocytes, Hevin was expressed at lower levels on DIV9 but was upregulated on DIV14 and 21 (Fig. 30A). In contrast, glypican6 protein levels remained unaltered, and TSP1 was downregulated between DIV14 and DIV21 (although the Western blot was much less clear than for Hevin). Since, like Syt7, Hevin was upregulated between DIV9 and DIV14, we next investigated if Hevin co-localises with Syt7-harboured vesicles in co-culture or NB+H astrocytes. We found that astrocytes expressed both Hevin and Syt7 by immunocytochemistry, and several (but not all) Hevin puncta co-localised with Syt7 vesicles (Fig. 30B).

In summary, astrocytes developmentally regulated both Hevin and Syt7 expression, and Hevin co-localised with a subset of several Syt7 vesicles, suggesting that Hevin may be a cargo that is transported by some Syt7-harboured vesicles to be released during synaptogenesis.

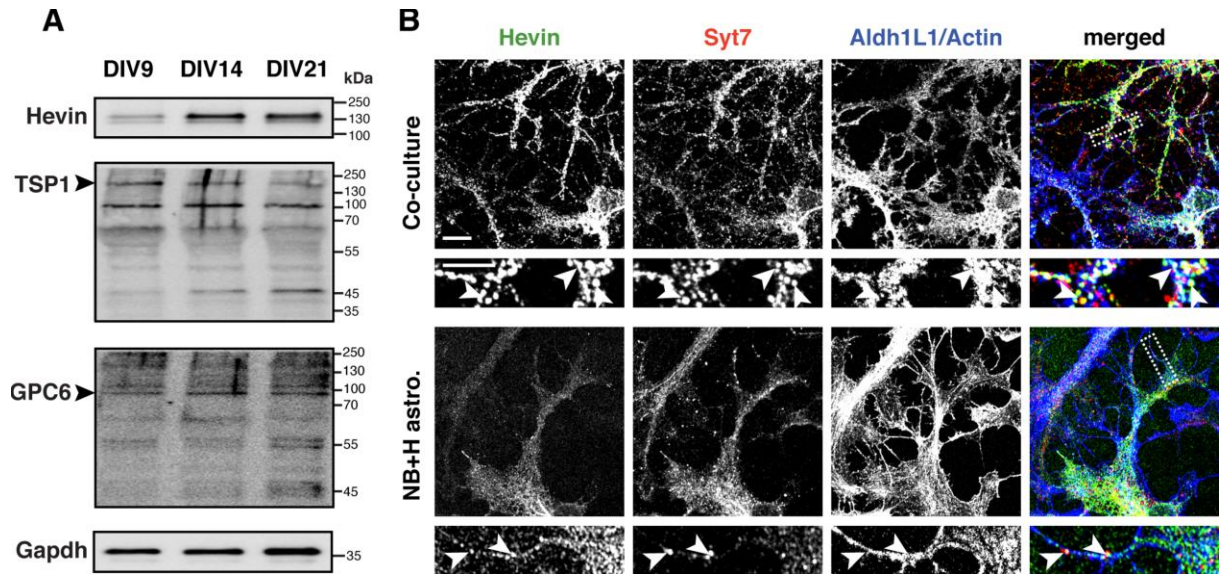


Fig. 30: Hevin is developmentally regulated in astrocytes, and partly co-localises with Syt7

A Western blot analysis of different synaptogenic factors expressed by NB+H astrocytes on DIV9, 14, and 21. Hevin is predicted to run at 75 kDa, but migrates at \approx 130 kDa according to the manufacturer and Kuckdereli et al. (2011); thrombospondin1 (TSP1) runs between 150 and 180 kDa; glypican6 (GPC6) runs at 85-95 kDa. Hevin expression is upregulated on DIV14 and 21, whereas TSP1 and GPC6 expression remains unaltered. Gapdh serves as a loading control (note that the same Gapdh blot appears in Fig. 28, where samples were processed together). Western blots were prepared by Dr. Saheeb Ahmed (European Neuroscience Institute, Göttingen). **B** Immunocytochemistry of DIV14 co-cultures and DIV16 NB+H astrocytes shows that several Syt7 puncta co-localise with Hevin (arrowheads). Images per experiment: $n=6$ for all conditions in **B**. Scalebar = 10 μ m and 5 μ m for zoom-ins.

5. Discussion

Synaptic signalling and plasticity are not solely a neuronal matter: Astrocytes greatly affect synapse function, e.g. by taking up excess neurotransmitters from, and releasing glial factors into, the synaptic cleft (Barker and Ullian, 2010; Perea et al., 2009), or by influencing synapse development (Clarke and Barres, 2013; Eroglu and Barres, 2010). To influence synaptic signalling, plasticity, and development, astrocytic factors must be released somehow, but the release mechanism is unclear. So far, several models for the underlying molecular mechanism were suggested, including vesicle-associated proteins which promote astrocytic exocytosis from small synaptic-like microvesicles, dense core vesicles, or lysosomes (Santello et al., 2012). Although astrocytes express several vesicle-associated proteins that could steer vesicular release, controlled vesicular exocytosis in astrocytes is under debate (Fiacco et al., 2009; Hamilton and Attwell, 2010; Martineau, 2013; Sloan and Barres, 2014b; Vardjan and Zorec, 2015).

Therefore, the goal of this project was to analyse the potential role of vesicle-associated proteins in astrocytic vesicle fusion, and the effects of astrocytic vesicle fusion on synaptic function.

5.1 Astrocyte morphology and protein expression depend on the medium

To study the recycling and molecular composition of astrocytic vesicles, we first needed a cell culture system that allowed us to focus on astrocytes only (without surrounding neurones that also express some of the vesicle-associated proteins found in astrocytes). However, protocols for growing astrocyte monocultures are suboptimal in that they are lengthy (3 months for iPSC-derived astrocytes (Krencik and Zhang, 2011)), generate polygonal, reactive astrocytes (MD method (McCarthy and de Vellis, 1980)), or produce very low yields of stellate astrocytes using relatively expensive reagents (IP method (Foo et al., 2011)). Thus, we developed a high-yield, fast, economical, and simple protocol for growing stellate “NB+H” astrocyte monocultures in chemically defined, serum-free medium.

NB+H astrocytes were similar to astrocytes co-cultured with neurones and to “*in vivo*-like” IP astrocytes (Foo et al., 2011) by morphology and protein expression, e.g. they featured thin processes and astrocyte-specific proteins. Also, NB+H astrocytes contained lower levels of Vimentin than MD astrocytes, which marks immature and reactive astrocytes (Dahl et al., 1981; Pixley and de Vellis, 1984; Schnitzer et al., 1981), and higher levels of S100 β , which labels mature astrocytes that lost their neural stem cell potential (Raponi et al., 2007), than MD and IP astrocytes. This indicates that NB+H astrocytes are more “*in vivo*-like” and more mature than MD astrocytes. In addition, NB+H cultures were free of other glia and neurones.

Our Western blot analysis showed that IP astrocytes expressed the lowest Vimentin levels (i.e. fewer immature or reactive astrocytes), compared with other culture methods we tested, but this may be due to either the IP method itself, or to the tissue age, since IP astrocytes are usually prepared from P7 tissue. To test this, we prepared viable and stellate NB+H astrocytes from P7 tissue, which is the source of IP astrocytes, and compared the morphology in P7-derived NB+H and IP astrocytes. In both cases, astrocytes appeared stellate, although NB+H astrocytes showed lower Gfap expression levels by immunostaining. In future experiments, comparing Vimentin and S100 β expression levels might reveal if NB+H and IP astrocytes maturity still differs when dissected from similarly aged tissue. The maximal tissue age reported to successfully generate IP astrocytes is P14, whereas NB+H astrocytes can likely be derived from older (or even adult) tissue, too, since the core technique (the MD method) successfully generates adult-derived astrocyte cultures (Schwartz and Wilson, 1992; Souza et al., 2013).

For astrocytes prepared by any protocol, we found that the medium composition defined the morphology: Growing astrocytes in Neurobasal medium with the growth factor HBEGF always generated stellate cells. When cultured in NB+H, IP astrocytes downregulated Gfap expression to near-undetectable levels, a sign of non-reactive cortical astrocytes similar to *in vivo* conditions. Thus, immunopanning may yield more “*in vivo*-like” astrocytes when using NB+H medium rather than NB+H with DMEM as described by Foo et al. (2011).

HBEGF belongs to the epidermal growth factor family (Prigent and Lemoine, 1992; Raab and Klagsbrun, 1997) and induces downstream transcriptional changes (Korotkevych et al., 2015). By binding to the ErbB3 receptor, HBEGF may indirectly induce proliferation, cell migration, differentiation, or apoptosis (Citri and Yarden, 2006; Galati, 2012). IP astrocytes are thought to require HBEGF to prevent apoptosis (Foo et al., 2011), yet we found that astrocytes proliferate less without HBEGF, but still survive. In line with our findings, a recent study comparing 2D to 3D mouse cultures also reports astrocyte survival but less proliferation in the absence of HBEGF (Puschmann et al., 2014). However, Puschmann et al. (2014) claimed that astrocytes partially de-differentiate in the presence of HBEGF. We did not observe any de-differentiation in the presence of HBEGF, but we only used half the concentration of HBEGF that Puschmann et al. used, and allowed astrocytes to mature for at least 16 days (versus 8-10 days in Puschmann et al.). In line with Puschmann et al., our findings suggest that HBEGF promotes astrocyte proliferation and stellate morphology without any de-differentiation effects at the concentrations and culture times we used to generate NB+H astrocytes.

Recently, astrocytes derived from human fetal tissue were successfully grown in serum-containing medium in 3D matrices (Placone et al., 2015); yet how such human cultures would look with HBEGF as a substitute for serum is not yet known and signifies another potential role for HBEGF in cell culture systems.

In summary, astrocytes change morphology and protein expression depending on the medium they are grown in. In particular, we found that HBEGF induces stellate astrocyte morphology, and this effect was strongest when adding HBEGF to Neurobasal medium.

5.2 Ca^{2+} signalling differs amongst astrocyte culture methods

Astrocytes communicate largely through Ca^{2+} signalling, where Ca^{2+} sources include internal Ca^{2+} stores (e.g. the endoplasmic reticulum or mitochondria) and extracellular Ca^{2+} (transported into the cell by transporters or voltage- and ligand-operated channels) (Deitmer et al., 2009). Until recently, astrocytic Ca^{2+} signalling was studied by patch-clamp recordings (e.g. as in Zur Nieden and Deitmer (2006)) or by loading organic Ca^{2+} indicator dyes into the cell (e.g. Fluo-4, Oregon Green BAPTA1, or rhod-2 (Nimmerjahn et al., 2004; Takano et al., 2006)). Genetically encoded Ca^{2+} indicators (GECIs) are now widely used, where the Gfap promoter-driven membrane-tethered Lck-GCaMP3 was shown to be superior to organic Ca^{2+} indicator dyes (Shigetomi et al., 2013a) for measuring Ca^{2+} responses in astrocytes: Lck-GCaMP3 allows visualisation of Ca^{2+} fluctuations in even the fine astrocytic processes, whereas the commonly used Fluo-4 detects mainly somatic $[\text{Ca}^{2+}]$ changes (Reeves et al., 2011). Therefore, we analysed astrocytic Ca^{2+} signalling using Lck-GCaMP3, where its expression was driven with an astrocyte-specific Gfap promoter.

5.2.1 Astrocytic Ca²⁺ signalling occurs in somata, branchlets, and microdomains

As in astrocytes in brain slices (Shigetomi et al., 2013a) and *in vivo* (Srinivasan et al., 2015), our data from cultured NB+H astrocytes show that Lck-GCaMP reports Ca²⁺ signalling across the entire territory of astrocytes, segregated into three domains: somata, branchlets, and microdomains. In somata, the Ca²⁺ event amplitude was similar in all cultures tested (co-culture, MD, IP, and NB+H). In branchlets, amplitude was also similar between culture preparations (except for a slightly higher amplitude in MD astrocytes). This suggests that the amplitude of somatic and branchlet Ca²⁺ fluctuations is conserved in astrocytes of different culture types.

In contrast, Ca²⁺ event duration in somata, branchlets, and microdomains was more variable across all cultures. However, NB+H astrocyte event duration in all three compartments was comparable to co-cultured (more *in vivo*-like) astrocytes. In contrast, MD and IP astrocytes event durations did not resemble those of co-cultures. Microdomains always produced the highest-amplitude, shortest Ca²⁺ events compared with somata and branchlets (in all culture types). Microdomains of co-culture astrocytes exhibited significantly lower Ca²⁺ event amplitude than monoculture astrocytes. Thus, in the absence of neurones, astrocytes showed more pronounced microdomain responses. However, microdomains in all cultures showed similar Ca²⁺ event frequency.

Our results are comparable to Ca²⁺ fluctuations in brain slices (Shigetomi et al., 2013a) and *in vivo* (Srinivasan et al., 2015): Ca²⁺ event frequency and amplitude are similar as summarised in Table 2 (although standard error values are high in some cases). In contrast, Ca²⁺ event duration was longer in cultured astrocytes than in astrocytes in brain slices and *in vivo*. This could be a result of the stringent criteria we applied to define Ca²⁺ events, in which we chose thresholds such that we could be sure of “real” events, which may exclude smaller events that are closer to the noise. Although our culture experiments cannot be directly compared to brain slices or *in vivo* data, given possible differences in methods and analysis, the similarity in Ca²⁺ event frequency and amplitude suggests that co-culture and NB+H (but not MD and IP) astrocytes are a good model for studying Ca²⁺ fluctuations in cultures.

Table 2: Comparing our results on astrocytic Ca²⁺ signalling to slices and *in vivo* data

Tables summarising the frequency, amplitude, and duration of Ca²⁺ signalling events from our culture analysis (see **Fig. 13BC**) to slices (Shigetomi et al., 2013a) and *in vivo* (Srinivasan et al., 2015) data. Although the differences in experimental setups do not allow for a direct comparison, this summary illustrates that Ca²⁺ signalling in cultures (*in vitro*) is similar to Ca²⁺ signalling in slices (*in situ*) or *in vivo*. Apart from half-width values for data from slices (derived from Cyto-GCaMP3 experiments), all data were generated using membrane-tethered Lck-GCaMP3.

Frequency (events / ROI / min)

	<i>in vivo</i>	<i>in situ</i>	<i>in vitro</i>			
			Co	NB+H	MD	IP
somata	1.1 ± 0.3	0.74 ± 0.4	1.2 ± 0.8	0.8 ± 0.5	0.3 ± 0.3	0.15 ± 0.17
branchlets	0.5 ± 0.02	1.4 ± 0.07	0.9 ± 0.27	0.7 ± 0.3	0.08 ± 0.1	0.04 ± 0.04
micros	0.4 ± 0.01	?	0.4 ± 0.07	0.5 ± 0.07	0.4 ± 0.06	0.2 ± 0.03

Amplitude (dF/F)

	<i>in vivo</i>	<i>in situ</i>	<i>in vitro</i>			
			Co	NB+H	MD	IP
somata	3.0 ± 0.3	1.45 ± 0.1	1.3 ± 0.9	2.1 ± 2.0	1.7 ± 1.7	1.8 ± 0.2
branchlets	2.3 ± 0.1	1.5 ± 0.05	2.3 ± 1.4	2.1 ± 1.4	3.1 ± 1.9	1.8 ± 0.6
micros	5.0 ± 0.4	?	3.8 ± 2.0	4.3 ± 1.8	4.2 ± 1.6	5.0 ± 1.8

Half-width (s) / “duration”

	<i>in vivo</i>	<i>in situ</i>	<i>in vitro</i>			
			Co	NB+H	MD	IP
somata	3.3 ± 0.2	2.5 ± 0.2	13.5 ± 6.9	7.1 ± 6.3	36.2 ± 23.4	40.6 ± 2.1
branchlets	2.9 ± 0.05	2.9 ± 0.3	6.7 ± 5.1	9.6 ± 6.8	19.5 ± 14.2	27.5 ± 24.9
micros	1.6 ± 0.02	2.5 ± 0.3	2.3 ± 2.0	4.1 ± 3.1	1.1 ± 0.3	1.1 ± 0.2

5.2.2 Co-culture and NB+H astrocytes exhibit similar Ca^{2+} signalling profiles

Ca^{2+} event duration in co-culture and NB+H astrocytes was more similar to Ca^{2+} event duration in brain slices and *in vivo* than that of MD and IP astrocytes (Table 2). Moreover, no or very few events were detected in somata and branchlets of MD and IP astrocytes, i.e. Ca^{2+} fluctuation frequency in brain slices / *in vivo* was generally more similar to that of co-culture and NB+H astrocytes.

While microdomain Ca^{2+} event frequency was comparable across all cultures (around 0.4 events / min), somata and branchlets showed two ranges of Ca^{2+} event frequencies: (1) 0.8 to 1.2 events / min occurred in co-culture and NB+H astrocytes, and (2) < 0.2 events / min occurred in MD and IP astrocytes.

Moreover, Ca^{2+} events had shorter durations in somata and branchlets, and longer durations in microdomains of co-culture and NB+H astrocytes; the opposite was true for MD and IP astrocytes. Thus, differences in Ca^{2+} event duration also divided cell cultures into two groups (co-culture / NB+H astrocytes versus MD / IP astrocytes).

What mechanism underlies differences in Ca^{2+} fluctuations in different domains? It was hypothesised that astrocytic Ca^{2+} activity depends on inositol triphosphate type 2 receptor (IP3R2)-dependent release from internal Ca^{2+} stores in the endoplasmic reticulum, since *Ip3r2*^{-/-} mouse astrocytes no longer show Ca^{2+} fluctuations as measured by organic Ca^{2+} indicator dyes (Agulhon et al., 2010; Petracicz et al., 2008). However, when membrane-tethered GECIs were used to visualise Ca^{2+} activity in awake adult *Ip3r2*^{-/-} mice, Ca^{2+} fluctuations persisted (although at decreased frequency, amplitude, and duration), and depleting intracellular Ca^{2+} stores with cyclopiazonic acid in wild-type mice yielded similar Ca^{2+} fluctuations as in *Ip3r2*^{-/-} mice (Srinivasan et al., 2015). These Ca^{2+} fluctuations made up half or more of the total branchlet and microdomain Ca^{2+} activity and were IP3R2-independent. In addition to intracellular Ca^{2+} stores, branchlet and microdomain Ca^{2+} fluctuations employ extracellular Ca^{2+} : removing extracellular Ca^{2+} abolishes branchlet and microdomain Ca^{2+} activity, and subsequently restoring extracellular Ca^{2+} causes branchlet and microdomain Ca^{2+} fluctuations to reappear. Such transmembrane Ca^{2+} fluxes may be due to Ca^{2+} channels (e.g. TRPA1 channels) and transporters (e.g. the $\text{Na}^+/\text{Ca}^{2+}$ exchanger) that traffic extracellular Ca^{2+} into the cytosol (Kirischuk et al., 1997; Minelli et al., 2007; Shigetomi et al., 2013b).

Following these observations, it would be interesting to test how cyclopiazonic acid and Ca^{2+} -free extracellular solution affect astrocytic Ca^{2+} events in cell cultures. If in cultures, astrocyte subcompartments (partly) rely on both IP3R2-dependent release from intracellular Ca^{2+} stores and extracellular Ca^{2+} via Ca^{2+} channels for fast and local Ca^{2+} events as in brain slices, Ca^{2+} fluctuations should decrease in response to cyclopiazonic acid, Ca^{2+} -free extracellular solution, or both. Somata, branchlets, and microdomains may also access different Ca^{2+} sources in cultured astrocytes. As detected by organic Ca^{2+} indicator dyes, removing extracellular Ca^{2+} has a direct, negative effect on astrocytic Ca^{2+} event frequency of expanded events (i.e. larger amplitude in several neighbouring domains) but not single domains (Di Castro et al., 2011). The same study found a branchlet event frequency of 1.8 events / min, i.e. much lower than in Lck-GCaMP-based *in vivo* experiments, stressing that GECIs are more sophisticated than organic dyes for measuring astrocytic Ca^{2+} signalling.

We successfully expressed Lck-GCaMP3 in cultured astrocytes, and found that the Ca^{2+} activity in NB+H astrocytes mimics brain slice and *in vivo* Ca^{2+} fluctuations. This illustrates that monitoring Ca^{2+} signalling in a culture system closer to an *in vivo*-like state is possible. This allows the study of astrocytes isolated from neuronal influence, but also permits imaging all processes of an astrocyte within a small z plane due to the monoculture's 2D nature. Our study is the first to analyse Ca^{2+} signalling in IP astrocytes transduced with Lck-GCaMP3, and the first to compare astrocytic Ca^{2+} signalling of somata, branchlets, and microdomains across different cell cultures using the semi-automated software GECIquant. Therefore, further studies are required to validate our findings.

If astrocyte Ca^{2+} signalling in the soma differs from branchlets and microdomains, which processes do these three domains compute? As for somatic Ca^{2+} fluctuations, both our results and previous studies show that these Ca^{2+} transients are much slower and often less frequent than branchlet and microdomain Ca^{2+} events. Slow somatic Ca^{2+} signalling is associated with prolonged blood-oxygen-level-dependent signals (Schulz et al., 2012). However, the slow nature of somatic Ca^{2+} fluctuations also led some groups to question how relevant astrocytic Ca^{2+} signalling is for neurovascular coupling (Nizar et al., 2013). Yet, further Ca^{2+} studies using Fluo-4 and GECIs in astrocytes revealed that vascular responses are functionally and temporally linked to astrocytic Ca^{2+} signalling, but that a majority of these events appear in branchlets (Kim et al., 2015b; Otsu et al., 2015). Thus, Ca^{2+} fluctuations in the somata and branchlets of astrocytes may relate to more large-scale events like vascular responses.

Apart from a putative role in neurovascular coupling, Ca^{2+} fluctuations in astrocytic branchlets may also reflect neighbouring axonal firing, since adding tetrodotoxin to hippocampal slices significantly decreases astrocytic Ca^{2+} signalling (Serrano et al., 2006). Further, Ca^{2+} signalling in hypothalamic astrocytes evokes increased synaptic currents, but only in neuronal processes directly bordering the astrocyte with increased Ca^{2+} activity (Gordon et al., 2009). In response to synaptic activity, Ca^{2+} fluctuations in astrocytic branchlets increase, resulting in gliotransmitter release, which in turn affects basal synaptic transmission (Panatier et al., 2011). Taken together, these findings suggest that Ca^{2+} signalling in astrocytic branchlets may mediate communication between single astrocytes and neurones, e.g. via gliotransmitter release.

While Ca^{2+} signalling in astrocytic branchlets diminishes when neurones are treated with tetrodotoxin, microdomain Ca^{2+} fluctuations persist (Di Castro et al., 2011). Thus, microdomain Ca^{2+} concentration likely is not influenced by neuronal firing, but may change if these fine astrocytic processes detect spontaneous synaptic activity.

As individual synapses can function independently in neurones, microdomains and branchlets may present an analogous structure in astrocytes that can quickly respond to local challenges, e.g. synaptic signalling and plasticity at tripartite synapses.

5.3 Astrocytes express some vesicle-associated proteins, including synaptotagmins

Astrocytes feature several vesicular organelles, including endocytic clathrin-coated vesicles and multivesicular bodies, but also putative exocytotic vesicles ranging from 30 to 300 nm in diameter (Bezzi et al., 2004; Martineau et al., 2013; Singh et al., 2014). We also found vesicular organelles in astrocytes by electron microscopy, and further detected several vesicle-associated proteins in astrocytes in Western blots. We validated previous reports of syntaxin1 and Vamp2 in astrocytes (Jeftinija et al., 1997; Parpura et al., 1995), and further found endogenous Vamp4 in astrocytes, which had only been reported in the Golgi body of oligodendrocytic glia before (Feldmann et al., 2009). MD astrocytes likely recycle the neuromodulator tPA via Vamp4, since transfected EGFP-Vamp4 co-localises with exogenously applied tPA in MD astrocytes (Cassé et al., 2012). Therefore, it would be interesting to test if exogenous tPA is also recycled via Vamp4-harboured vesicles in more *in vivo*-like NB+H astrocytes.

In neurones, syntaxin1 and Vamp2 form the SNARE complex (together with Snap25) for exocytotic synaptic vesicle fusion (Hanson et al., 1997; Jahn and Scheller, 2006). Similarly, astrocytic syntaxin1 and Vamp2 may control exocytotic astrocytic vesicle fusion with Snap23, the astrocytic homologue of Snap25 (Hepp et al., 1999; Montana et al., 2004; Wilhelm et al., 2004). While neuronal exocytotic synaptic vesicles also pass through docking and priming stages before being released (Südhof, 2013), there is yet no evidence for the molecules that mediate these processes in astrocytes, i.e. Munc13 isoforms, RIM active zone proteins, or vesicle-associated Rab3a (Fiacco et al., 2009). We found no Rab3a in astrocytes, but other proteins remain to be tested. While the lack of similar vesicle docking / priming molecules in astrocytes as compared with neurones supports the view that there is no controlled exocytotic vesicle release in astrocytes, astrocytes may simply employ other molecules for vesicle docking and priming. For instance, Snap23, which astrocytes express, mediates secretory granule docking in endocrine cells (Chieriegatti et al., 2004), similar to Snap25, which regulates synaptic vesicle docking in neurones (Mohrman et al., 2013; de Wit et al., 2009). Alternatively, astrocyte vesicles may dock and fuse at the right place and time by other, as of yet unknown mechanisms.

Nonetheless, the pool of astrocytic vesicle-associated proteins is extensive, and the interactions between individual proteins are still being investigated, e.g. in addition to Vamp2 and Vamp4, astrocytes also express Vamp3 (Li et al., 2015; Parpura et al., 1995; Schubert et

al., 2011) and syntaxin isoforms 2, 3, and 4 (Paco et al., 2009; Tao-Cheng et al., 2015). Astrocytes may also express more vesicle-associated proteins than tested here, which further Western blot analysis will show.

In addition to SNARE proteins, we also found that astrocytes express vGluT isoform 3, which transports glutamate into synaptic vesicles in neurones (Freneau et al., 2002; Nelson et al., 2014). Since astrocytes were also suggested to release gliotransmitters like glutamate via exocytotic vesicles (Martineau, 2013; Santello et al., 2012), glutamate would first have to be loaded into these vesicles, e.g. via vGluTs. Several groups found one or more of the three vGluT isoforms in astrocytes (Anlauf and Derouiche, 2005; Bezzi et al., 2004; Montana et al., 2004), although other reports claim that astrocytes express no vGluTs at all (Li et al., 2013). In line with this, (2011) observed no glutamate release when stimulating MD and IP astrocytes with ATP. However, astrocytes released glutamate in several other studies both in cell culture (Araque et al., 1999; Hassinger et al., 1995; Parpura et al., 1994) and in brain slices (Angulo et al., 2004; Bezzi et al., 2004; Fellin et al., 2004; Jourdain et al., 2007), and immunogold cytochemistry revealed glutamate on small synaptic-like microvesicles in astrocytes in the adult hippocampus (Bergersen et al., 2012). Further, immunogold-labelling in astrocytes revealed vGluT3 as the most abundant isoform *in vivo* (Ormel et al., 2012). Unlike vGluT1 or 2, vGluT3 overexpression increased glutamate release from cultured astrocytes (Ni and Parpura, 2009). These studies illustrate that vGluT3 may be involved in glutamate release from astrocytes by exocytotic vesicles.

In general, regulated vesicular exocytosis in astrocytes is still under debate (Hamilton and Attwell, 2010; Parpura and Zorec, 2010; Sahlender et al., 2014; Sloan and Barres, 2014b). This debate partly comes from inconsistent findings in MD astrocytes, e.g. some studies find Vamp2 in astrocytes (Araque et al., 2000; Bezzi et al., 1998; Coco et al., 2003; Crippa et al., 2006), which was challenged by a report (Li et al., 2015) using similar culture conditions that include serum-containing media that are prone to varying quality. Other groups identified Vamp2 co-localisation with more established astrocyte markers like Gfap in brain slices using 3D reconstruction methods (Bergami et al., 2008), which provide better resolution than optical planes. Using the NB+H monoculture protocol for stellate astrocytes, with a defined medium that does not contain serum, we found that astrocytes express Vamp2 via both Western blot analysis and immunocytochemistry. In addition, astrocytic vesicles can be isolated using anti-Vamp2 antibodies (Martineau et al., 2013), and Vamp2-harboured vesicles are highly mobile (Singh et al., 2014) but mediate slow vesicular release (Zorec et al., 2015)

If astrocytes also control regulated vesicle fusion, this would implicate another class of molecules, which in neurones initiates vesicle fusion by sensing local intracellular $[Ca^{2+}]$ elevations: synaptotagmins (Syts). Since we showed that Ca^{2+} signalling in cultured astrocytes is spatially divided into different cellular subcompartments (soma, branchlets, microdomains) as *in vivo*, with domain-specific kinetics, local Ca^{2+} fluctuations may well be involved in regulated vesicle exocytosis in astrocytes. Indeed, astrocytes express both mRNA (Mittelsteadt et al., 2009) and protein of several Syt isoforms (Cahoy et al., 2008; Zhang et al., 2004a). In line with this study, we found that cultured astrocytes express Syt isoforms 4, 7, 11, as reported in Mittelsteadt et al., and 17 (but not 1, 3, and 5). Overall, our data show that astrocytes express vesicle-associated proteins that are central mediators of exocytotic vesicle fusion.

5.4 Vamp2 and Syt7 mark distinct vesicle populations in astrocytes

Our immunostainings of Vamp2 and Syt7 vesicles showed punctate protein distribution in astrocytes, with an enrichment of signal in astrocytic processes (in those cultures with stellate morphology). Similarly, Vamp2- and Syt7-harboured vesicles recycled in fine astrocytic processes when stimulated with glutamate. The majority of GFP-Vamp2-harboured vesicles recycled in basal, non-stimulated conditions (2 mM KCl), where only a fraction of GFP-Vamp2 remained within the cell membrane and was not internalised by recycling vesicles. These findings from cultured astrocytes hint at constitutive recycling of vesicles that include Syt7 and Vamp2.

At 4 °C, vesicle trafficking is inhibited (Kuismanen and Saraste, 1989). Although a slight decrease in vesicle recycling was observed in internalisation assays of GFP-Vamp2-transfected astrocytes, most anti-GFP antibodies were still taken up by cells at 4 °C in our experiments. Since we did not observe a dramatic decrease in vesicle recycling at 4 °C versus 37 °C, we concluded that inhibiting membrane trafficking at 4 °C might have failed. However, other studies also show no change or only a slight reduction in vesicular antibody uptake at 4 °C (Helmy et al., 2006; Iglesias-Bartolomé et al., 2006).

In internalisation assays, both Vamp2- and Syt7-harboured vesicles recycled. Since Vamp2 and Syt1 are both essential parts of the SNARE complex in neurones, Vamp2 and astrocytic Syt isoforms may also act together in astrocytes. In neurones, Vamp2 catalyses membrane fusion and stabilises the SNARE complex (Schoch et al., 2001), and the Ca²⁺ sensor Syt1 is required for fast, synchronous vesicle release in neurones (Geppert et al., 1994). *Vamp2*^{-/-}, *Syt1*^{-/-}, and *Syt2*^{-/-} mutants show a severe phenotype and die soon after birth (Pang et al., 2006), whereas mutants lacking other Syt isoforms in the brain have milder phenotypes, e.g. deficits in learning and memory as the *Syt4*^{-/-} mutant (Ferguson et al., 2000).

Due to the differential roles of Syts in neurones, we hypothesised that astrocytes may also employ Vamp2 alongside several Syts for different aspects of vesicle fusion (e.g. transient versus full fusion, or fusion of different vesicle or organelle types). Despite their similar staining patterns and recycling in internalisation assays, Syt7 and Vamp2 did not co-localise. Therefore, we concluded that Syt7 and Vamp2 are associated with different vesicle subtypes in cultured astrocytes.

Apart from Vamp2 and Syt7, we also performed internalisation assays using Syt17 as a negative control, since this Syt isoform lacks a transmembrane domain (Fukuda and Mikoshiba, 2001b) and the GFP domain of GFP-Syt17 is therefore not exposed to the vesicular lumen. Syt17 is associated with vesicular membranes, however, and appears in mass spectrometric analyses of purified synaptic vesicles alongside other (transmembrane domain-containing) Syt isoforms (Takamori et al., 2006). Therefore, Syt17-harboured vesicles may recycle in astrocytes, but this would not be detected by internalisation assays. However, total internal reflection fluorescence microscopy of MD astrocytes transfected with pHluorin-coupled Syt17 revealed spontaneous pH-dependent GFP fluorescence changes indicating vesicle fusion with the membrane (Anne Wolfes, unpublished data). Further, Syt7 and 17 were reported to selectively recycle in axons (and not dendrites) of neurones, assayed by pHluorin-Syt reporter constructs (Dean et al., 2012). In our experiments, Syt17 worked as a negative control (suggesting that Syt17 does indeed lack a transmembrane domain), and we saw no internalisation of GFP antibodies by GFP-Syt17 expressing cells in stimulated or unstimulated conditions. In a study referring to Syt17 as B/K protein, Syt17 localised to the trans-Golgi network (where proteins are assembled for lysosomal, secretory vesicle, or transport to the cell membrane) of PC12 cells (Fukuda and Mikoshiba, 2001a). Thus, it may be interesting to test which subcellular compartments Syt17 localises to in astrocytes.

5.4.1 Vamp2 is rarely localised to endosomes in astrocytes

Previously, Vamp2 was found on endocytotic / recycling vesicles in neurones and HeLa cells (Bonanomi et al., 2007; Koo et al., 2011; Zylbersztejn et al., 2012). In rat kidney, Vamp2 mediates endosomal fusion of vesicles (Jo et al., 1995). We therefore also tested if Vamp2 is localised to astrocytic endosomes. Vamp2 and early (EEA1-positive) as well as late (Rab7-positive) endosomal markers only partly co-localised, and only in MD astrocyte cultures. While this implies that MD astrocytes may express Vamp2 on endosomal vesicles, it also stresses the difference between the polygonal MD astrocytes and stellate astrocytes of other culture types; Vamp2 is rarely localised on endosomes in MD astrocytes, and likely exempt from endosomes in more *in vivo*-like astrocyte cultures.

If Vamp2 is not localised to endosomes, lysosomes and small exocytotic vesicles are other candidates for Vamp2 integration. In astrocytes in mouse hippocampal cultures, both lysosomes and small exocytotic vesicles fuse with the membrane in a Ca^{2+} -dependent manner (Liu et al., 2011). In the same study, Vamp2 and Vamp3 co-localised to small vesicles (but not lysosomes), and glutamate release (but not lysosomal membrane fusion) was Vamp2-dependent (as TeNT blocked it). Thus, these small vesicles were required for release of glutamate, as suggested in previous studies (Crippa et al., 2006; Martineau et al., 2008), so that both Vamp2 and Vamp3 may be involved in the exocytosis of small vesicles in astrocytes.

5.4.2 Syt7 is not localised to lysosomes

In contrast to Vamp2, where most reports focus on neuronal exocytotic vesicles, Syt7 is associated with lysosomes in rat kidney and mouse embryonic fibroblasts (Jaiswal et al., 2004; Martinez et al., 2000; Rao et al., 2004), and in hippocampal neurones (Monterrat et al., 2007). Functionally, Syt7 was further associated with Ca^{2+} -dependent lysosomal exocytosis, where Syt7 influences the formation of lysosomal fusion pores (Jaiswal et al., 2004). In PC12 cells, Syt7 localises to lysosomes and large dense-core vesicles, but not to synaptic-like microvesicles (Fukuda et al., 2002, 2004).

Because Syt7 mediates lysosomal exocytosis in fibroblasts and PC12 cells and lysosomes are the main vesicular organelle implicated in astrocytic exocytosis (Li et al., 2008), we hypothesised that Syt7 may be present on lysosomes to regulate their fusion in astrocytes. However, our immunocytochemistry analysis revealed that in cultured astrocytes, Syt7 does not co-localise with lysosomes. Since GFP-Syt7 internalisation assays showed that Syt7-harboured vesicles recycle, however, we conclude that Syt7 localises to other vesicular organelles that undergo active recycling.

Compared with Syt1, the Ca^{2+} sensitivity of Syt7 is ≈ 400 -fold higher (Bhalla et al., 2005). Syt7 was suggested as a Ca^{2+} sensor in asynchronous vesicle release, since the disassembly kinetics of Syt7 (assayed *in vitro* using liposomes) are the slowest amongst all Syts (Hui et al., 2005). These properties make Syt7 a good candidate for mediating Ca^{2+} -dependent vesicular fusion in astrocytes, where Ca^{2+} concentrations may be lower than in neuronal active zones following an action potential, and thus require a higher affinity Ca^{2+} sensor. Ca^{2+} -dependent vesicle fusion of both lysosomes and small vesicles occurs in cultured mouse hippocampal astrocytes, where small vesicles release glutamate (Liu et al., 2011) and may release other cargo. Glutamate release from astrocytes significantly decreases (but does not vanish) when Vamp2 (and Vamp3) are blocked with clostridial toxins (Liu et al. 2011). Since in our cultures, Syts did not co-localise with Vamp2 in astrocytes, only a fraction of glutamate release may be mediated by Syt7-harboured vesicles, if any. However, Syt7-harboured vesicles may contain other cargo than glutamate, as is discussed in chapter 5.6.

5.5 Astrocytic Syt7 is involved in synaptogenesis

The goal of this project was to identify molecules involved in astrocyte vesicle fusion at synaptic interfaces. Here, we focused on Syt7, which we found expressed in astrocytes and which has a very high Ca^{2+} sensitivity (Bhalla et al., 2005) (see previous chapter). According to our findings, Syt7 may be involved in synaptogenesis. During prenatal development and several days before synapse formation, most neurones of the central nervous system innervate their future targets (Pfrieger and Barres, 1996). However, synapses only form after astroglialogenesis begins (Ullian et al., 2001). In general, astrocytes shape synaptogenesis by releasing different synaptogenic factors both in cultures and *in vivo* (Eroglu, 2009; McKellar and Shatz, 2009).

We found that when astrocytes (but not neurones) lack Syt7, synapse number decreases significantly. When DIV14 neurones cultured with *Syt7^{-/-}* astrocytes were stimulated, synaptic vesicles recycled normally, suggesting that synaptic function is unaffected, and only synapse number is reduced. Our results suggest that astrocytic Syt7 is involved in synaptogenesis, but do not show whether this is due to changes in synapse formation, stabilisation, or elimination. In cultures, synapse formation and stabilisation occur between DIV10 and DIV14 in hippocampal neurones (Goslin et al., 1990), and synapse elimination occurs between DIV6 and 11 in corticospinal neurones (Ohno and Sakurai, 2005). Considering that our results showed a $\approx 50\%$ decrease in synapse number, but not a complete loss of synapses in DIV14 cultures, we propose that astrocytic Syt7 plays a role in synaptic refinement rather than formation. In line with this, removing astrocytic trophic support from co-cultures (in which synapses had begun to form) on DIV7 causes most synapses to disappear by DIV14 (Ullian et al., 2001). If Syt7 plays a role in synapse formation, we might therefore expect a more dramatic effect on synapse loss than a reduction by 50%. Thus, Syt7 in astrocytes may more likely support synaptic stabilisation or refinement.

Our data do not directly address whether fewer synapses form, or whether synapses form normally but are not stabilised. Interestingly, *Syt7^{-/-}* mice showed no neuronal phenotype (Chakrabarti et al., 2003) and no change in neurotransmitter release and short-term plasticity (Maximov et al., 2008). Given unaffected neuronal networks in *Syt7^{-/-}* mice, there are two possible explanations of reduced synapse numbers on cultured *Syt7^{-/-}* astrocytes: (1) fewer synapses form in the absence of Syt7, so that fewer synapses compete for stabilisation, i.e. there is less synapse elimination, but the number of synaptic connections is the same as in

wild-type; (2) synapses form but are not stabilised, possibly creating a lower threshold for synapse elimination, and a higher turnover of synapses during development, but still leading to synaptic refinement. In both scenarios, functional neuronal network are established despite reduced synapse formation, or reduced synapse formation due to the absence of Syt7 in astrocytes – evolutionarily, this would imply that synapse elimination only arose because having many synapses compete for stabilisation is a good thing (possibly to guarantee enough functional synaptic connections); yet it is strange that *Syt7*^{-/-} mice are unaffected by less stringent synapse competition and elimination. Considering that in humans, atypical wiring may have mild symptoms (e.g. as in autism spectrum disorders), it is possible that more delicate, milder aspects of the *Syt7*^{-/-} phenotype have been overlooked.

Since no neuronal phenotype was reported for *Syt7*^{-/-} mice, removing astrocytic Syt7 may have a more pronounced effect in cultures than *in vivo*. Therefore, it would be interesting to compare cortical synapse numbers at different developmental stages of *Syt7*^{-/-} mice (or mice lacking Syt7 only in astrocytes, e.g. under an astrocyte-specific promoter like *Gfap*, used for knockdown). To find out whether synapse formation, stabilisation, or elimination involves astrocytic Syt7 and how this is reflected *in vivo*, more detailed analyses are required, e.g. studying synaptic strength in *Syt7*^{-/-} early postnatal versus adolescent and adult mutant mice to assess if synapses are stabilised and functionally normal compared with Wt animals. In light of normal neuronal function in *Syt7*^{-/-} mice, Syt7 may only be involved during a small time window of synaptogenesis, so that any impairments due to Syt7 absence in astrocytes may only have minor consequences.

In summary, astrocytic Syt7 is involved in the synaptogenesis of cultured neurones, but to what extent this is true *in vivo* remains to be tested.

5.6 Astrocytes developmentally regulate Syt7 and Hevin

Astrocytes developmentally regulate Syt7, where the 46 kDa isoform is upregulated between DIV14 and 16. This roughly matches *Drosophila* Syt7 expression, which is only upregulated as the nervous system begins to form (Adolfson et al., 2004). Since synapse numbers are decreased in DIV14 neurones co-cultured with *Syt7*^{-/-} astrocytes, we hypothesise that astrocytes mediate synapse number by releasing glial factors from Syt7-harbouring vesicles.

Synaptogenesis is affected by several astrocyte-secreted proteins, e.g. Hevin, SPARC, thrombospondins (TSPs), and glypicans (Allen et al., 2012; Eroglu, 2009; Jones and Bouvier, 2014). *Hevin*^{-/-} mice have fewer excitatory synapses, and *Sparc*^{-/-} mice have more (Kucukdereli et al., 2011). Synapse number is unaltered in *Tsp1*^{-/-} or *Tsp2*^{-/-} mice, but decreases by 40% in *Tsp1*^{-/-}/*Tsp2*^{-/-} double knockout mice at P8, and by 25% at P21 (Christopherson et al., 2005). *Gpc4*^{-/-} mouse synapses are defective due to impaired glutamate receptor clustering (Allen et al., 2012). Amongst these astrocyte-secreted proteins, Hevin and SPARC are complementary positive and negative regulators of synapse formation, respectively (Kucukdereli et al., 2011), and astrocyte leaflets (which contact synapses) contain Hevin (Lively and Brown, 2008a; Lively et al., 2007).

In our study, we found that cultured astrocytes upregulate Hevin (but not glypican6) expression between DIV9 and DIV14, and might slightly downregulate TSP1 expression on DIV21 (repetition is required to quantify changes in protein level). Similarly, astrocytes developmentally upregulate Hevin (at a time point comparable to our findings) and TSP1 *in vivo* (Iruela-Arispe et al., 1993; Kucukdereli et al., 2011), and release these glial factors to promote synaptogenesis (Christopherson et al., 2005; Hughes et al., 2010). We further found that Syt7-harbouring vesicles partly co-localise with Hevin. Since Hevin is released by astrocytes, and Syt7 is a Ca²⁺ sensor on vesicular organelles (e.g. synaptic vesicles in neurones (Liu et al., 2014) or lysosomes in fibroblasts (Martinez et al., 2000)), Hevin may be the cargo of vesicles whose molecular fusion mechanism involves Syt7.

Based on our findings that synapse number decreases only by half in neurones grown on *Syt7*^{-/-} astrocytes, we argued that astrocytic Syt7 affects synaptic refinement rather than synapse formation. Interestingly, astrocytes were reported to regulate synaptic refinement through Hevin (Risher et al., 2014), which supports our proposition that astrocytes regulate the refinement but not formation of synapses through Syt7. Specifically, thalamocortical synaptic connections are reduced in the *Hevin*^{-/-} mouse cortex, whereas dendritic spines with

multiple excitatory synaptic connections increase. Injecting Hevin directly into *Hevin*^{-/-} mouse cortices at P13 rescued this effect and promoted significantly more thalamocortical synapses after three days. This shows that astrocyte-derived Hevin is required for normal synaptic connectivity of long-distance projections of the thalamocortical tract. The results of this *Hevin*^{-/-} mouse model analysis correlate with our observations that Hevin and Syt7 partially co-localise, and that cortical neurones have fewer synapses in the absence of astrocytic Syt7 (Fig. 31).

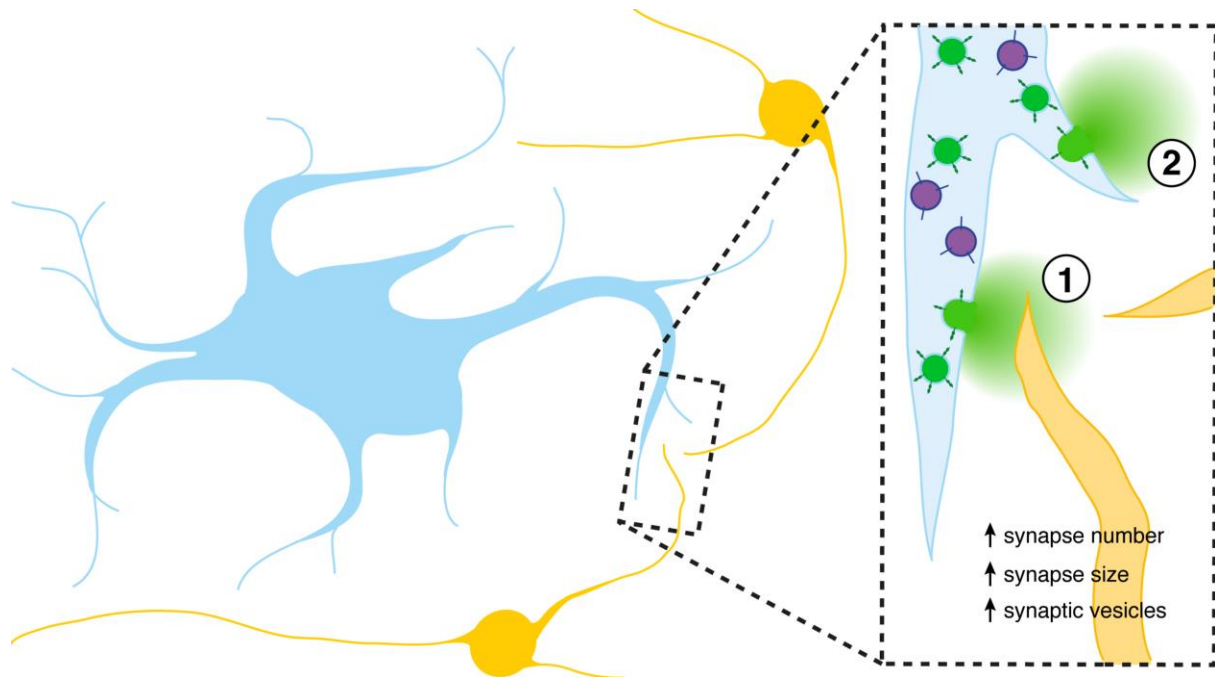


Fig. 31: Model of Hevin released from astrocytes during synaptogenesis

Schematic model of our findings. Astrocytes (blue) support and regulate synaptogenesis of nearby developing neurones (orange). In astrocytic processes, Vamp2 is localised to some vesicles (purple), while Syt7 is localised to other vesicles (green). Syt7-harboured vesicles may traffic Hevin to the cell surface to release Hevin either locally to nearby developing synaptic connections (1) or globally, to release Hevin throughout the extracellular matrix (2). Astrocyte-derived Hevin release promotes synapse number, size, and synaptic vesicle number (Kucukdereli et al., 2011). This model can be applied to cell interactions *in vivo* and in co-cultures of astrocytes and neurones.

However, since we did not find complete co-localisation of Syt7 and Hevin, Syt7-harboured vesicles may contain other cargo (e.g. TSP1). To test if Syt7 and Hevin are functionally linked, recombinant Hevin could be used to potentially rescue synapse number in neurones cultured with *Syt7*^{-/-} astrocytes. Since Hevin and SPARC both regulate synapse formation in a complementary fashion (either by enhancing or reducing synapse number), it is also possible that Syt7-harboured vesicles traffic SPARC. However, synapse numbers

remain the same when culturing Wt neurones with *Sparc*^{-/-} or with Wt astrocytes (Jones et al., 2011), unlike our results of culturing Wt neurones with *Syt7*^{-/-} versus Wt astrocytes.

Little is known about how astrocytes release synaptogenic factors at the right place and time in the developing nervous system (Allen, 2013; Clarke and Barres, 2013). To test if astrocytes not only express *Syt7* in culture but also *in vivo*, FACS-based astrocyte isolation from *Tg{Gfap::Gfp}* or *Tg{Aldh1L1::Gfp}* mice would be useful for analysing how *Syt7* (and synaptogenic factors) are regulated at different developmental stages. Understanding the molecular mechanisms by which glial cells shape neuronal networks would not only advance general knowledge on nervous system development, but may also aid in treatment of neurological diseases. Synapse refinement, which may be promoted by astrocytic *Syt7*, is a crucial step in nervous system development, without which neuronal networks become dysfunctional (Doll and Broadie, 2014; West and Greenberg, 2011). Not only neurones, but astrocytes too play an important role in neurodevelopmental diseases (Yang et al., 2013). Common symptoms in autism, schizophrenia, fragile X syndrome, and Down's syndrome include cognitive impairment, epileptic seizures, and often abnormal synapse formation or function – all of which are associated with astrocytic function (Molofsky et al., 2012). On a molecular level, Hevin (which partly co-localised with *Syt7*) protein levels decrease following induced epileptic seizures in rodents, after which Hevin was associated with excitatory, but not inhibitory synaptic markers (Lively and Brown, 2008b). These findings suggest that Hevin is involved in synaptic modifications that underlie epileptogenesis. Another example comes from a mouse model of the fragile X syndrome, which showed reduced pre- and postsynaptic protein clusters at synapses and abnormal dendrite morphology, which was rescued by co-culturing mutant neurones with Wt astrocytes (Jacobs and Doering, 2010). In the reverse approach, culturing Wt neurones with astrocytes from Down's syndrome patients reduced dendritic spine number and neuronal activity, and caused abnormal dendritic spine morphology (Garcia et al., 2010). This effect was rescued by adding TSP1, illustrating that astrocyte-secreted factors can restore neuronal connections in neurodevelopmental disease.

Given the importance of astrocyte-secreted factors for developing synaptic connections, astrocytes represent an important target for therapeutic disease management. Thus, understanding how astrocytes release glial factors is essential not only for understanding the relationship between glia and neurones, but also for developing therapeutic agents to treat neurodevelopmental diseases.

5.7 Conclusion and future directives

In support of regulated vesicular exocytosis, this study confirmed that cultured astrocytes express several vesicle-associated proteins (that were previously linked to gliotransmitter release), and showed that Vamp2- and Syt7-harboured vesicles recycle in a similar fashion, although Vamp2 and Syt7 do not localise to the same vesicles. Interestingly, Syt7 and the synaptogenic factor Hevin are developmentally regulated by astrocytes, and partly co-localise in cultured astrocytes. Moreover, synapse number decreases if astrocytes (but not neurones) lack Syt7. To understand how astrocytes release synaptogenic factors, future experiments could address if other Syts and synaptogenic factors are developmentally regulated, and analyse Syt-regulated vesicle fusion mechanisms *in vivo*, e.g. by re-visiting *Syt7^{-/-}* mouse behaviour in the light of astrocytic functional changes.

To analyse vesicular release of glial compounds in astrocytes, we developed a fast, simple, and economical protocol for growing a high yield of stellate astrocytes. These cultures exhibited Ca^{2+} event frequency, amplitude, and duration similar to astrocytes co-cultured with neurones, but different from MD and IP astrocytes. These Ca^{2+} fluctuations and their subcellular localisations were comparable to those of astrocytes in brain slices and *in vivo*, suggesting that cultured astrocytes may employ similar Ca^{2+} signalling profiles. With this new protocol for astrocyte monocultures, follow-up experiments could investigate if astrocytic Ca^{2+} signalling and nearby Syt-mediated vesicle trafficking are linked, e.g. by monitoring Ca^{2+} signalling (using GCaMPs) together with astrocyte vesicle recycling (by transfecting cells with Syt7 coupled to a red pHluorin reporter). Alternatively, since improved red genetically encoded Ca^{2+} indicators like RCaMP2 are now available (Inoue et al., 2015), astrocytic Syt kinetics could be deciphered by simultaneous imaging of Ca^{2+} (through RCaMP2) and Syts coupled to green pH-sensitive fluorescent indicators of vesicle endo- / exocytosis called pHluorins (Miesenböck et al., 1998). In the absence of astrocytic (but not neuronal) Syt7, synapse numbers decrease, i.e. this astrocytic Syt isoform affects synaptic interfaces. Whether or not this happens at tripartite synapses, where astrocytic leaflets enwrap neuronal connections, or whether Syt7-harboured vesicles mediate the global release of synaptogenic factors, remains to be tested.

Astrocyte-derived synaptogenic factors are implicated in several common neurodevelopmental diseases like epilepsy or Down's syndrome. Therefore, studying astrocytic vesicular release mechanisms may help clarify how astrocytes affect synaptogenesis and thus neuronal network function in health and disease.

Bibliography

- Adolfson, B., Saraswati, S., Yoshihara, M., and Littleton, J.T. (2004). Synaptotagmins are trafficked to distinct subcellular domains including the postsynaptic compartment. *J. Cell Biol.* *166*, 249–260.
- Agulhon, C., Fiacco, T.A., and McCarthy, K.D. (2010). Hippocampal short- and long-term plasticity are not modulated by astrocyte Ca²⁺ signaling. *Science* *327*, 1250–1254.
- Allen, N.J. (2013). Role of glia in developmental synapse formation. *Curr. Opin. Neurobiol.* *23*, 1027–1033.
- Allen, N.J., Bennett, M.L., Foo, L.C., Wang, G.X., Chakraborty, C., Smith, S.J., and Barres, B.A. (2012). Astrocyte glypicans 4 and 6 promote formation of excitatory synapses via GluA1 AMPA receptors. *Nature* *486*, 410–414.
- Anderson, C.M., Bergher, J.P., and Swanson, R.A. (2004). ATP-induced ATP release from astrocytes. *J. Neurochem.* *88*, 246–256.
- Andrews, N.W., and Chakrabarti, S. (2005). There's more to life than neurotransmission: the regulation of exocytosis by synaptotagmin VII. *Trends Cell Biol.* *15*, 626–631.
- Angulo, M.C., Kozlov, A.S., Charpak, S., and Audinat, E. (2004). Glutamate released from glial cells synchronizes neuronal activity in the hippocampus. *J. Neurosci. Off. J. Soc. Neurosci.* *24*, 6920–6927.
- Anlauf, E., and Derouiche, A. (2005). Astrocytic exocytosis vesicles and glutamate: a high-resolution immunofluorescence study. *Glia* *49*, 96–106.
- Arango Duque, G., Fukuda, M., and Descoteaux, A. (2013). Synaptotagmin XI regulates phagocytosis and cytokine secretion in macrophages. *J. Immunol. Baltim. Md 1950* *190*, 1737–1745.
- Arantes, R.M.E., and Andrews, N.W. (2006). A role for synaptotagmin VII-regulated exocytosis of lysosomes in neurite outgrowth from primary sympathetic neurons. *J. Neurosci. Off. J. Soc. Neurosci.* *26*, 4630–4637.
- Araque, A., and Navarrete, M. (2010). Glial cells in neuronal network function. *Philos. Trans. R. Soc. Lond. B. Biol. Sci.* *365*, 2375–2381.
- Araque, A., Parpura, V., Sanzgiri, R.P., and Haydon, P.G. (1999). Tripartite synapses: glia, the unacknowledged partner. *Trends Neurosci.* *22*, 208–215.
- Araque, A., Li, N., Doyle, R.T., and Haydon, P.G. (2000). SNARE protein-dependent glutamate release from astrocytes. *J. Neurosci. Off. J. Soc. Neurosci.* *20*, 666–673.
- Baker, D.A., Shen, H., and Kalivas, P.W. (2002). Cystine/glutamate exchange serves as the source for extracellular glutamate: modifications by repeated cocaine administration. *Amino Acids* *23*, 161–162.

- Ballas, N., Lioy, D.T., Grunseich, C., and Mandel, G. (2009). Non-cell autonomous influence of MeCP2-deficient glia on neuronal dendritic morphology. *Nat. Neurosci.* *12*, 311–317.
- Bal-Price, A., Moneer, Z., and Brown, G.C. (2002). Nitric oxide induces rapid, calcium-dependent release of vesicular glutamate and ATP from cultured rat astrocytes. *Glia* *40*, 312–323.
- Barbe, M.T., Monyer, H., and Bruzzone, R. (2006). Cell-cell communication beyond connexins: the pannexin channels. *Physiol. Bethesda Md* *21*, 103–114.
- Barker, A.J., and Ullian, E.M. (2010). Astrocytes and synaptic plasticity. *Neurosci. Rev. J. Bringing Neurobiol. Neurol. Psychiatry* *16*, 40–50.
- Barres, B.A. (1991). Five electrophysiological properties of glial cells. *Ann. N. Y. Acad. Sci.* *633*, 248–254.
- Bauer, D., Haroutunian, V., Meador-Woodruff, J.H., and McCullumsmith, R.E. (2010). Abnormal glycosylation of EAAT1 and EAAT2 in prefrontal cortex of elderly patients with schizophrenia. *Schizophr. Res.* *117*, 92–98.
- Bennett, M.R. (2009). Synapse formation and regression in the cortex during adolescence and in schizophrenia. *Med. J. Aust.* *190*, S14–S16.
- Bergami, M., Santi, S., Formaggio, E., Cagnoli, C., Verderio, C., Blum, R., Berninger, B., Matteoli, M., and Canossa, M. (2008). Uptake and recycling of pro-BDNF for transmitter-induced secretion by cortical astrocytes. *J. Cell Biol.* *183*, 213–221.
- Bergersen, L.H., and Gundersen, V. (2009). Morphological evidence for vesicular glutamate release from astrocytes. *Neuroscience* *158*, 260–265.
- Bergersen, L.H., Morland, C., Ormel, L., Rinholm, J.E., Larsson, M., Wold, J.F.H., Røe, A.T., Stranna, A., Santello, M., Bouvier, D., et al. (2012). Immunogold detection of L-glutamate and D-serine in small synaptic-like microvesicles in adult hippocampal astrocytes. *Cereb. Cortex N. Y. N 1991* *22*, 1690–1697.
- Bezzi, P., Carmignoto, G., Pasti, L., Vesce, S., Rossi, D., Rizzini, B.L., Pozzan, T., and Volterra, A. (1998). Prostaglandins stimulate calcium-dependent glutamate release in astrocytes. *Nature* *391*, 281–285.
- Bezzi, P., Gundersen, V., Galbete, J.L., Seifert, G., Steinhäuser, C., Pilati, E., and Volterra, A. (2004). Astrocytes contain a vesicular compartment that is competent for regulated exocytosis of glutamate. *Nat. Neurosci.* *7*, 613–620.
- Bhalla, A., Tucker, W.C., and Chapman, E.R. (2005). Synaptotagmin isoforms couple distinct ranges of Ca²⁺, Ba²⁺, and Sr²⁺ concentration to SNARE-mediated membrane fusion. *Mol. Biol. Cell* *16*, 4755–4764.
- Bhalla, A., Chicka, M.C., and Chapman, E.R. (2008). Analysis of the synaptotagmin family during reconstituted membrane fusion. Uncovering a class of inhibitory isoforms. *J. Biol. Chem.* *283*, 21799–21807.

- Bittner, C.X., Valdebenito, R., Ruminot, I., Loaiza, A., Larenas, V., Sotelo-Hitschfeld, T., Moldenhauer, H., San Martín, A., Gutiérrez, R., Zambrano, M., et al. (2011). Fast and reversible stimulation of astrocytic glycolysis by K⁺ and a delayed and persistent effect of glutamate. *J. Neurosci. Off. J. Soc. Neurosci.* *31*, 4709–4713.
- Bonanomi, D., Rusconi, L., Colombo, C.A., Benfenati, F., and Valtorta, F. (2007). Synaptophysin I selectively specifies the exocytic pathway of synaptobrevin 2/VAMP2. *Biochem. J.* *404*, 525–534.
- Bowser, D.N., and Khakh, B.S. (2007). Two forms of single-vesicle astrocyte exocytosis imaged with total internal reflection fluorescence microscopy. *Proc. Natl. Acad. Sci. U. S. A.* *104*, 4212–4217.
- Bozzi, Y., Casarosa, S., and Caleo, M. (2012). Epilepsy as a neurodevelopmental disorder. *Front. Psychiatry* *3*, 19.
- Brenner, M., Goldman, J.E., Quinlan, R.A., and Messing, A. (2009). Alexander Disease: A Genetic Disorder of Astrocytes. In *Astrocytes in (Patho)Physiology of the Nervous System*, P.G. Haydon, and V. Parpura, eds. (Springer US), pp. 591–648.
- Cahoy, J.D., Emery, B., Kaushal, A., Foo, L.C., Zamanian, J.L., Christopherson, K.S., Xing, Y., Lubischer, J.L., Krieg, P.A., Krupenko, S.A., et al. (2008). A transcriptome database for astrocytes, neurons, and oligodendrocytes: a new resource for understanding brain development and function. *J. Neurosci. Off. J. Soc. Neurosci.* *28*, 264–278.
- Caleo, M. (2009). Epilepsy: synapses stuck in childhood. *Nat. Med.* *15*, 1126–1127.
- Carlsen, E.M., and Perrier, J.-F. (2014). Purines released from astrocytes inhibit excitatory synaptic transmission in the ventral horn of the spinal cord. *Front. Neural Circuits* *8*, 60.
- Cassé, F., Bardou, I., Danglot, L., Briens, A., Montagne, A., Parcq, J., Alahari, A., Galli, T., Vivien, D., and Docagne, F. (2012). Glutamate controls tPA recycling by astrocytes, which in turn influences glutamatergic signals. *J. Neurosci. Off. J. Soc. Neurosci.* *32*, 5186–5199.
- Chahrour, M., and Zoghbi, H.Y. (2007). The story of Rett syndrome: from clinic to neurobiology. *Neuron* *56*, 422–437.
- Chakrabarti, S., Kobayashi, K.S., Flavell, R.A., Marks, C.B., Miyake, K., Liston, D.R., Fowler, K.T., Gorelick, F.S., and Andrews, N.W. (2003). Impaired membrane resealing and autoimmune myositis in synaptotagmin VII-deficient mice. *J. Cell Biol.* *162*, 543–549.
- Chapman, E.R. (2002). Synaptotagmin: a Ca²⁺ sensor that triggers exocytosis? *Nat. Rev. Mol. Cell Biol.* *3*, 498–508.
- Chieragatti, E., Chicka, M.C., Chapman, E.R., and Baldini, G. (2004). SNAP-23 functions in docking/fusion of granules at low Ca²⁺. *Mol. Biol. Cell* *15*, 1918–1930.
- Christopherson, K.S., Ullian, E.M., Stokes, C.C.A., Mallowney, C.E., Hell, J.W., Agah, A., Lawler, J., Mosher, D.F., Bornstein, P., and Barres, B.A. (2005). Thrombospondins are astrocyte-secreted proteins that promote CNS synaptogenesis. *Cell* *120*, 421–433.

- Citri, A., and Yarden, Y. (2006). EGF-ERBB signalling: towards the systems level. *Nat. Rev. Mol. Cell Biol.* *7*, 505–516.
- Clarke, L.E., and Barres, B.A. (2013). Emerging roles of astrocytes in neural circuit development. *Nat. Rev. Neurosci.* *14*, 311–321.
- Coco, S., Calegari, F., Pravettoni, E., Pozzi, D., Taverna, E., Rosa, P., Matteoli, M., and Verderio, C. (2003). Storage and release of ATP from astrocytes in culture. *J. Biol. Chem.* *278*, 1354–1362.
- Cotrina, M.L., Lin, J.H., Alves-Rodrigues, A., Liu, S., Li, J., Azmi-Ghadimi, H., Kang, J., Naus, C.C., and Nedergaard, M. (1998). Connexins regulate calcium signaling by controlling ATP release. *Proc. Natl. Acad. Sci. U. S. A.* *95*, 15735–15740.
- Cotrina, M.L., Lin, J.H., López-García, J.C., Naus, C.C., and Nedergaard, M. (2000). ATP-mediated glia signaling. *J. Neurosci. Off. J. Soc. Neurosci.* *20*, 2835–2844.
- Craxton, M. (2010). A manual collection of Syt, Esyt, Rph3a, Rph3al, Doc2, and Dblc2 genes from 46 metazoan genomes--an open access resource for neuroscience and evolutionary biology. *BMC Genomics* *11*, 37.
- Crippa, D., Schenk, U., Francolini, M., Rosa, P., Verderio, C., Zonta, M., Pozzan, T., Matteoli, M., and Carmignoto, G. (2006). Synaptobrevin2-expressing vesicles in rat astrocytes: insights into molecular characterization, dynamics and exocytosis. *J. Physiol.* *570*, 567–582.
- Dahl, G. (2015). ATP release through pannexon channels. *Philos. Trans. R. Soc. Lond. B. Biol. Sci.* *370*.
- Dahl, D., Rueger, D.C., Bignami, A., Weber, K., and Osborn, M. (1981). Vimentin, the 57 000 molecular weight protein of fibroblast filaments, is the major cytoskeletal component in immature glia. *Eur. J. Cell Biol.* *24*, 191–196.
- Dallwig, R., Vitten, H., and Deitmer, J.W. (2000). A novel barium-sensitive calcium influx into rat astrocytes at low external potassium. *Cell Calcium* *28*, 247–259.
- Dani, J.W., Chernjavsky, A., and Smith, S.J. (1992). Neuronal activity triggers calcium waves in hippocampal astrocyte networks. *Neuron* *8*, 429–440.
- Deák, F., Schoch, S., Liu, X., Südhof, T.C., and Kavalali, E.T. (2004). Synaptobrevin is essential for fast synaptic-vesicle endocytosis. *Nat. Cell Biol.* *6*, 1102–1108.
- Dean, C., Liu, H., Dunning, F.M., Chang, P.Y., Jackson, M.B., and Chapman, E.R. (2009). Synaptotagmin-IV modulates synaptic function and long-term potentiation by regulating BDNF release. *Nat. Neurosci.* *12*, 767–776.
- Dean, C., Dunning, F.M., Liu, H., Bomba, E., Bharat, V., Ahmed, S., and Chapman, E.R. (2012). Axonal and dendritic synaptotagmin isoforms revealed by a pHluorin-syt functional screen. *Mol. Biol. Cell.*

- Deitmer, J.W., Singaravelu, K., and Lohr, C. (2009). Calcium ion signaling in astrocytes. In *Astrocytes in (Patho)Physiology of the Nervous System*, P.G. Haydon, and V. Parpura, eds. (Springer US), pp. 201–224.
- Delépine, C., Nectoux, J., Letourneur, F., Baud, V., Chelly, J., Billuart, P., and Bienvenu, T. (2015). Astrocyte Transcriptome from the Mecp2(308)-Truncated Mouse Model of Rett Syndrome. *Neuromolecular Med.*
- Del Puerto, A., Wandosell, F., and Garrido, J.J. (2013). Neuronal and glial purinergic receptors functions in neuron development and brain disease. *Front. Cell. Neurosci.* 7, 197.
- Deneen, B., Ho, R., Lukaszewicz, A., Hochstim, C.J., Gronostajski, R.M., and Anderson, D.J. (2006). The transcription factor NFIA controls the onset of gliogenesis in the developing spinal cord. *Neuron* 52, 953–968.
- Di Castro, M.A., Chuquet, J., Liaudet, N., Bhaukaurally, K., Santello, M., Bouvier, D., Tiret, P., and Volterra, A. (2011). Local Ca²⁺ detection and modulation of synaptic release by astrocytes. *Nat. Neurosci.* 14, 1276–1284.
- Dichter, M.A. (1978). Rat cortical neurons in cell culture: culture methods, cell morphology, electrophysiology, and synapse formation. *Brain Res.* 149, 279–293.
- Doll, C.A., and Broadie, K. (2014). Impaired activity-dependent neural circuit assembly and refinement in autism spectrum disorder genetic models. *Front. Cell. Neurosci.* 8, 30.
- Donato, R., Cannon, B.R., Sorci, G., Riuzzi, F., Hsu, K., Weber, D.J., and Geczy, C.L. (2013). Functions of S100 proteins. *Curr. Mol. Med.* 13, 24–57.
- Draper, J.S., Moore, H.D., Ruban, L.N., Gokhale, P.J., and Andrews, P.W. (2004). Culture and characterization of human embryonic stem cells. *Stem Cells Dev.* 13, 325–336.
- Du, F., Qian, Z.M., Zhu, L., Wu, X.M., Qian, C., Chan, R., and Ke, Y. (2010). Purity, cell viability, expression of GFAP and bystin in astrocytes cultured by different procedures. *J. Cell. Biochem.* 109, 30–37.
- Duan, S., Anderson, C.M., Keung, E.C., Chen, Y., Chen, Y., and Swanson, R.A. (2003). P2X7 receptor-mediated release of excitatory amino acids from astrocytes. *J. Neurosci. Off. J. Soc. Neurosci.* 23, 1320–1328.
- Dutly, F., and Schwab, M.E. (1991). Neurons and astrocytes influence the development of purified O-2A progenitor cells. *Glia* 4, 559–571.
- Eroglu, C. (2009). The role of astrocyte-secreted matricellular proteins in central nervous system development and function. *J. Cell Commun. Signal.* 3, 167–176.
- Eroglu, C., and Barres, B.A. (2010). Regulation of synaptic connectivity by glia. *Nature* 468, 223–231.
- Faber-Elman, A., Solomon, A., Abraham, J.A., Marikovsky, M., and Schwartz, M. (1996). Involvement of wound-associated factors in rat brain astrocyte migratory response to axonal injury: in vitro simulation. *J. Clin. Invest.* 97, 162–171.

- Fan, G., Martinowich, K., Chin, M.H., He, F., Fouse, S.D., Hutnick, L., Hattori, D., Ge, W., Shen, Y., Wu, H., et al. (2005). DNA methylation controls the timing of astroglialogenesis through regulation of JAK-STAT signaling. *Dev. Camb. Engl.* *132*, 3345–3356.
- Feldmann, A., Winterstein, C., White, R., Trotter, J., and Krämer-Albers, E.-M. (2009). Comprehensive analysis of expression, subcellular localization, and cognate pairing of SNARE proteins in oligodendrocytes. *J. Neurosci. Res.* *87*, 1760–1772.
- Fellin, T., Pascual, O., Gobbo, S., Pozzan, T., Haydon, P.G., and Carmignoto, G. (2004). Neuronal synchrony mediated by astrocytic glutamate through activation of extrasynaptic NMDA receptors. *Neuron* *43*, 729–743.
- Fellin, T., Sul, J.-Y., D’Ascenzo, M., Takano, H., Pascual, O., and Haydon, P.G. (2006a). Bidirectional astrocyte-neuron communication: the many roles of glutamate and ATP. *Novartis Found. Symp.* *276*, 208–217; discussion 217–221, 233–237, 275–281.
- Fellin, T., Pozzan, T., and Carmignoto, G. (2006b). Purinergic receptors mediate two distinct glutamate release pathways in hippocampal astrocytes. *J. Biol. Chem.* *281*, 4274–4284.
- Fellin, T., Halassa, M.M., Terunuma, M., Succol, F., Takano, H., Frank, M., Moss, S.J., and Haydon, P.G. (2009). Endogenous nonneuronal modulators of synaptic transmission control cortical slow oscillations in vivo. *Proc. Natl. Acad. Sci. U. S. A.* *106*, 15037–15042.
- Ferguson, G.D., Anagnostaras, S.G., Silva, A.J., and Herschman, H.R. (2000). Deficits in memory and motor performance in synaptotagmin IV mutant mice. *Proc. Natl. Acad. Sci. U. S. A.* *97*, 5598–5603.
- Ferguson, G.D., Wang, H., Herschman, H.R., and Storm, D.R. (2004a). Altered hippocampal short-term plasticity and associative memory in synaptotagmin IV (-/-) mice. *Hippocampus* *14*, 964–974.
- Ferguson, G.D., Herschman, H.R., and Storm, D.R. (2004b). Reduced anxiety and depression-like behavior in synaptotagmin IV (-/-) mice. *Neuropharmacology* *47*, 604–611.
- Fernandez-Fernandez, S., Almeida, A., and Bolaños, J.P. (2012). Antioxidant and bioenergetic coupling between neurons and astrocytes. *Biochem. J.* *443*, 3–11.
- Fiacco, T.A., Agulhon, C., and McCarthy, K.D. (2009). Sorting out astrocyte physiology from pharmacology. *Annu. Rev. Pharmacol. Toxicol.* *49*, 151–174.
- Fields, R.D., and Stevens-Graham, B. (2002). New insights into neuron-glia communication. *Science* *298*, 556–562.
- Fields, R.D., Araque, A., Johansen-Berg, H., Lim, S.-S., Lynch, G., Nave, K.-A., Nedergaard, M., Perez, R., Sejnowski, T., and Wake, H. (2014). Glial biology in learning and cognition. *Neurosci. Rev. J. Bringing Neurobiol. Neurol. Psychiatry* *20*, 426–431.
- Flannery, A.R., Czibener, C., and Andrews, N.W. (2010). Palmitoylation-dependent association with CD63 targets the Ca²⁺ sensor synaptotagmin VII to lysosomes. *J. Cell Biol.* *191*, 599–613.

- Foo, L.C. (2013a). Purification of astrocytes from transgenic rodents by fluorescence-activated cell sorting. *Cold Spring Harb. Protoc.* 2013, 551–560.
- Foo, L.C. (2013b). Purification of rat and mouse astrocytes by immunopanning. *Cold Spring Harb. Protoc.* 2013.
- Foo, L.C., and Dougherty, J.D. (2013). Aldh1L1 is expressed by postnatal neural stem cells in vivo. *Glia* 61, 1533–1541.
- Foo, L.C., Allen, N.J., Bushong, E.A., Ventura, P.B., Chung, W.-S., Zhou, L., Cahoy, J.D., Daneman, R., Zong, H., Ellisman, M.H., et al. (2011). Development of a method for the purification and culture of rodent astrocytes. *Neuron* 71, 799–811.
- Freeman, M.R. (2010). Specification and morphogenesis of astrocytes. *Science* 330, 774–778.
- Fremeau, R.T., Burman, J., Qureshi, T., Tran, C.H., Proctor, J., Johnson, J., Zhang, H., Sulzer, D., Copenhagen, D.R., Storm-Mathisen, J., et al. (2002). The identification of vesicular glutamate transporter 3 suggests novel modes of signaling by glutamate. *Proc. Natl. Acad. Sci. U. S. A.* 99, 14488–14493.
- Fukuda, M., and Mikoshiba, K. (2001a). The N-terminal cysteine cluster is essential for membrane targeting of B/K protein. *Biochem. J.* 360, 441–448.
- Fukuda, M., and Mikoshiba, K. (2001b). Characterization of KIAA1427 protein as an atypical synaptotagmin (Syt XIII). *Biochem. J.* 354, 249–257.
- Fukuda, M., Ogata, Y., Saegusa, C., Kanno, E., and Mikoshiba, K. (2002). Alternative splicing isoforms of synaptotagmin VII in the mouse, rat and human. *Biochem. J.* 365, 173–180.
- Fukuda, M., Kanno, E., Satoh, M., Saegusa, C., and Yamamoto, A. (2004). Synaptotagmin VII is targeted to dense-core vesicles and regulates their Ca²⁺-dependent exocytosis in PC12 cells. *J. Biol. Chem.* 279, 52677–52684.
- Galati, R. (2012). The Role of Cyclooxygenase-2, Epidermal Growth Factor Receptor and Aromatase in Malignant Mesothelioma. In *Malignant Mesothelioma*, C. Belli, ed. (InTech),.
- Garcia, O., Torres, M., Helguera, P., Coskun, P., and Busciglio, J. (2010). A role for thrombospondin-1 deficits in astrocyte-mediated spine and synaptic pathology in Down's syndrome. *PLoS One* 5, e14200.
- García-Marín, V., García-López, P., and Freire, M. (2007). Cajal's contributions to glia research. *Trends Neurosci.* 30, 479–487.
- Ge, W.-P., Miyawaki, A., Gage, F.H., Jan, Y.N., and Jan, L.Y. (2012). Local generation of glia is a major astrocyte source in postnatal cortex. *Nature* 484, 376–380.
- Geppert, M., Goda, Y., Hammer, R.E., Li, C., Rosahl, T.W., Stevens, C.F., and Südhof, T.C. (1994). Synaptotagmin I: a major Ca²⁺ sensor for transmitter release at a central synapse. *Cell* 79, 717–727.

- Glantz, L.A., and Lewis, D.A. (2000). Decreased dendritic spine density on prefrontal cortical pyramidal neurons in schizophrenia. *Arch. Gen. Psychiatry* 57, 65–73.
- Gómez-Gonzalo, M., Losi, G., Chiavegato, A., Zonta, M., Cammarota, M., Brondi, M., Vetri, F., Uva, L., Pozzan, T., de Curtis, M., et al. (2010). An excitatory loop with astrocytes contributes to drive neurons to seizure threshold. *PLoS Biol.* 8, e1000352.
- Gordon, G.R.J., Iremonger, K.J., Kantevari, S., Ellis-Davies, G.C.R., MacVicar, B.A., and Bains, J.S. (2009). Astrocyte-mediated distributed plasticity at hypothalamic glutamate synapses. *Neuron* 64, 391–403.
- Goslin, K., Schreyer, D.J., Skene, J.H., and Banker, G. (1990). Changes in the distribution of GAP-43 during the development of neuronal polarity. *J. Neurosci. Off. J. Soc. Neurosci.* 10, 588–602.
- Hagerman, P.J., and Stafstrom, C.E. (2009). Origins of epilepsy in fragile X syndrome. *Epilepsy Curr. Am. Epilepsy Soc.* 9, 108–112.
- Hamilton, N.B., and Attwell, D. (2010). Do astrocytes really exocytose neurotransmitters? *Nat. Rev. Neurosci.* 11, 227–238.
- Han, D.W., Greber, B., Wu, G., Tapia, N., Araúz-Bravo, M.J., Ko, K., Bernemann, C., Stehling, M., and Schöler, H.R. (2011). Direct reprogramming of fibroblasts into epiblast stem cells. *Nat. Cell Biol.* 13, 66–71.
- Han, X., Chen, M., Wang, F., Windrem, M., Wang, S., Shanz, S., Xu, Q., Oberheim, N.A., Bekar, L., Betstadt, S., et al. (2013). Forebrain engraftment by human glial progenitor cells enhances synaptic plasticity and learning in adult mice. *Cell Stem Cell* 12, 342–353.
- Hanson, P.I., Heuser, J.E., and Jahn, R. (1997). Neurotransmitter release - four years of SNARE complexes. *Curr. Opin. Neurobiol.* 7, 310–315.
- Härtel, K., Singaravelu, K., Kaiser, M., Neusch, C., Hülsmann, S., and Deitmer, J.W. (2007). Calcium influx mediated by the inwardly rectifying K⁺ channel Kir4.1 (KCNJ10) at low external K⁺ concentration. *Cell Calcium* 42, 271–280.
- Hassinger, T.D., Atkinson, P.B., Strecker, G.J., Whalen, L.R., Dudek, F.E., Kossel, A.H., and Kater, S.B. (1995). Evidence for glutamate-mediated activation of hippocampal neurons by glial calcium waves. *J. Neurobiol.* 28, 159–170.
- He, F., Ge, W., Martinowich, K., Becker-Catania, S., Coskun, V., Zhu, W., Wu, H., Castro, D., Guillemot, F., Fan, G., et al. (2005). A positive autoregulatory loop of Jak-STAT signaling controls the onset of astrogenesis. *Nat. Neurosci.* 8, 616–625.
- Helmy, K.Y., Katschke, K.J., Gorgani, N.N., Kljavin, N.M., Elliott, J.M., Diehl, L., Scales, S.J., Ghilardi, N., and van Lookeren Campagne, M. (2006). CR1g: a macrophage complement receptor required for phagocytosis of circulating pathogens. *Cell* 124, 915–927.
- Henneberger, C., Papouin, T., Oliet, S.H.R., and Rusakov, D.A. (2010). Long-term potentiation depends on release of D-serine from astrocytes. *Nature* 463, 232–236.

- Hepp, R., Perraut, M., Chasserot-Golaz, S., Galli, T., Aunis, D., Langley, K., and Grant, N.J. (1999). Cultured glial cells express the SNAP-25 analogue SNAP-23. *Glia* 27, 181–187.
- Hughes, E.G., Elmariah, S.B., and Balice-Gordon, R.J. (2010). Astrocyte secreted proteins selectively increase hippocampal GABAergic axon length, branching, and synaptogenesis. *Mol. Cell. Neurosci.* 43, 136–145.
- Hui, E., Bai, J., Wang, P., Sugimori, M., Llinas, R.R., and Chapman, E.R. (2005). Three distinct kinetic groupings of the synaptotagmin family: candidate sensors for rapid and delayed exocytosis. *Proc. Natl. Acad. Sci. U. S. A.* 102, 5210–5214.
- Hur, Y.S., Kim, K.D., Paek, S.H., and Yoo, S.H. (2010). Evidence for the existence of secretory granule (dense-core vesicle)-based inositol 1,4,5-trisphosphate-dependent Ca²⁺ signaling system in astrocytes. *PLoS One* 5, e11973.
- Iglesias-Bartolomé, R., Crespo, P.M., Gomez, G.A., and Daniotti, J.L. (2006). The antibody to GD3 ganglioside, R24, is rapidly endocytosed and recycled to the plasma membrane via the endocytic recycling compartment. Inhibitory effect of brefeldin A and monensin. *FEBS J.* 273, 1744–1758.
- Innocenti, B., Parpura, V., and Haydon, P.G. (2000). Imaging extracellular waves of glutamate during calcium signaling in cultured astrocytes. *J. Neurosci. Off. J. Soc. Neurosci.* 20, 1800–1808.
- Inoue, M., Takeuchi, A., Horigane, S., Ohkura, M., Gengyo-Ando, K., Fujii, H., Kamijo, S., Takemoto-Kimura, S., Kano, M., Nakai, J., et al. (2015). Rational design of a high-affinity, fast, red calcium indicator R-CaMP2. *Nat. Methods* 12, 64–70.
- Iruela-Arispe, M.L., Liska, D.J., Sage, E.H., and Bornstein, P. (1993). Differential expression of thrombospondin 1, 2, and 3 during murine development. *Dev. Dyn. Off. Publ. Am. Assoc. Anat.* 197, 40–56.
- Ishibashi, T., Dakin, K.A., Stevens, B., Lee, P.R., Kozlov, S.V., Stewart, C.L., and Fields, R.D. (2006). Astrocytes promote myelination in response to electrical impulses. *Neuron* 49, 823–832.
- Jacob, P.F., Vaz, S.H., Ribeiro, J.A., and Sebastião, A.M. (2014). P2Y1 receptor inhibits GABA transport through a calcium signalling-dependent mechanism in rat cortical astrocytes. *Glia* 62, 1211–1226.
- Jacobs, S., and Doering, L.C. (2010). Astrocytes prevent abnormal neuronal development in the fragile x mouse. *J. Neurosci. Off. J. Soc. Neurosci.* 30, 4508–4514.
- Jahn, R., and Fasshauer, D. (2012). Molecular machines governing exocytosis of synaptic vesicles. *Nature* 490, 201–207.
- Jahn, R., and Scheller, R.H. (2006). SNAREs--engines for membrane fusion. *Nat. Rev. Mol. Cell Biol.* 7, 631–643.
- Jaiswal, J.K., Chakrabarti, S., Andrews, N.W., and Simon, S.M. (2004). Synaptotagmin VII restricts fusion pore expansion during lysosomal exocytosis. *PLoS Biol.* 2, E233.

- Jaiswal, J.K., Fix, M., Takano, T., Nedergaard, M., and Simon, S.M. (2007). Resolving vesicle fusion from lysis to monitor calcium-triggered lysosomal exocytosis in astrocytes. *Proc. Natl. Acad. Sci. U. S. A.* *104*, 14151–14156.
- Jeftinija, S.D., Jeftinija, K.V., and Stefanovic, G. (1997). Cultured astrocytes express proteins involved in vesicular glutamate release. *Brain Res.* *750*, 41–47.
- Jo, I., Harris, H.W., Amendt-Raduege, A.M., Majewski, R.R., and Hammond, T.G. (1995). Rat kidney papilla contains abundant synaptobrevin protein that participates in the fusion of antidiuretic hormone-regulated water channel-containing endosomes in vitro. *Proc. Natl. Acad. Sci. U. S. A.* *92*, 1876–1880.
- Jones, E.V., and Bouvier, D.S. (2014). Astrocyte-secreted matricellular proteins in CNS remodelling during development and disease. *Neural Plast.* *2014*, 321209.
- Jones, E.V., Bernardinelli, Y., Tse, Y.C., Chierzi, S., Wong, T.P., and Murai, K.K. (2011). Astrocytes control glutamate receptor levels at developing synapses through SPARC-beta-integrin interactions. *J. Neurosci. Off. J. Soc. Neurosci.* *31*, 4154–4165.
- Jourdain, P., Bergersen, L.H., Bhaukaurally, K., Bezzi, P., Santello, M., Domercq, M., Matute, C., Tonello, F., Gundersen, V., and Volterra, A. (2007). Glutamate exocytosis from astrocytes controls synaptic strength. *Nat. Neurosci.* *10*, 331–339.
- Kaiser, O., Aliuos, P., Wissel, K., Lenarz, T., Werner, D., Reuter, G., Kral, A., and Warnecke, A. (2013). Dissociated neurons and glial cells derived from rat inferior colliculi after digestion with papain. *PLoS One* *8*, e80490.
- Kang, N., Peng, H., Yu, Y., Stanton, P.K., Guilarte, T.R., and Kang, J. (2013). Astrocytes release d-serine by a large vesicle. *Neuroscience* *240*, 243–257.
- Khakh, B.S., and McCarthy, K.D. (2015). Astrocyte calcium signaling: from observations to functions and the challenges therein. *Cold Spring Harb. Perspect. Biol.* *7*, a020404.
- Kim, H., Lee, B.-H., Choi, S.-H., Kim, H.-J., Jung, S.-W., Hwang, S.-H., Rhim, H., Kim, H.-C., Cho, I.-H., and Nah, S.-Y. (2015a). Gintoin stimulates gliotransmitter release in cortical primary astrocytes. *Neurosci. Lett.* *603*, 19–24.
- Kim, K.J., Iddings, J.A., Stern, J.E., Blanco, V.M., Croom, D., Kirov, S.A., and Filosa, J.A. (2015b). Astrocyte contributions to flow/pressure-evoked parenchymal arteriole vasoconstriction. *J. Neurosci. Off. J. Soc. Neurosci.* *35*, 8245–8257.
- Kimelberg, H.K., Anderson, E., and Kettenmann, H. (1990). Swelling-induced changes in electrophysiological properties of cultured astrocytes and oligodendrocytes. II. Whole-cell currents. *Brain Res.* *529*, 262–268.
- Kirischuk, S., Kettenmann, H., and Verkhratsky, A. (1997). Na⁺/Ca²⁺ exchanger modulates kainate-triggered Ca²⁺ signaling in Bergmann glial cells in situ. *FASEB J. Off. Publ. Fed. Am. Soc. Exp. Biol.* *11*, 566–572.
- Koo, S.J., Markovic, S., Puchkov, D., Mahrenholz, C.C., Beceren-Braun, F., Maritzen, T., Dornedde, J., Volkmer, R., Oschkinat, H., and Haucke, V. (2011). SNARE motif-mediated

sorting of synaptobrevin by the endocytic adaptors clathrin assembly lymphoid myeloid leukemia (CALM) and AP180 at synapses. *Proc. Natl. Acad. Sci. U. S. A.* *108*, 13540–13545.

Kornblum, H.I., Zurcher, S.D., Werb, Z., Derynck, R., and Seroogy, K.B. (1999). Multiple trophic actions of heparin-binding epidermal growth factor (HB-EGF) in the central nervous system. *Eur. J. Neurosci.* *11*, 3236–3246.

Korotkevych, N.V., Labyntsev, A.J., Kolybo, D.V., and Komisarenko, S.V. (2015). The Soluble Heparin-Binding EGF-Like Growth Factor Stimulates EGF Receptor Trafficking to the Nucleus. *PLoS One* *10*, e0127887.

Kotlikoff, M.I. (2007). Genetically encoded Ca²⁺ indicators: using genetics and molecular design to understand complex physiology. *J. Physiol.* *578*, 55–67.

Krencik, R., and Zhang, S.-C. (2011). Directed differentiation of functional astroglial subtypes from human pluripotent stem cells. *Nat. Protoc.* *6*, 1710–1717.

Kucukdereli, H., Allen, N.J., Lee, A.T., Feng, A., Ozlu, M.I., Conatser, L.M., Chakraborty, C., Workman, G., Weaver, M., Sage, E.H., et al. (2011). Control of excitatory CNS synaptogenesis by astrocyte-secreted proteins Hevin and SPARC. *Proc. Natl. Acad. Sci. U. S. A.* *108*, E440–E449.

Kuga, N., Sasaki, T., Takahara, Y., Matsuki, N., and Ikegaya, Y. (2011). Large-scale calcium waves traveling through astrocytic networks in vivo. *J. Neurosci. Off. J. Soc. Neurosci.* *31*, 2607–2614.

Kuismanen, E., and Saraste, J. (1989). Low temperature-induced transport blocks as tools to manipulate membrane traffic. *Methods Cell Biol.* *32*, 257–274.

Kuo, C.-L., Oyler, G., and Shoemaker, C.B. (2010). Lipid and cationic polymer based transduction of botulinum holotoxin, or toxin protease alone, extends the target cell range and improves the efficiency of intoxication. *Toxicol. Off. J. Int. Soc. Toxicology* *55*, 619–629.

Lang, T., and Jahn, R. (2008). Core proteins of the secretory machinery. *Handb. Exp. Pharmacol.* 107–127.

LaRochelle, W.J. (2009). A Sensitive Method to Quantitatively Detect Total Protein on Membranes after Electrophoretic Transfer Using Avidin- or Streptavidin-Biotin. In *The Protein Protocols Handbook*, J.M. Walker, ed. (Totowa, NJ: Humana Press), pp. 771–777.

Li, D., Ropert, N., Koulakoff, A., Giaume, C., and Oheim, M. (2008). Lysosomes are the major vesicular compartment undergoing Ca²⁺-regulated exocytosis from cortical astrocytes. *J. Neurosci. Off. J. Soc. Neurosci.* *28*, 7648–7658.

Li, D., Héroult, K., Silm, K., Evrard, A., Wojcik, S., Oheim, M., Herzog, E., and Ropert, N. (2013). Lack of evidence for vesicular glutamate transporter expression in mouse astrocytes. *J. Neurosci. Off. J. Soc. Neurosci.* *33*, 4434–4455.

Li, D., Héroult, K., Zylbersztein, K., Lauterbach, M.A., Guillon, M., Oheim, M., and Ropert, N. (2015). Astrocyte VAMP3 vesicles undergo Ca²⁺-independent cycling and modulate glutamate transporter trafficking. *J. Physiol.* *593*, 2807–2832.

- Lioy, D.T., Garg, S.K., Monaghan, C.E., Raber, J., Foust, K.D., Kaspar, B.K., Hirrlinger, P.G., Kirchhoff, F., Bissonnette, J.M., Ballas, N., et al. (2011). A role for glia in the progression of Rett's syndrome. *Nature* *475*, 497–500.
- Liu, H., Bai, H., Hui, E., Yang, L., Evans, C.S., Wang, Z., Kwon, S.E., and Chapman, E.R. (2014). Synaptotagmin 7 functions as a Ca²⁺-sensor for synaptic vesicle replenishment. *eLife* *3*.
- Liu, T., Sun, L., Xiong, Y., Shang, S., Guo, N., Teng, S., Wang, Y., Liu, B., Wang, C., Wang, L., et al. (2011). Calcium triggers exocytosis from two types of organelles in a single astrocyte. *J. Neurosci. Off. J. Soc. Neurosci.* *31*, 10593–10601.
- Lively, S., and Brown, I.R. (2008a). Localization of the extracellular matrix protein SC1 coincides with synaptogenesis during rat postnatal development. *Neurochem. Res.* *33*, 1692–1700.
- Lively, S., and Brown, I.R. (2008b). The extracellular matrix protein SC1/hevin localizes to excitatory synapses following status epilepticus in the rat lithium-pilocarpine seizure model. *J. Neurosci. Res.* *86*, 2895–2905.
- Lively, S., Ringuette, M.J., and Brown, I.R. (2007). Localization of the extracellular matrix protein SC1 to synapses in the adult rat brain. *Neurochem. Res.* *32*, 65–71.
- Maienschein, V., Marxen, M., Volkandt, W., and Zimmermann, H. (1999). A plethora of presynaptic proteins associated with ATP-storing organelles in cultured astrocytes. *Glia* *26*, 233–244.
- Malarkey, E.B., and Parpura, V. (2008). Mechanisms of glutamate release from astrocytes. *Neurochem. Int.* *52*, 142–154.
- Malarkey, E.B., and Parpura, V. (2011). Temporal characteristics of vesicular fusion in astrocytes: examination of synaptobrevin 2-laden vesicles at single vesicle resolution. *J. Physiol.* *589*, 4271–4300.
- Martineau, M. (2013). Gliotransmission: focus on exocytotic release of L-glutamate and D-serine from astrocytes. *Biochem. Soc. Trans.* *41*, 1557–1561.
- Martineau, M., Galli, T., Baux, G., and Mothet, J.-P. (2008). Confocal imaging and tracking of the exocytotic routes for D-serine-mediated gliotransmission. *Glia* *56*, 1271–1284.
- Martineau, M., Shi, T., Puyal, J., Knolhoff, A.M., Dulong, J., Gasnier, B., Klingauf, J., Sweedler, J.V., Jahn, R., and Mothet, J.-P. (2013). Storage and Uptake of D-Serine into Astrocytic Synaptic-Like Vesicles Specify Gliotransmission. *J. Neurosci. Off. J. Soc. Neurosci.* *33*, 3413–3423.
- Martinez, I., Chakrabarti, S., Hellevik, T., Morehead, J., Fowler, K., and Andrews, N.W. (2000). Synaptotagmin VII regulates Ca²⁺-dependent exocytosis of lysosomes in fibroblasts. *J. Cell Biol.* *148*, 1141–1149.
- Maximov, A., Lao, Y., Li, H., Chen, X., Rizo, J., Sørensen, J.B., and Südhof, T.C. (2008). Genetic analysis of synaptotagmin-7 function in synaptic vesicle exocytosis. *Proc. Natl. Acad. Sci. U. S. A.* *105*, 3986–3991.

- McCarthy, K.D., and de Vellis, J. (1980). Preparation of separate astroglial and oligodendroglial cell cultures from rat cerebral tissue. *J. Cell Biol.* 85, 890–902.
- McKellar, C.E., and Shatz, C.J. (2009). Synaptogenesis in purified cortical subplate neurons. *Cereb. Cortex N. Y. N* 1991 19, 1723–1737.
- Melone, M., Bellesi, M., Ducati, A., Iacoangeli, M., and Conti, F. (2011). Cellular and Synaptic Localization of EAAT2a in Human Cerebral Cortex. *Front. Neuroanat.* 4, 151.
- Messam, C.A., Hou, J., and Major, E.O. (2000). Coexpression of nestin in neural and glial cells in the developing human CNS defined by a human-specific anti-nestin antibody. *Exp. Neurol.* 161, 585–596.
- Miesenböck, G., De Angelis, D.A., and Rothman, J.E. (1998). Visualizing secretion and synaptic transmission with pH-sensitive green fluorescent proteins. *Nature* 394, 192–195.
- Miller, F.D., and Gauthier, A.S. (2007). Timing is everything: making neurons versus glia in the developing cortex. *Neuron* 54, 357–369.
- Minelli, A., Castaldo, P., Gobbi, P., Salucci, S., Magi, S., and Amoroso, S. (2007). Cellular and subcellular localization of Na⁺-Ca²⁺ exchanger protein isoforms, NCX1, NCX2, and NCX3 in cerebral cortex and hippocampus of adult rat. *Cell Calcium* 41, 221–234.
- Mittelstaedt, T., Seifert, G., Álvarez-Barón, E., Steinhäuser, C., Becker, A.J., and Schoch, S. (2009). Differential mRNA expression patterns of the synaptotagmin gene family in the rodent brain. *J. Comp. Neurol.* 512, 514–528.
- Moghaddam, B., and Javitt, D. (2012). From revolution to evolution: the glutamate hypothesis of schizophrenia and its implication for treatment. *Neuropsychopharmacol. Off. Publ. Am. Coll. Neuropsychopharmacol.* 37, 4–15.
- Mohrmann, R., de Wit, H., Connell, E., Pinheiro, P.S., Leese, C., Bruns, D., Davletov, B., Verhage, M., and Sørensen, J.B. (2013). Synaptotagmin interaction with SNAP-25 governs vesicle docking, priming, and fusion triggering. *J. Neurosci. Off. J. Soc. Neurosci.* 33, 14417–14430.
- Molofsky, A.V., Krencik, R., Krenick, R., Ullian, E.M., Ullian, E., Tsai, H., Deneen, B., Richardson, W.D., Barres, B.A., and Rowitch, D.H. (2012). Astrocytes and disease: a neurodevelopmental perspective. *Genes Dev.* 26, 891–907.
- Montana, V., Ni, Y., Sunjara, V., Hua, X., and Parpura, V. (2004). Vesicular glutamate transporter-dependent glutamate release from astrocytes. *J. Neurosci. Off. J. Soc. Neurosci.* 24, 2633–2642.
- Montana, V., Malarkey, E.B., Verderio, C., Matteoli, M., and Parpura, V. (2006). Vesicular transmitter release from astrocytes. *Glia* 54, 700–715.
- Monterrat, C., Grise, F., Benassy, M.N., Hémar, A., and Lang, J. (2007). The calcium-sensing protein synaptotagmin 7 is expressed on different endosomal compartments in endocrine, neuroendocrine cells or neurons but not on large dense core vesicles. *Histochem. Cell Biol.* 127, 625–632.

- Mothet, J.P., Parent, A.T., Wolosker, H., Brady, R.O., Linden, D.J., Ferris, C.D., Rogawski, M.A., and Snyder, S.H. (2000). D-serine is an endogenous ligand for the glycine site of the N-methyl-D-aspartate receptor. *Proc. Natl. Acad. Sci. U. S. A.* *97*, 4926–4931.
- Mothet, J.-P., Pollegioni, L., Ouanounou, G., Martineau, M., Fossier, P., and Baux, G. (2005). Glutamate receptor activation triggers a calcium-dependent and SNARE protein-dependent release of the gliotransmitter D-serine. *Proc. Natl. Acad. Sci. U. S. A.* *102*, 5606–5611.
- Mullis, K., Faloona, F., Scharf, S., Saiki, R., Horn, G., and Erlich, H. (1986). Specific enzymatic amplification of DNA in vitro: the polymerase chain reaction. *Cold Spring Harb. Symp. Quant. Biol.* *51 Pt 1*, 263–273.
- Nakai, J., Ohkura, M., and Imoto, K. (2001). A high signal-to-noise Ca²⁺ probe composed of a single green fluorescent protein. *Nat. Biotechnol.* *19*, 137–141.
- Navarrete, M., Perea, G., Fernandez de Sevilla, D., Gómez-Gonzalo, M., Núñez, A., Martín, E.D., and Araque, A. (2012). Astrocytes mediate in vivo cholinergic-induced synaptic plasticity. *PLoS Biol.* *10*, e1001259.
- Nedergaard, M. (1994). Direct signaling from astrocytes to neurons in cultures of mammalian brain cells. *Science* *263*, 1768–1771.
- Nedergaard, M., Ransom, B., and Goldman, S.A. (2003). New roles for astrocytes: redefining the functional architecture of the brain. *Trends Neurosci.* *26*, 523–530.
- Nelson, A.B., Bussert, T.G., Kreitzer, A.C., and Seal, R.P. (2014). Striatal cholinergic neurotransmission requires VGLUT3. *J. Neurosci. Off. J. Soc. Neurosci.* *34*, 8772–8777.
- Nett, W.J., Oloff, S.H., and McCarthy, K.D. (2002). Hippocampal astrocytes in situ exhibit calcium oscillations that occur independent of neuronal activity. *J. Neurophysiol.* *87*, 528–537.
- Newman, E.A., and Zahs, K.R. (1998). Modulation of neuronal activity by glial cells in the retina. *J. Neurosci. Off. J. Soc. Neurosci.* *18*, 4022–4028.
- Ni, Y., and Parpura, V. (2009). Dual regulation of Ca²⁺-dependent glutamate release from astrocytes: vesicular glutamate transporters and cytosolic glutamate levels. *Glia* *57*, 1296–1305.
- Nimmerjahn, A., Kirchhoff, F., Kerr, J.N.D., and Helmchen, F. (2004). Sulforhodamine 101 as a specific marker of astroglia in the neocortex in vivo. *Nat. Methods* *1*, 31–37.
- Nizar, K., Uhlirva, H., Tian, P., Saisan, P.A., Cheng, Q., Reznichenko, L., Weldy, K.L., Steed, T.C., Sridhar, V.B., MacDonald, C.L., et al. (2013). In vivo stimulus-induced vasodilation occurs without IP₃ receptor activation and may precede astrocytic calcium increase. *J. Neurosci. Off. J. Soc. Neurosci.* *33*, 8411–8422.
- Oberheim, N.A., Wang, X., Goldman, S., and Nedergaard, M. (2006). Astrocytic complexity distinguishes the human brain. *Trends Neurosci.* *29*, 547–553.
- Ohno, T., and Sakurai, M. (2005). Critical period for activity-dependent elimination of corticospinal synapses in vitro. *Neuroscience* *132*, 917–922.

- Ormel, L., Stensrud, M.J., Chaudhry, F.A., and Gundersen, V. (2012). A distinct set of synaptic-like microvesicles in astroglial cells contain VGLUT3. *Glia* 60, 1289–1300.
- Otsu, Y., Couchman, K., Lyons, D.G., Collot, M., Agarwal, A., Mallet, J.-M., Pfrieger, F.W., Bergles, D.E., and Charpak, S. (2015). Calcium dynamics in astrocyte processes during neurovascular coupling. *Nat. Neurosci.* 18, 210–218.
- Paco, S., Margelí, M.A., Olkkonen, V.M., Imai, A., Blasi, J., Fischer-Colbrie, R., and Aguado, F. (2009). Regulation of exocytotic protein expression and Ca²⁺-dependent peptide secretion in astrocytes. *J. Neurochem.* 110, 143–156.
- Panatier, A., Theodosis, D.T., Mothet, J.-P., Touquet, B., Pollegioni, L., Poulain, D.A., and Oliet, S.H.R. (2006). Glia-derived D-serine controls NMDA receptor activity and synaptic memory. *Cell* 125, 775–784.
- Panatier, A., Vallée, J., Haber, M., Murai, K.K., Lacaille, J.-C., and Robitaille, R. (2011). Astrocytes are endogenous regulators of basal transmission at central synapses. *Cell* 146, 785–798.
- Pang, Z.P., Melicoff, E., Padgett, D., Liu, Y., Teich, A.F., Dickey, B.F., Lin, W., Adachi, R., and Südhof, T.C. (2006). Synaptotagmin-2 is essential for survival and contributes to Ca²⁺ triggering of neurotransmitter release in central and neuromuscular synapses. *J. Neurosci. Off. J. Soc. Neurosci.* 26, 13493–13504.
- Parpura, V., and Zorec, R. (2010). Gliotransmission: Exocytotic release from astrocytes. *Brain Res. Rev.* 63, 83–92.
- Parpura, V., Basarsky, T.A., Liu, F., Jeftinija, K., Jeftinija, S., and Haydon, P.G. (1994). Glutamate-mediated astrocyte-neuron signalling. *Nature* 369, 744–747.
- Parpura, V., Fang, Y., Basarsky, T., Jahn, R., and Haydon, P.G. (1995). Expression of synaptobrevin II, cellubrevin and syntaxin but not SNAP-25 in cultured astrocytes. *FEBS Lett.* 377, 489–492.
- Parri, R., and Crunelli, V. (2003). An astrocyte bridge from synapse to blood flow. *Nat. Neurosci.* 6, 5–6.
- Parri, H.R., Gould, T.M., and Crunelli, V. (2001). Spontaneous astrocytic Ca²⁺ oscillations in situ drive NMDAR-mediated neuronal excitation. *Nat. Neurosci.* 4, 803–812.
- Pascual, O., Casper, K.B., Kubera, C., Zhang, J., Revilla-Sanchez, R., Sul, J.-Y., Takano, H., Moss, S.J., McCarthy, K., and Haydon, P.G. (2005). Astrocytic purinergic signaling coordinates synaptic networks. *Science* 310, 113–116.
- Pasti, L., Zonta, M., Pozzan, T., Vicini, S., and Carmignoto, G. (2001). Cytosolic calcium oscillations in astrocytes may regulate exocytotic release of glutamate. *J. Neurosci. Off. J. Soc. Neurosci.* 21, 477–484.
- Perea, G., Navarrete, M., and Araque, A. (2009). Tripartite synapses: astrocytes process and control synaptic information. *Trends Neurosci.* 32, 421–431.

- Petravicz, J., Fiacco, T.A., and McCarthy, K.D. (2008). Loss of IP₃ receptor-dependent Ca²⁺ increases in hippocampal astrocytes does not affect baseline CA1 pyramidal neuron synaptic activity. *J. Neurosci. Off. J. Soc. Neurosci.* *28*, 4967–4973.
- Pfrieger, F.W. (2002). Role of glia in synapse development. *Curr. Opin. Neurobiol.* *12*, 486–490.
- Pfrieger, F.W., and Barres, B.A. (1996). New views on synapse-glia interactions. *Curr. Opin. Neurobiol.* *6*, 615–621.
- Pixley, S.K., and de Vellis, J. (1984). Transition between immature radial glia and mature astrocytes studied with a monoclonal antibody to vimentin. *Brain Res.* *317*, 201–209.
- Placone, A.L., McGuiggan, P.M., Bergles, D.E., Guerrero-Cazares, H., Quiñones-Hinojosa, A., and Searson, P.C. (2015). Human astrocytes develop physiological morphology and remain quiescent in a novel 3D matrix. *Biomaterials* *42*, 134–143.
- Potokar, M., Stenovec, M., Kreft, M., Kreft, M.E., and Zorec, R. (2008). Stimulation inhibits the mobility of recycling peptidergic vesicles in astrocytes. *Glia* *56*, 135–144.
- Pouget, J.-T., Toulme, E., Martinez, A., Choquet, D., Hosy, E., and Boué-Grabot, E. (2014). ATP P_{2X} receptors downregulate AMPA receptor trafficking and postsynaptic efficacy in hippocampal neurons. *Neuron* *83*, 417–430.
- Prada, I., Marchaland, J., Podini, P., Magrassi, L., D'Alessandro, R., Bezzi, P., and Meldolesi, J. (2011). REST/NRSF governs the expression of dense-core vesicle gliosecretion in astrocytes. *J. Cell Biol.* *193*, 537–549.
- Prebil, M., Jensen, J., Zorec, R., and Kreft, M. (2011). Astrocytes and energy metabolism. *Arch. Physiol. Biochem.* *117*, 64–69.
- Prigent, S.A., and Lemoine, N.R. (1992). The type 1 (EGFR-related) family of growth factor receptors and their ligands. *Prog. Growth Factor Res.* *4*, 1–24.
- Puschmann, T.B., Zandén, C., De Pablo, Y., Kirchhoff, F., Pekna, M., Liu, J., and Pekny, M. (2013). Bioactive 3D cell culture system minimizes cellular stress and maintains the in vivo-like morphological complexity of astroglial cells. *Glia* *61*, 432–440.
- Puschmann, T.B., Zandén, C., Lebkuechner, I., Philippot, C., de Pablo, Y., Liu, J., and Pekny, M. (2014). HB-EGF affects astrocyte morphology, proliferation, differentiation, and the expression of intermediate filament proteins. *J. Neurochem.* *128*, 878–889.
- Queiroz, G., Meyer, D.K., Meyer, A., Starke, K., and von Kügelgen, I. (1999). A study of the mechanism of the release of ATP from rat cortical astroglial cells evoked by activation of glutamate receptors. *Neuroscience* *91*, 1171–1181.
- Raab, G., and Klagsbrun, M. (1997). Heparin-binding EGF-like growth factor. *Biochim. Biophys. Acta* *1333*, F179–F199.
- Ramamoorthy, P., and Whim, M.D. (2008). Trafficking and fusion of neuropeptide Y-containing dense-core granules in astrocytes. *J. Neurosci. Off. J. Soc. Neurosci.* *28*, 13815–13827.

- Rao, S.K., Huynh, C., Proux-Gillardeaux, V., Galli, T., and Andrews, N.W. (2004). Identification of SNAREs involved in synaptotagmin VII-regulated lysosomal exocytosis. *J. Biol. Chem.* *279*, 20471–20479.
- Raponi, E., Agenes, F., Delphin, C., Assard, N., Baudier, J., Legraverend, C., and Deloulme, J.-C. (2007). S100B expression defines a state in which GFAP-expressing cells lose their neural stem cell potential and acquire a more mature developmental stage. *Glia* *55*, 165–177.
- Reeves, A.M.B., Shigetomi, E., and Khakh, B.S. (2011). Bulk loading of calcium indicator dyes to study astrocyte physiology: key limitations and improvements using morphological maps. *J. Neurosci. Off. J. Soc. Neurosci.* *31*, 9353–9358.
- Ribeiro, C.S., Reis, M., Panizzutti, R., de Miranda, J., and Wolosker, H. (2002). Glial transport of the neuromodulator D-serine. *Brain Res.* *929*, 202–209.
- Risher, W.C., Patel, S., Kim, I.H., Uezu, A., Bhagat, S., Wilton, D.K., Pilaz, L.-J., Singh Alvarado, J., Calhan, O.Y., Silver, D.L., et al. (2014). Astrocytes refine cortical connectivity at dendritic spines. *eLife* *3*.
- Rose, C.R., and Karus, C. (2013). Two sides of the same coin: sodium homeostasis and signaling in astrocytes under physiological and pathophysiological conditions. *Glia* *61*, 1191–1205.
- Rosenberg, P.A., Knowles, R., Knowles, K.P., and Li, Y. (1994). Beta-adrenergic receptor-mediated regulation of extracellular adenosine in cerebral cortex in culture. *J. Neurosci. Off. J. Soc. Neurosci.* *14*, 2953–2965.
- Rossi, D.J., Oshima, T., and Attwell, D. (2000). Glutamate release in severe brain ischaemia is mainly by reversed uptake. *Nature* *403*, 316–321.
- Sahlender, D.A., Savtchouk, I., and Volterra, A. (2014). What do we know about gliotransmitter release from astrocytes? *Philos. Trans. R. Soc. Lond. B Biol. Sci.* *369*, 20130592.
- Saiki, R.K., Gelfand, D.H., Stoffel, S., Scharf, S.J., Higuchi, R., Horn, G.T., Mullis, K.B., and Erlich, H.A. (1988). Primer-directed enzymatic amplification of DNA with a thermostable DNA polymerase. *Science* *239*, 487–491.
- Sankowski, R., Mader, S., and Valdés-Ferrer, S.I. (2015). Systemic inflammation and the brain: novel roles of genetic, molecular, and environmental cues as drivers of neurodegeneration. *Front. Cell. Neurosci.* *9*, 28.
- Santello, M., Calì, C., and Bezzi, P. (2012). Gliotransmission and the tripartite synapse. *Adv. Exp. Med. Biol.* *970*, 307–331.
- Sasaki, T., Kuga, N., Namiki, S., Matsuki, N., and Ikegaya, Y. (2011). Locally synchronized astrocytes. *Cereb. Cortex N. Y. N 1991* *21*, 1889–1900.
- Scemes, E., and Giaume, C. (2006). Astrocyte calcium waves: what they are and what they do. *Glia* *54*, 716–725.

- Schafer, D.P., Lehrman, E.K., Kautzman, A.G., Koyama, R., Mardinly, A.R., Yamasaki, R., Ransohoff, R.M., Greenberg, M.E., Barres, B.A., and Stevens, B. (2012). Microglia sculpt postnatal neural circuits in an activity and complement-dependent manner. *Neuron* *74*, 691–705.
- Schafer, D.P., Lehrman, E.K., and Stevens, B. (2013). The “quad-partite” synapse: microglia-synapse interactions in the developing and mature CNS. *Glia* *61*, 24–36.
- Schell, M.J., Molliver, M.E., and Snyder, S.H. (1995). D-serine, an endogenous synaptic modulator: localization to astrocytes and glutamate-stimulated release. *Proc. Natl. Acad. Sci. U. S. A.* *92*, 3948–3952.
- Schiavo, G., Osborne, S.L., and Sgouros, J.G. (1998). Synaptotagmins: more isoforms than functions? *Biochem. Biophys. Res. Commun.* *248*, 1–8.
- Schiavo, G., Matteoli, M., and Montecucco, C. (2000). Neurotoxins affecting neuroexocytosis. *Physiol. Rev.* *80*, 717–766.
- Schiffer, D., Giordana, M.T., Migheli, A., Giaccone, G., Pezzotta, S., and Mauro, A. (1986). Glial fibrillary acidic protein and vimentin in the experimental glial reaction of the rat brain. *Brain Res.* *374*, 110–118.
- Schnitzer, J., Franke, W.W., and Schachner, M. (1981). Immunocytochemical demonstration of vimentin in astrocytes and ependymal cells of developing and adult mouse nervous system. *J. Cell Biol.* *90*, 435–447.
- Schoch, S., Deák, F., Königstorfer, A., Mozhayeva, M., Sara, Y., Südhof, T.C., and Kavalali, E.T. (2001). SNARE function analyzed in synaptobrevin/VAMP knockout mice. *Science* *294*, 1117–1122.
- Schubert, V., Bouvier, D., and Volterra, A. (2011). SNARE protein expression in synaptic terminals and astrocytes in the adult hippocampus: A comparative analysis. *Glia* *59*, 1472–1488.
- Schulz, K., Sydekum, E., Krueppel, R., Engelbrecht, C.J., Schlegel, F., Schröter, A., Rudin, M., and Helmchen, F. (2012). Simultaneous BOLD fMRI and fiber-optic calcium recording in rat neocortex. *Nat. Methods* *9*, 597–602.
- Schwartz, J.P., and Wilson, D.J. (1992). Preparation and characterization of type 1 astrocytes cultured from adult rat cortex, cerebellum, and striatum. *Glia* *5*, 75–80.
- Segovia, M., Alés, E., Montes, M.A., Bonifas, I., Jemal, I., Lindau, M., Maximov, A., Südhof, T.C., and Alvarez de Toledo, G. (2010). Push-and-pull regulation of the fusion pore by synaptotagmin-7. *Proc. Natl. Acad. Sci. U. S. A.* *107*, 19032–19037.
- Seifert, G., and Steinhäuser, C. (2013). Neuron-astrocyte signaling and epilepsy. *Exp. Neurol.* *244*, 4–10.
- Sergent-Tanguy, S., Chagneau, C., Neveu, I., and Naveilhan, P. (2003). Fluorescent activated cell sorting (FACS): a rapid and reliable method to estimate the number of neurons in a mixed population. *J. Neurosci. Methods* *129*, 73–79.

- Serrano, A., Haddjeri, N., Lacaille, J.-C., and Robitaille, R. (2006). GABAergic network activation of glial cells underlies hippocampal heterosynaptic depression. *J. Neurosci. Off. J. Soc. Neurosci.* *26*, 5370–5382.
- Sherwood, C.C., Stimpson, C.D., Raghanti, M.A., Wildman, D.E., Uddin, M., Grossman, L.I., Goodman, M., Redmond, J.C., Bonar, C.J., Erwin, J.M., et al. (2006). Evolution of increased glia-neuron ratios in the human frontal cortex. *Proc. Natl. Acad. Sci. U. S. A.* *103*, 13606–13611.
- Shigetomi, E., Kracun, S., and Khakh, B.S. (2010a). Monitoring astrocyte calcium microdomains with improved membrane targeted GCaMP reporters. *Neuron Glia Biol.* *6*, 183–191.
- Shigetomi, E., Kracun, S., Sofroniew, M.V., and Khakh, B.S. (2010b). A genetically targeted optical sensor to monitor calcium signals in astrocyte processes. *Nat. Neurosci.* *13*, 759–766.
- Shigetomi, E., Bushong, E.A., Hausteiner, M.D., Tong, X., Jackson-Weaver, O., Kracun, S., Xu, J., Sofroniew, M.V., Ellisman, M.H., and Khakh, B.S. (2013a). Imaging calcium microdomains within entire astrocyte territories and endfeet with GCaMPs expressed using adeno-associated viruses. *J. Gen. Physiol.* *141*, 633–647.
- Shigetomi, E., Jackson-Weaver, O., Huckstepp, R.T., O’Dell, T.J., and Khakh, B.S. (2013b). TRPA1 channels are regulators of astrocyte basal calcium levels and long-term potentiation via constitutive D-serine release. *J. Neurosci. Off. J. Soc. Neurosci.* *33*, 10143–10153.
- Singh, P., Jorgačevski, J., Kreft, M., Grubišić, V., Stout, R.F., Potokar, M., Parpura, V., and Zorec, R. (2014). Single-vesicle architecture of synaptobrevin2 in astrocytes. *Nat. Commun.* *5*, 3780.
- Sloan, S.A., and Barres, B.A. (2014a). Mechanisms of astrocyte development and their contributions to neurodevelopmental disorders. *Curr. Opin. Neurobiol.* *27*, 75–81.
- Sloan, S.A., and Barres, B.A. (2014b). Looks Can Be Deceiving: Reconsidering the Evidence for Gliotransmission. *Neuron* *84*, 1112–1115.
- Sontheimer, H. (1994). Voltage-dependent ion channels in glial cells. *Glia* *11*, 156–172.
- Sosinsky, G.E., Boassa, D., Dermietzel, R., Duffy, H.S., Laird, D.W., MacVicar, B., Naus, C.C., Penuela, S., Scemes, E., Spray, D.C., et al. (2011). Pannexin channels are not gap junction hemichannels. *Channels Austin Tex* *5*, 193–197.
- Souza, D.G., Bellaver, B., Souza, D.O., and Quincozes-Santos, A. (2013). Characterization of adult rat astrocyte cultures. *PloS One* *8*, e60282.
- Srinivasan, R., Huang, B.S., Venugopal, S., Johnston, A.D., Chai, H., Zeng, H., Golshani, P., and Khakh, B.S. (2015). Ca²⁺ signaling in astrocytes from *Ip3r2*(^{-/-}) mice in brain slices and during startle responses in vivo. *Nat. Neurosci.* *18*, 708–717.
- Steiner, J., Bernstein, H.-G., Bogerts, B., Gos, T., Richter-Landsberg, C., Wunderlich, M.T., and Keilhoff, G. (2008). S100B is expressed in, and released from, OLN-93 oligodendrocytes: Influence of serum and glucose deprivation. *Neuroscience* *154*, 496–503.

- Steinhäuser, C. (1993). Electrophysiologic characteristics of glial cells. *Hippocampus* 3 *Spec No*, 113–123.
- Südhof, T.C. (2002). Synaptotagmins: why so many? *J. Biol. Chem.* 277, 7629–7632.
- Südhof, T.C. (2013). Neurotransmitter release: the last millisecond in the life of a synaptic vesicle. *Neuron* 80, 675–690.
- Sun, W., McConnell, E., Pare, J.-F., Xu, Q., Chen, M., Peng, W., Lovatt, D., Han, X., Smith, Y., and Nedergaard, M. (2013). Glutamate-dependent neuroglial calcium signaling differs between young and adult brain. *Science* 339, 197–200.
- Szatkowski, M., Barbour, B., and Attwell, D. (1990). Non-vesicular release of glutamate from glial cells by reversed electrogenic glutamate uptake. *Nature* 348, 443–446.
- Takamori, S., Holt, M., Stenius, K., Lemke, E.A., Grønborg, M., Riedel, D., Urlaub, H., Schenck, S., Brügger, B., Ringler, P., et al. (2006). Molecular anatomy of a trafficking organelle. *Cell* 127, 831–846.
- Takano, T., Kang, J., Jaiswal, J.K., Simon, S.M., Lin, J.H.-C., Yu, Y., Li, Y., Yang, J., Dienel, G., Zielke, H.R., et al. (2005). Receptor-mediated glutamate release from volume sensitive channels in astrocytes. *Proc. Natl. Acad. Sci. U. S. A.* 102, 16466–16471.
- Takano, T., Tian, G.-F., Peng, W., Lou, N., Libionka, W., Han, X., and Nedergaard, M. (2006). Astrocyte-mediated control of cerebral blood flow. *Nat. Neurosci.* 9, 260–267.
- Tao-Cheng, J.-H., Pham, A., Yang, Y., Winters, C.A., Gallant, P.E., and Reese, T.S. (2015). Syntaxin 4 is concentrated on plasma membrane of astrocytes. *Neuroscience* 286, 264–271.
- Tian, L., Hires, S.A., and Looger, L.L. (2012). Imaging neuronal activity with genetically encoded calcium indicators. *Cold Spring Harb. Protoc.* 2012, 647–656.
- Tong, X., Shigetomi, E., Looger, L.L., and Khakh, B.S. (2013). Genetically encoded calcium indicators and astrocyte calcium microdomains. *Neurosci. Rev. J. Bringing Neurobiol. Neurol. Psychiatry* 19, 274–291.
- Torres, A., Wang, F., Xu, Q., Fujita, T., Dobrowolski, R., Willecke, K., Takano, T., and Nedergaard, M. (2012). Extracellular Ca²⁺ acts as a mediator of communication from neurons to glia. *Sci. Signal.* 5, ra8.
- Ullian, E.M., Sapperstein, S.K., Christopherson, K.S., and Barres, B.A. (2001). Control of synapse number by glia. *Science* 291, 657–661.
- Uniprot Consortium (2012). Reorganizing the protein space at the Universal Protein Resource (UniProt). *Nucleic Acids Res.* 40, D71–D75.
- Vardjan, N., and Zorec, R. (2015). Excitable Astrocytes: Ca(2+)- and cAMP-Regulated Exocytosis. *Neurochem. Res.*
- Verderio, C., Coco, S., Rossetto, O., Montecucco, C., and Matteoli, M. (1999). Internalization and proteolytic action of botulinum toxins in CNS neurons and astrocytes. *J. Neurochem.* 73, 372–379.

- Verkhatsky, A. (2009). Neurotransmitter Receptors in Astrocytes. In *Astrocytes in (Patho)Physiology of the Nervous System*, P.G. Haydon, and V. Parpura, eds. (Springer US), pp. 49–67.
- Verkhatsky, A., and Parpura, V. (2010). Recent advances in (patho)physiology of astroglia. *Acta Pharmacol. Sin.* *31*, 1044–1054.
- Verkhatsky, A., and Steinhäuser, C. (2000). Ion channels in glial cells. *Brain Res. Brain Res. Rev.* *32*, 380–412.
- Volkandt, W. (2002). Vesicular release mechanisms in astrocytic signalling. *Neurochem. Int.* *41*, 301–306.
- Volterra, A., and Meldolesi, J. (2005). Astrocytes, from brain glue to communication elements: the revolution continues. *Nat. Rev. Neurosci.* *6*, 626–640.
- Volterra, A., Bezzi, P., Rizzini, B.L., Trotti, D., Ullensvang, K., Danbolt, N.C., and Racagni, G. (1996). The competitive transport inhibitor L-trans-pyrrolidine-2, 4-dicarboxylate triggers excitotoxicity in rat cortical neuron-astrocyte co-cultures via glutamate release rather than uptake inhibition. *Eur. J. Neurosci.* *8*, 2019–2028.
- Volterra, A., Liaudet, N., and Savtchouk, I. (2014). Astrocyte Ca²⁺ signalling: an unexpected complexity. *Nat. Rev. Neurosci.* *15*, 327–335.
- Walsh, C.A., Morrow, E.M., and Rubenstein, J.L.R. (2008). Autism and brain development. *Cell* *135*, 396–400.
- Walz, W. (2000). Role of astrocytes in the clearance of excess extracellular potassium. *Neurochem. Int.* *36*, 291–300.
- Wang, P., Chicka, M.C., Bhalla, A., Richards, D.A., and Chapman, E.R. (2005). Synaptotagmin VII is targeted to secretory organelles in PC12 cells, where it functions as a high-affinity calcium sensor. *Mol. Cell. Biol.* *25*, 8693–8702.
- Wang, X., Lou, N., Xu, Q., Tian, G.-F., Peng, W.G., Han, X., Kang, J., Takano, T., and Nedergaard, M. (2006). Astrocytic Ca²⁺ signaling evoked by sensory stimulation in vivo. *Nat. Neurosci.* *9*, 816–823.
- Warr, O., Takahashi, M., and Attwell, D. (1999). Modulation of extracellular glutamate concentration in rat brain slices by cystine-glutamate exchange. *J. Physiol.* *514 (Pt 3)*, 783–793.
- West, A.E., and Greenberg, M.E. (2011). Neuronal activity-regulated gene transcription in synapse development and cognitive function. *Cold Spring Harb. Perspect. Biol.* *3*.
- Whitelam, G. (1995). Immunocytochemical methods and protocols edited by Lorette C. Javois. *Mol. Biotechnol.* *3*, 76–76.
- Wilhelm, A., Volkandt, W., Langer, D., Nolte, C., Kettenmann, H., and Zimmermann, H. (2004). Localization of SNARE proteins and secretory organelle proteins in astrocytes in vitro and in situ. *Neurosci. Res.* *48*, 249–257.

- Williams, S.M., Diaz, C.M., Macnab, L.T., Sullivan, R.K.P., and Pow, D.V. (2006). Immunocytochemical analysis of D-serine distribution in the mammalian brain reveals novel anatomical compartmentalizations in glia and neurons. *Glia* 53, 401–411.
- de Wit, H., Walter, A.M., Milosevic, I., Gulyás-Kovács, A., Riedel, D., Sørensen, J.B., and Verhage, M. (2009). Synaptotagmin-1 docks secretory vesicles to syntaxin-1/SNAP-25 acceptor complexes. *Cell* 138, 935–946.
- Wolosker, H., Blackshaw, S., and Snyder, S.H. (1999). Serine racemase: a glial enzyme synthesizing D-serine to regulate glutamate-N-methyl-D-aspartate neurotransmission. *Proc. Natl. Acad. Sci. U. S. A.* 96, 13409–13414.
- Woo, D.H., Han, K.-S., Shim, J.W., Yoon, B.-E., Kim, E., Bae, J.Y., Oh, S.-J., Hwang, E.M., Marmorstein, A.D., Bae, Y.C., et al. (2012). TREK-1 and Best1 channels mediate fast and slow glutamate release in astrocytes upon GPCR activation. *Cell* 151, 25–40.
- Yang, Y., Vidensky, S., Jin, L., Jie, C., Lorenzini, I., Frankl, M., and Rothstein, J.D. (2011). Molecular comparison of GLT1+ and ALDH1L1+ astrocytes in vivo in astroglial reporter mice. *Glia* 59, 200–207.
- Yang, Y., Higashimori, H., and Morel, L. (2013). Developmental maturation of astrocytes and pathogenesis of neurodevelopmental disorders. *J. Neurodev. Disord.* 5, 22.
- Ye, Z.-C., Wyeth, M.S., Baltan-Tekkok, S., and Ransom, B.R. (2003). Functional hemichannels in astrocytes: a novel mechanism of glutamate release. *J. Neurosci. Off. J. Soc. Neurosci.* 23, 3588–3596.
- Zamanian, J.L., Xu, L., Foo, L.C., Nouri, N., Zhou, L., Giffard, R.G., and Barres, B.A. (2012). Genomic analysis of reactive astrogliosis. *J. Neurosci. Off. J. Soc. Neurosci.* 32, 6391–6410.
- Zhang, J., Wang, H., Ye, C., Ge, W., Chen, Y., Jiang, Z., Wu, C., Poo, M., and Duan, S. (2003). ATP released by astrocytes mediates glutamatergic activity-dependent heterosynaptic suppression. *Neuron* 40, 971–982.
- Zhang, Q., Fukuda, M., Van Bockstaele, E., Pascual, O., and Haydon, P.G. (2004a). Synaptotagmin IV regulates glial glutamate release. *Proc. Natl. Acad. Sci. U. S. A.* 101, 9441–9446.
- Zhang, Q., Pangrsic, T., Kreft, M., Krzan, M., Li, N., Sul, J.-Y., Halassa, M., Van Bockstaele, E., Zorec, R., and Haydon, P.G. (2004b). Fusion-related release of glutamate from astrocytes. *J. Biol. Chem.* 279, 12724–12733.
- Zhang, Z., Chen, G., Zhou, W., Song, A., Xu, T., Luo, Q., Wang, W., Gu, X., and Duan, S. (2007). Regulated ATP release from astrocytes through lysosome exocytosis. *Nat. Cell Biol.* 9, 945–953.
- Zorec, R., Verkhratsky, A., Rodríguez, J.J., and Parpura, V. (2015). Astrocytic vesicles and gliotransmitters: Slowness of vesicular release and synaptobrevin2-laden vesicle nanoarchitecture. *Neuroscience*.

Zur Nieden, R., and Deitmer, J.W. (2006). The role of metabotropic glutamate receptors for the generation of calcium oscillations in rat hippocampal astrocytes in situ. *Cereb. Cortex N. Y. N* 1991 *16*, 676–687.

Zylbersztejn, K., Petkovic, M., Burgo, A., Deck, M., Garel, S., Marcos, S., Bloch-Gallego, E., Nothias, F., Serini, G., Bagnard, D., et al. (2012). The vesicular SNARE Synaptobrevin is required for Semaphorin 3A axonal repulsion. *J. Cell Biol.* *196*, 37–46.

Curriculum Vitae

EDUCATION

- Sept. 2015 PhD in “Molecular Physiology of the Brain” at the Göttingen Graduate School for Neurosciences, Biophysics, and Molecular Biosciences (GGNB), Germany
“Mechanisms of astrocyte vesicle fusion at synaptic interfaces”
(supervisor: Camin Dean, PhD)
- May 2012 M.Sc. in Neural, Developmental, and Behavioral Biology at the University of Göttingen, Germany
“Neurones and astrocytes in deep discussion: Synaptotagmins of tripartite synapses” (supervisor: Camin Dean, PhD)
- June 2010 B.Sc. (Honours) in Neuroscience at the University College London, UK
“Basal lamina proteins in eye morphogenesis: An analysis of wild-type and *rx3* mutant zebrafish” (supervisor: Prof. Stephen Wilson)

RESEARCH & PROFESSIONAL EXPERIENCE

- 2012 – 2015 PhD student at the European Neuroscience Institute in Göttingen, Germany
Responsibilities: project planning, cell culture- and whole brain samplebased protein biochemistry and microscopy, data analysis and figure preparation (ImageJ, MetaMorph, Photoshop, Adobe Illustrator), conference visits (incl. posters and presentations, see below), and the preparation of two research articles (one submitted recently).
- 2011 Biochemistry teaching assistant for medical students at the University of Göttingen, Germany
- 2009 Student research assistant in the Department of Neurogenetics, Max Planck Institute for Experimental Medicine, Göttingen, Germany
“Proteins of the murine axogliasome” (supervisor: Dr. Hauke Werner)
Responsibilities: project planning, sciatic nerve and whole brain preparation, protein biochemistry (myelin purification by sucrose gradient centrifugation, immunoblotting), lab seminar presentations.
- 2008, 2009 Internships in the Department of Neurogenetics, Max Planck Institute for Experimental Medicine, Göttingen, Germany
“*Plp*^{-/-} mouse myelin proteomics” (2009, supervisor: Dr. Hauke Werner)
“Myelin protein redundancy of M6A and M6B protein” (2008, supervisor: Dr. Ursula Fünfschilling)
- 2008 Internship in the Department of Neurology and Clinical Neurophysiology, Hanover Medical School, Germany
“Fumaric acid application to the cuprizone model of CNS demyelination” (supervisor: Dr. Moharreggh-Khiabani)

CONFERENCES

- 2015 Gordon Research Conference on Glial Biology in Ventura, USA; incl. poster presentation
- 11th meeting of the German Neuroscience Society (NWG) in Göttingen, Germany; incl. talk “Calcium signalling and vesicle-related proteins in different astrocyte culture types”
- 2014 “Astrocytes in Health and Neurodegenerative Disease” in London, UK; incl. poster presentation
- 2013 Gordon Research Conference on Glial Biology in Ventura, USA; incl. poster presentation
- 10th meeting of the German Neuroscience Society (NWG) in Göttingen; incl. talk “Molecular Mechanisms of Astrocyte Vesicle Release at Synaptic Interfaces”

EXTRACURRICULAR ENGAGEMENT

- 2013 – 2014 Chair of the “Women’s Careers & Networks 2014” symposium on female advance in science (20/11/14), Göttingen, Germany
- 2013 – 2015 Student representative of my PhD programme
- 2013 Organiser of the “Game of Brains” symposium (29/10/13), Göttingen, Germany
- 2012 Chair and only organiser of the “Masters Club Career Day”
- 2011 – 2012 Student representative of my M.Sc. programme
- 2010 – 2012 Co-founder and head of the University of Göttingen “Masters Club”

AWARDS & CERTIFICATES

- 2014, 2015 Travel grants for conferences in the UK and USA (from the GGNB)
- 2013 2nd place of the NeuroDoWo 2013 presentation competition
- 2013 Certificate with distinction for the course “Writing in the Sciences”
 by Kristin Sainani, PhD, Stanford University (through Coursera.org)
- 2011 2nd place at the “Science Slam” in Göttingen
- 2010 Short-term scholarship (incl. financial support) from the University of Göttingen
- 2009, 2010 Student Ambassador Certificate from the University College London